AD-A171 591 THE LARGE STRAIN CONTROLLED RATE OF STRAIN (LSCRS) 1/2
DEVICE FOR CONSOLIDATI..(U) ARMY ENGINEER WATERWAYS
EXPERIMENT STATION VICKSBURG MS GEOTE.. K W CARGILL
UNCLASSIFIED JUL 86 WES/TR/GL-86-13 F/G 8/13 NL

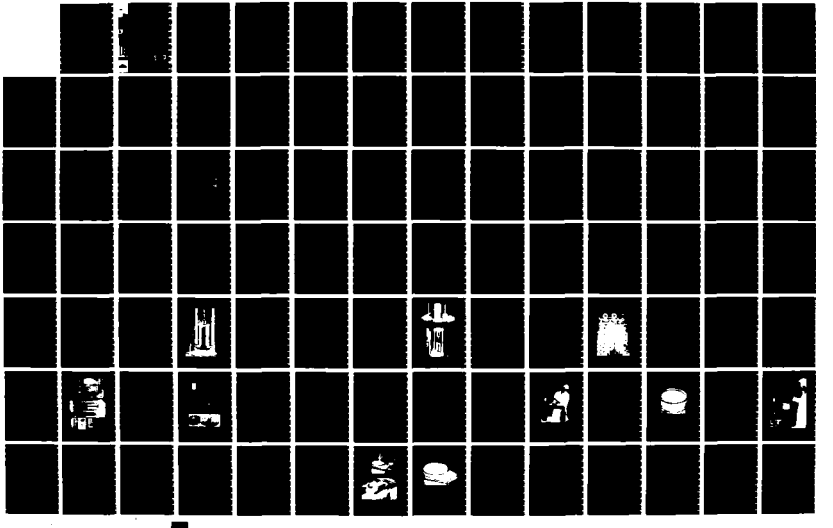

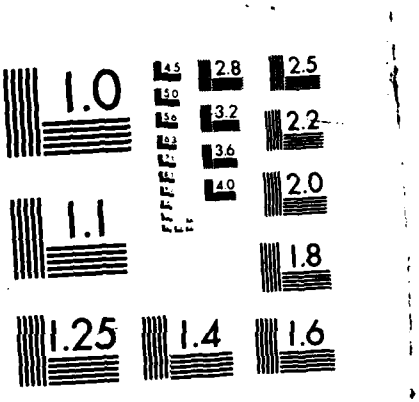
1.0
1.1
1.25
1.4
1.6
1.8
2.0
2.2
2.5
2.8
3.2
3.6
4.0
4.5
5.0
5.6

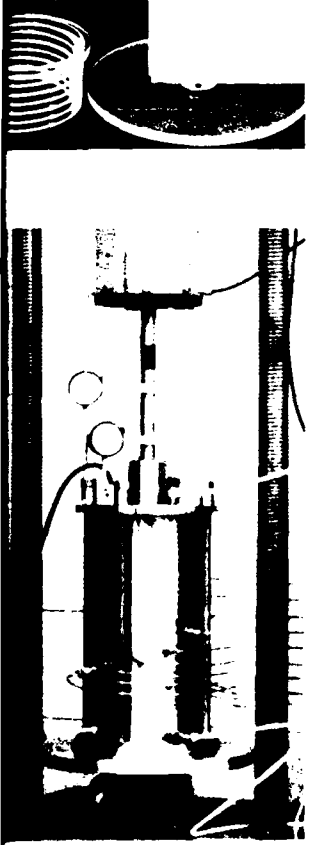

(12)

TECHNICAL REPORT GL-86-13

THE LARGE STRAIN, CONTROLLED RATE OF STRAIN (LSCRS) DEVICE FOR CONSOLIDATION TESTING OF SOFT FINE-GRAINED SOILS

by

Kenneth W. Cargill

Geotechnical Laboratory

DEPARTMENT OF THE ARMY
Waterways Experiment Station, Corps of Engineers
PO Box 631, Vicksburg, Mississippi 39180-0631

July 1986
Final Report

Prepared for DEPARTMENT OF THE ARMY
US Army Corps of Engineers
Washington, DC 20314-1000

Under CWIS Work Unit No. 31173, Task 34

Destroy this report when no longer needed. Do not return it to the originator.

The findings in this report are not to be construed as an official Department of the Army position unless so designated by other authorized documents.

This program is furnished by the Government and is accepted and used by the recipient with the express understanding that the United States Government makes no warranties, expressed or implied, concerning the accuracy, completeness, reliability, usability, or suitability for any particular purpose of the information and data contained in this program or furnished in connection therewith, and the United States shall be under no liability whatsoever to any person by reason of any use made thereof. The program belongs to the Government. Therefore, the recipient further agrees not to assert any proprietary rights therein or to represent this program to anyone as other than a Government program.

The contents of this report are not to be used for advertising, publication, or promotional purposes. Citation of trade names does not constitute an official endorsement or approval of the use of such commercial products.

Unclassified
SECURITY CLASSIFICATION OF THIS PAGE

ADA 171591

REPORT DOCUMENTATION PAGE

Form Approved
OMB No 0704-0188
Exp Date Jun 30, 1986

1a REPORT SECURITY CLASSIFICATION Unclassified	1b RESTRICTIVE MARKINGS
2a SECURITY CLASSIFICATION AUTHORITY	3 DISTRIBUTION / AVAILABILITY OF REPORT Approved for public release; distribution unlimited.
2b DECLASSIFICATION / DOWNGRADING SCHEDULE	
4 PERFORMING ORGANIZATION REPORT NUMBER(S) Technical Report GL-86-13	5 MONITORING ORGANIZATION REPORT NUMBER(S)
6a NAME OF PERFORMING ORGANIZATION USAEWES Geotechnical Laboratory 6b OFFICE SYMBOL (If applicable) WESGE-GC	7a NAME OF MONITORING ORGANIZATION
6c ADDRESS (City, State, and ZIP Code) PO Box 631 Vicksburg, MS 39180-0631	7b ADDRESS (City, State, and ZIP Code)
8a NAME OF FUNDING / SPONSORING ORGANIZATION US Army Corps of Engineers 8b OFFICE SYMBOL (If applicable) DAEN-CWO-R	9 PROCUREMENT INSTRUMENT IDENTIFICATION NUMBER CWIS Work Unit No. 31173
8c ADDRESS (City, State, and ZIP Code) Washington, DC 20314-1000	10 SOURCE OF FUNDING NUMBERS PROGRAM ELEMENT NO. / PROJECT NO / TASK NO 34 / WORK UNIT ACCESSION NO

11 TITLE (Include Security Classification)
The Large Strain, Controlled Rate of Strain (LSCRS) Device for Consolidation Testing of Soft Fine-Grained Soils

12 PERSONAL AUTHOR(S)
Cargill, Kenneth W.

13a TYPE OF REPORT	13b TIME COVERED	14 DATE OF REPORT (Year, Month, Day)	15 PAGE COUNT
Final report	FROM _____ TO _____	July 1986	187

16 SUPPLEMENTARY NOTATION
Available from National Technical Information Service, 5285 Port Royal Road, Springfield, VA 22161.

17 COSATI CODES			18 SUBJECT TERMS (Continue on reverse if necessary and identify by block number)	
FIELD	GROUP	SUB-GROUP	Containment areas	Finite strain theory
			Dredged material	Self-weight consolidation
			Finite strain consolidation	Slurried soil

19. ABSTRACT (Continue on reverse if necessary and identify by block number)

The development of a new device for consolidation testing of very soft fine-grained soils such as dredged materials is described. The new device, is capable of Large Strains at a Controlled Rate of Strain, and is referred to as LSCRS. The development of a self-weight consolidation device to supplement LSCRS testing is also described.

A mathematical model of the LSCRS test is first given in terms of the finite strain consolidation theory. Possible initial conditions are discussed and boundary conditions for singly and doubly drained cases are derived. Then, by the computer program CRST (also developed in this study), the effects of various test parameters at constant and variable strain rates are demonstrated. This leads to the definition of an idealized test.

The physical attributes of the LSCRS test device and self-weight consolidation
(Continued)

20 DISTRIBUTION / AVAILABILITY OF ABSTRACT	21 ABSTRACT SECURITY CLASSIFICATION
☒ UNCLASSIFIED/UNLIMITED ☐ SAME AS RPT ☐ DTIC USERS	Unclassified
22a NAME OF RESPONSIBLE INDIVIDUAL	22b TELEPHONE (Include Area Code) / 22c OFFICE SYMBOL

DD FORM 1473, 84 MAR 83 APR edition may be used until exhausted
All other editions are obsolete

SECURITY CLASSIFICATION OF THIS PAGE
Unclassified

19. ABSTRACT (Continued).

device are documented along with both testing and data interpretation procedures. The aim of these tests is the definition of the void ratio-effective stress and void ratio-permeability relationships for soft soils throughout the full range of possible void ratios at which they might exist in the field. Analysis of LSCRS test data is accomplished by the computer program LSCRS.

A testing program for three typical edged material slurries is described, and the relationships derived from the tests are compared to previous oedometer tests.

Appendices to the report contain user's guides and listings for the computer programs CRST and LSCRS. Figures depicting the results of self-weight consolidation tests and the excess pore pressure distribution from LSCRS tests are also included.

PREFACE

The investigation reported herein was sponsored by the Office, Chief of Engineers (OCE), US Army as a part of CWIS Work Unit No. 31173, "Special Studies for Civil Works Soils Problems," Task 34, Finite Strain Theory of Consolidation.

The study was conducted at the US Army Engineer Waterways Experiment Station (WES) by the Soil Mechanics Division (SMD) of the Geotechnical Laboratory (GL), WES. This report and computer programs were written by MAJ K. W. Cargill, SMD, GL, WES.

The work was conducted under the overall supervision of Dr. W. F. Marcuson III, Chief, GL, and under the direct supervision of Mr. C. L. McAnear, Chief, SMD, GL.

COL Allen F. Grum, USA, was the former Director of WES. COL Dwayne G. Lee, CE, is the present Commander and Director. Dr. Robert W. Whalin is Technical Director.

CONTENTS

CONVERSION FACTORS, NON-SI TO SI (METRIC)
UNITS OF MEASUREMENT

Non-SI units of measurement used in this report can be converted to SI (metric) units as follows:

Multiply	By	To Obtain
acres	4046.873	square metres
cubic yards	0.7645549	cubic metres
feet	0.3048	metres
inches	2.54	centimetres
pounds (force) per square foot	47.88026	pascals
pounds (force) per square inch	6.894757	kilopascals
pounds (mass) per cubic foot	16.01846	kilograms per cubis metre
pounds (mass) per cubic inch	27.6799	grams per cubic centimetre
square feet	0.09290304	square metres
square inches	6.4516	square centimetres
tons (force) per square foot	95.76052	kilopascals

THE LARGE STRAIN, CONTROLLED RATE OF STRAIN (LSCRS) DEVICE FOR CONSOLIDATION TESTING OF SOFT FINE-GRAINED SOILS

PART I: INTRODUCTION

1. The geotechnical engineer's ability to mathematically model complex behavior in soil mediums, in general, vastly exceeds his capability to define those properties of the soil which influence or control the behavior being analyzed. While the early pioneers of soil mechanics have certainly provided classic devices for characterizing most soils with parameters useful in many of the constitutive models programmed for today's computers, there are many instances where needed parameters cannot be directly measured in conventional testing devices and must be deduced or extrapolated from conventional testing results. It could be argued that the random nature of typical soil deposits will ultimately place a bound on the accuracy of any mathematical model, but until laboratory testing techniques for determination of soil parameters match the requirements of the constitutive model, calculation accuracy will always be lower than it should. This report will document efforts to devise and perform state-of-the-art one-dimensional consolidation testing on very soft fine-grained soils.

Background

2. Historically, consolidation calculations have been almost exclusively performed on normally consolidated or overconsolidated clays from foundations or embankments. References to soft soils usually pertained to the

upper levels of normally consolidated highly plastic clays or organic silt or clay deposits. The consolidation process and controlling properties in all but the very softest of these soils were adequately defined in terms of the conventional small strain or Terzaghi theory of consolidation and the parameters obtained from a conventional oedometer test in the laboratory. Some of the better solutions based on the Terzaghi governing equation are illustrated by Olson and Ladd (1979).

3. Recently, however, there has been considerable interest in the consolidation behavior of very soft soils. Soils so soft they are more appropriately described as slurries. Examples of such materials include sediments dredged from rivers and harbors to improve navigation, the clay by-product left after extraction of phosphate from its ore, and fine-grained tailings from uranium, tar sand, and other mining operations. Consolidation of these slurries may begin at extremely high void ratios when compared to soils of normal geotechnical interest. In fact, Bromwell and Carrier (1979) have reported typical initial void ratios on the order of 50 for phosphatic clays.

4. The theoretical treatment of one-dimensional primary consolidation, many times due only to self weight, in these very soft slurried soils has been quite comprehensive since the proposal of the finite strain theory of consolidation by Gibson, England, and Hussey (1967). A mathematical model based on this finite strain theory is documented by Cargill (1982) and illustrates the detailed analysis available through computer programming of the solution to the general governing equation. However, this very sophisticated analysis procedure suddenly becomes somewhat crude when material properties based on consolidation testing in a void ratio range not applicable to the problem must be used.

5. The Corps of Engineers is interested in state-of-the-art consolidation predictions for very soft fine-grained soils primarily in relation to dredged material disposal within confined areas. As environmentally acceptable alternatives and available disposal areas decrease, it becomes increasingly important to utilize areas which are available in the most efficient and economical manner. To do so requires accurate and dependable consolidation predictions for the dredged material placed, which in turn requires very accurate and dependable knowledge of the properties controlling consolidation. The work is also applicable to primary consolidation of very soft foundation materials or anywhere the nonlinear nature of a material's properties and/or its self weight influences its consolidation.

Need for an LSCRS

6. To complete the ability for accurate consolidation predictions for soft fine-grained soils, existing theoretical and computational capabilities must be supplemented with improved methods for defining the extremely nonlinear soil properties at the high void ratios common to these slurried soils. More specifically, a device is required which can be used to directly measure the relationships between void ratio and effective stress and void ratio and permeability from a very low effective stress to the maximum stress the material will experience under field conditions and over very large strains. Additionally, the device should be strain controlled as opposed to the stress controlled oedometer-type test for maximum efficiency in time of testing. The large strain, controlled rate of strain (LSCRS) slurry consolidometer to be documented in this report is a prototype of such a device and will hopefully

contribute significantly to the base of soft soil testing experience and ultimately lead to the design of the ideal soft soil testing device.

Previous Work

7. There have been many attempts to improve on the original methods of performing consolidation tests as proposed by Terzaghi (1925). However, before the 1960's, improvements were mainly limited to testing mechanics and refinements in the basic test analysis procedure based on the conventional Terzaghi theory. Some of the more noteworthy efforts at unique consolidation testing methods are mentioned in the following paragraphs.

8. Smith and Wahls (1969) published the first comprehensive treatment of the constant rate of strain consolidation test (CRS test) for relatively thin and stiff (compared to newly deposited dredge material) samples as a substitute for the conventional oedometer test. A theory was developed which permitted the evaluation of the effective stress-void ratio and coefficient of consolidation-void ratio relationships. The analysis procedure depended on the void ratio being a linear function of time throughout the sample during the test. The work showed that there was good agreement between effective stress-void ratio relationships established by a conventional and CRS test when pore pressure did not exceed 50 percent of total stress. It also showed that the coefficient of consolidation-void ratio relationship from the CRS test was consistently higher than that from the conventional test, but agreement was still reasonably good. The authors concluded that the primary advantage of the CRS test was that it was a rapid method for obtaining consolidation characteristics.

9. Another CRS test methodology was presented by Wissa, et al. (1971). This procedure differed from the above mainly only in the assumptions of its theoretical basis. The test analysis allowed for a variable permeability and coefficient of volume compressibility with time, but required a constant coefficient of consolidation. The authors concluded that there was reasonably good agreement between results obtained from the CRS and conventional tests and that the CRS test was much faster.

10. Among the early attempts at defining the consolidation properties of a soil approaching the slurry consistency of dredged material is that reported by Monte and Krizek (1976). Although the primary intent of the article is the validation of a large strain mathematical model of consolidation, some interesting stress controlled testing techniques for relatively thick samples of soft fine-grained soils are given. The extremely nonlinear nature of the relationships between void ratio and logarithm of effective stress and between void ratio and logarithm of permeability through the transition from soil slurry to more solid soil is illustrated. The authors also concluded that the coefficient of permeability value measured will depend on whether the fluid is either passed through a fixed matrix of solid particles or squeezed from a deforming matrix. This suggests that the conventional direct measurement of permeability is inferior to a direct measurement during soil deformation.

11. In response to the problem of predicting consolidation settlements in the fine-grained clay slurry resulting from the phosphate mining industry in Florida, Bromwell and Carrier (1979) used a slurry consolidometer to define the clay's consolidation properties. The principle of the device is similar to the conventional oedometer except that a sample approximately 8 in. in diameter and 10 in. high could be accommodated and very small stresses could be imposed. The author's test procedure called for the clay slurry (at a

typical initial void ratio of 50) to be put in the consolidometer and allowed to undergo self-weight consolidation. By measuring pore pressure at the undrained sample bottom and noting the amount of settlement over a specific time interval during the self-weight phase, estimates of material permeability could be made for the higher average void ratios. After self-weight consolidation is complete, additional load increments are applied as in the oedometer test and results analyzed according to the Terzaghi theory. The chief disadvantages of this methodology are that it gives properties corresponding to the average void ratio of a relatively thick sample and requires literally months to complete each test.

12. Noting that the conventional oedometer test has limited applicability to very soft soil due to deficiencies in both theory and testing techniques, Umehara and Zen (1980) proposed another interpretation of CRS test results based on the large strain consolidation theory of Mikasa (1965). While their analysis procedure does offer some advantages, chief among its disadvantages are the assumptions of a constant coefficient of consolidation throughout the test and a constant compression index. However, in using their procedure to analyze consolidation in soft dredged materials, Umehara and Zen (1982) recognized the need for and should probably be credited with the idea of using a specially designed self-weight consolidation apparatus to supplement the effective stress-void ratio relationship in the low effective stress range not measurable in the CRS test apparatus.

13. Znidarcic (1982) has detailed the first CRS-type test whose analysis is based on the finite strain theory of consolidation, but without consideration of material self-weight. The test and analysis procedures were used with apparent success to define two very soft dredged materials as reported by Cargill (1983). The interpretation of these results requires a

deconvolution procedure to obtain the finite strain theory coefficient of consolidation which is assumed constant over a specified time interval. A coefficient of compressibility is obtained from directly measured stresses and pore pressures, and this is used with average void ratio values to deduce a void ratio-permeability relationship from the coefficient of consolidation. The primary disadvantages of the proposed procedures are the necessity for computer programming of the deconvolution technique and the assumption of a constant coefficient of consolidation throughout the sample during specified time periods.

Report Objectives

14. The purpose of this report is to document a new consolidation testing methodology based on the most general and complete theory describing one-dimensional primary consolidation to date; i.e., Gibson, England, and Hussey (1967). To show that material properties derived by this method correspond to or validate those derived by other methods is not an objective. Through use of the finite strain consolidation theory to understand the test and a series of direct measurements during the test, it is hoped that material properties more exact than ever before derived can be obtained. Basically, the new test will involve a large sample deformed under a controlled (not constant as in all previous work) rate of strain with pore pressure measurements throughout the sample and stress measurements at both ends, thus the acronym LSCRS.

15. More specifically, the report will:

a. Set forth the mathematical description of the test to include the governing equation, initial conditions, and boundary conditions.

b. Detail a parametric study of the test by computer simulation to define the features of an idealized test and procedure.

c. Describe testing hardware to include equipment construction and layout and auxiliary devices.

d. Outline all require test procedures from sample preparation to data collection.

e. Provide procedures for data interpretation and show how the basic soil consolidation properties are obtained.

f. Illustrate the device and analysis capabilities with the testing of several typical soft fine-grained soils.

PART II: MATHEMATICAL DESCRIPTION OF TEST

16. The theoretical basis for analyzing the proposed LSCRS test will be established in this part. There have been many variations of the theory of one-dimensional primary consolidation proposed since the original Terzaghi (1924) formulation. The most general and least restrictive of the proposals is the finite strain theory due to Gibson, England, and Hussey (1967). It can be shown that all other variations, including Terzaghi's, are merely special cases of the finite strain theory (Schiffman 1980 and Pane 1981). A complete mathematical statement of the test includes the general consolidation governing equation, sample initial conditions, and boundary conditions for the test.

Governing Equation

17. The governing equation for finite strain consolidation theory is based on the continuity of fluid flow in a differential soil element, Darcy's law, and the effective stress principle similar to the conventional consolidation theory. However, finite strain theory additionally considers vertical equilibrium of the soil mass, places no restriction on the form of the stress-strain relationship, allows for a variable coefficient of permeability, and accommodates any degree of strain. It is instructive to briefly go through the derivation of the governing equation so that an appreciation for its generality can be obtained.

18. Consider the differential soil element shown in Figure 1. The element is defined in space by the vertical coordinate ξ which is free to change with time so that the element continuously encloses the same solid

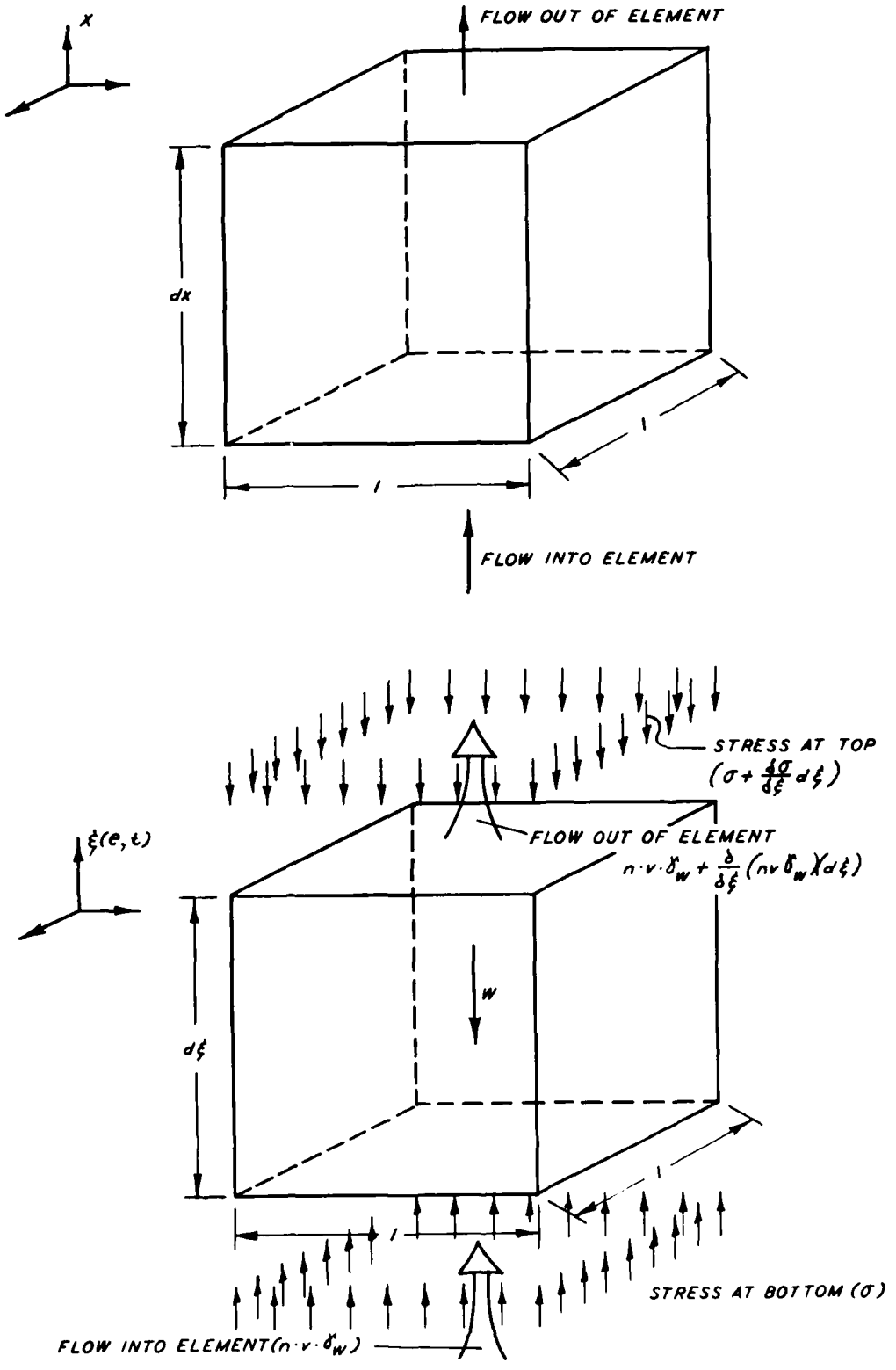

Figure 1. Equilibrium and flow conditions in a differential soil element

particles and has a constant unit plan area. Also shown in the figure are total stresses and flow conditions at the top and bottom of the element. The Terzaghi theory assumes that total stresses at top and bottom are equal (thus no material self-weight) and that the vertical coordinate does not materially change with time (small strains).

19. The weight W of the element (assumed fully saturated) is the sum of the weights of the pore fluid and solid particles. Thus

$$W = (e\gamma_w + \gamma_s) \frac{d\xi}{1 + e} \tag{1}$$

where

e = void ratio

γ_w = the unit weight of water

γ_s = the unit weight of the soil solid particles

Therefore, the total equilibrium of the soil mixture is given by

$$\sigma + \frac{\partial \sigma}{\partial \xi} d\xi + (e\gamma_w + \gamma_s) \frac{d\xi}{1 + e} - \sigma = 0 \tag{2}$$

where σ = the total stress. This means that

$$\frac{\partial \sigma}{\partial \xi} + \frac{e\gamma_w + \gamma_s}{1 + e} = 0 \tag{3}$$

20. It is also necessary to establish an expression for equilibrium of the pore fluid. If the total pore water pressure u_w is decomposed into its static and excess parts,

$$\frac{\partial u_w}{\partial \xi} - \frac{\partial u_o}{\partial \xi} - \frac{\partial u}{\partial \xi} = 0 \tag{4}$$

where

u_o = static pore water pressure

u = excess pore water pressure

But,

$$\frac{\partial u_o}{\partial \xi} = -\gamma_w \tag{5}$$

and, therefore,

$$\frac{\partial u_w}{\partial \xi} + \gamma_w - \frac{\partial u}{\partial \xi} = 0 \tag{6}$$

21. The equation of fluid continuity is derived similarly to that for conventional Terzaghi theory except that the fluid velocity (v) must be defined as a relative velocity equal to the difference in the velocities of the fluid and solids in the soil matrix:

$$v = v_f - v_s \tag{7}$$

The quantity of water flowing into the element, which is assumed to be completely saturated, per unit area can be calculated by the expression

$$n \cdot (v_f - v_s) \cdot \gamma_w \tag{8}$$

where n = volume porosity and also assumed to be the proportion of the cross-sectional area conducting fluid. The quantity of water flowing out of the element per unit area is

$$n \cdot (v_f - v_s) \cdot \gamma_w + \frac{\partial}{\partial \xi} \left[n \cdot (v_f - v_s) \cdot \gamma_w \right] d\xi \tag{9}$$

22. The difference in the quantity of water flowing in and the quantity flowing out of the element is equal to the time rate of change of the quantity of water in the element. The quantity of water in a saturated element per unit area can be written

$$n \cdot d\xi \cdot \gamma_w \tag{10}$$

or

$$\frac{e}{1 + e} \cdot d\xi \cdot \gamma_w \tag{11}$$

since

$$n = \frac{e}{1 + e} \tag{12}$$

Thus, the time rate of change is

$$\frac{\partial}{\partial t}\left(\frac{\gamma_w d\xi}{1 + e} \cdot e\right) \tag{13}$$

23. Equating this time rate of change to inflow minus outflow results in the equation

$$\frac{\partial}{\partial \xi}\left[\frac{e}{1 + e}(v_f - v_s)\right] d\xi + \frac{\partial}{\partial t}\left(\frac{d\xi}{1 + e} \cdot e\right) = 0 \tag{14}$$

after cancellation of the constant γ_w .

24. Now $d\xi/(1 + e)$ defines the volume of solids in the differential element; and since a time-dependent element enclosing the same solid volume throughout the consolidation process has been chosen, the quantity $d\xi/(1 + e)$ defines the volume of solids for all time. Equation 14 can therefore be reduced to

$$\frac{\partial}{\partial \xi}\left[\frac{e}{1 + e}(v_f - v_s)\right] + \frac{1}{1 + e}\frac{\partial e}{\partial t} + 0 \tag{15}$$

which is the equation of fluid continuity.

25. The velocity terms in the above equation may be eliminated by application of Darcy's law which can be written in terms of coordinates as

$$n(v_f - v_s) = -\frac{k}{\gamma_w}\frac{\partial u}{\partial \xi} \tag{16}$$

26. Equation 16 substituted into equation 15 results in

$$\frac{1}{\gamma_w}\frac{\partial}{\partial \xi}\left(k\frac{\partial u}{\partial \xi}\right) - \frac{1}{1+e}\frac{\partial e}{\partial t} = 0 \tag{17}$$

where k will <u>not</u> be assumed constant with respect to depth as in conventional theory but a function of the void ratio which varies with depth in the layer.

27. Through consideration of the effective stress principle

$$\sigma = \sigma' + u_w \tag{18}$$

where σ' = the effective stress or pressure between soil grains. The excess pore pressure term of Equation 6 can be written

$$\frac{\partial u}{\partial \xi} = \gamma_w + \frac{\partial \sigma}{\partial \xi} - \frac{\partial \sigma'}{\partial \xi} \tag{19}$$

Equation 17 can then be written

$$\frac{1}{\gamma_w}\frac{\partial}{\partial \xi}\left[k\left(\gamma_w + \frac{\partial \sigma}{\partial \xi} - \frac{\partial \sigma'}{\partial \xi}\right)\right] - \frac{1}{1+e}\frac{\partial e}{\partial t} = 0 \tag{20}$$

28. The term for total stress may be eliminated from the above by substitution of the relation in Equation 3 so that

$$\frac{1}{\gamma_w} \frac{\partial}{\partial \xi} \left[k \left(\gamma_w - \frac{e\gamma_w + \gamma_s}{1 + e} - \frac{\partial \sigma'}{\partial \xi} \right) \right] - \frac{1}{1 + e} \frac{\partial e}{\partial t} = 0 \qquad (21)$$

Equation 21 is the governing equation for finite strain consolidation, but this form is very difficult to solve because of the time dependency of the coordinate system.

29. Ortenblad (1930) proposed a coordinate system uniquely suited for calculating consolidation in soft materials such as fine-grained dredged fill. These reduced coordinates are based on the volume of solids in the consolidating layer and are therefore time-independent. Transformation between the time-dependent ξ coordinate and the time-independent z coordinate is accomplished by the equation

$$dz = \frac{d\xi}{1 + e} \qquad (22)$$

30. Additionally, by utilizing the chain rule for differentiation, the relationship

$$\frac{\partial F}{\partial z} = \frac{\partial F}{\partial \xi} \frac{d\xi}{dz} \qquad (23)$$

can be written where F is any function (see Gibson, Schiffman, and Cargill (1981) for a more mathematically correct treatment of this functional relationship).

31. Applying Equations 22 and 23 enables Equation 21 to be written

$$\frac{\partial}{\partial z}\left[\frac{k}{1+e}\left(1-\frac{\gamma_s}{\gamma_w}-\frac{1}{\gamma_w}\frac{\partial\sigma'}{\partial z}\right)\right]\frac{\partial e}{\partial t}=0 \tag{24}$$

or

$$(\gamma_s-\gamma_w)\frac{\partial}{\partial z}\left(\frac{k}{1+e}\right)+\frac{\partial}{\partial z}\left[\frac{k}{\gamma_w(1+e)}\frac{\partial\sigma'}{\partial z}\right]+\frac{\partial e}{\partial t}=0 \tag{25}$$

Again, by the chain rule of differentiation, the relationship

$$\frac{\partial F}{\partial z}=\frac{dF}{de}\frac{\partial e}{\partial z} \tag{26}$$

can be written and Equation 25 thus becomes

$$(\gamma_s-\gamma_w)\frac{d}{de}\left(\frac{k}{1+e}\right)\frac{\partial e}{\partial z}+\frac{\partial}{\partial z}\left[\frac{k}{\gamma_w(1+e)}\frac{d\sigma'}{de}\frac{\partial e}{\partial z}\right]+\frac{\partial e}{\partial t}=0 \tag{27}$$

which constitutes the governing equation of one-dimensional finite strain consolidation in terms of the void ratio e and the functions $k(e)$ and $\sigma'(e)$.

32. An analytical solution to Equation 27 is not practical, but once appropriate initial and boundary conditions are specified, its solution by numerical techniques is feasible with the aid of a computer (see Cargill 1982 for the solution of typical field consolidation problems). Of course, the relationships between permeability and void ratio and effective stress and void ratio must also be specified whenever the equation is used for consolidation prediction. The use of Equation 27 to deduce soil properties from measurements during a consolidation test is also not practical without first

making some simplifying assumptions. In this report, the governing equation will be used in a numerical simulation of the LSCRS test. The basic equation of continuity, effective stress principle, and Darcy's law will be used to analyze the test for determination of soil properties.

Initial Conditions

33. Regardless of whether consolidation is being calculated or a consolidation test is being analyzed for soil properties, a knowledge of initial conditions within the soil mass or sample is required before actual performance can be related to theoretical equations. The initial condition within a freshly deposited dredged material or soil slurry sample is often conveniently described in terms of its zero effective stress void ratio e_{oo}. This is defined as the void ratio existing in a soil slurry at the instant sedimentation stops and consolidation begins.

34. For the purposes of this report, the sedimentation process is considered operative when soil particles or flocs are descending through the water medium. The consolidation process is operative when soil particles or flocs are in contact forming a continuous soil matrix and water is being squeezed from the interstices. In a column of sedimenting/consolidating soil, the void ratio of material at the interface between sedimentation and consolidation should be at the void ratio corresponding to zero effective stress. However, Imai (1981) has presented test results which indicate that this interface void ratio is dependent on the initial void ratio of the slurry. Therefore, it is essential that any test performed to measure the zero effective stress void ratio (as is the self-weight consolidation test to be

described) be with a material whose initial void ratio is comparable to what it would be when deposited in the field.

35. Imai's data also exhibited the tendency for the effective stress-void ratio curves of the same material consolidated from varying initial void ratios to converge at an effective stress in the neighborhood of the 0.001 tsf stress ordinate. It is therefore expected that consolidation testing above this stress level will yield a unique effective stress-void ratio relationship for each material and that this relationship can be extrapolated toward the appropriate zero effective stress-void ratio based on self-weight consolidation tests on material at the initially deposited in situ void ratio.

36. There are two possible initial conditions in the LSCRS test. The first is when the sample is uniformly deposited at its previously determined zero effective stress-void ratio. In this case

$$e(z,t) = e_{oo} \quad , \quad 0 \leq z \leq \ell \text{ and } t = 0 \tag{28}$$

where ℓ = the total vertical height of solids.

37. This initial condition would be difficult to duplicate in anything but relatively thin samples since it is an instantaneous condition. It would also be more difficult to choose a proper strain rate for a sample initially at its zero effective stress void ratio since it would be consolidating under its own weight at the same time attempts are being made to strain it in a device.

38. The second possible initial condition is when the sample has undergone some degree of self-weight consolidation. In this case the initial void ratio distribution must be measured at the time the test is begun. In the absence of an accurate nondestructive technique of measuring void ratio, two

identical specimens can be built and allowed to consolidate under their own weight. At the time the test is begun, one specimen is sampled throughout its depth for void ratio determination by the equation

$$e(z,t) = \frac{G_s}{S} w(z,t) \quad , \quad 0 \leq z \leq \ell \text{ and } t = 0 \tag{29}$$

where

G_s = the specific gravity of soil solids

S = the saturation of the soil (assumed = 1.0)

w = water content at sampling point

There is also other information about the materials' effective stress-void ratio and permeability-void ratio relationships which can be obtained from such a procedure and will be discussed in a later part of the report.

Boundary Conditions

39. Any statement of the boundary conditions for consolidation testing under an imposed strain rate must be in terms of the basic equations used in deriving the consolidation governing equation. Znidarcic and Schiffman (1981) presented the first statement for a constant rate of strain test based on the finite strain theory of consolidation. However, their derivation of the moving boundary conditions require considerable insight into the problem, and therefore a less intuitive derivation will be presented here.

40. As previously stated, the objective of the LSCRS device is a controlled rate of strain consolidation test. While the strain rate may be changed during a test, the change is assumed instantaneous and final

conditions from the previous strain rate are initial conditions for the new strain rate. Thus boundary conditions can be stated as if the test were at a constant rate. Potential rebound within the soil due to going to a slower strain rate will be discussed in the next part.

One permeable and one impermeable boundary

41. The key to statement of a boundary condition for the imposed strain test is correct statement of the actual velocity of the fluid relative to the solid particles at each end of the sample tested. Consider first the test where one end of the specimen is fixed and undrained while the opposite end is drained and moved at a known rate as illustrated in Figure 2.

42. At the upper moving boundary, there is a discontinuity in the vertical velocity of the fluid. Since the total volume of solids and water does not change from that of the original test specimen, the absolute velocity of the fluid above the moving boundary is zero. But as the boundary moves downward and takes solid soil particles with it, the space formerly occupied by the solids must be filled with fluid. Thus just below the moving boundary there is a net flow of water upward into these previously occupied spaces.

43. From the definition of porosity n, it is possible to relate the volume of solids in an element of soil to the volume of voids in that same element by

$$V_s = \frac{1 - n}{n} V_v \tag{30}$$

where

V_s = volume of solids in a soil element

V_v = volume of voids in a soil element

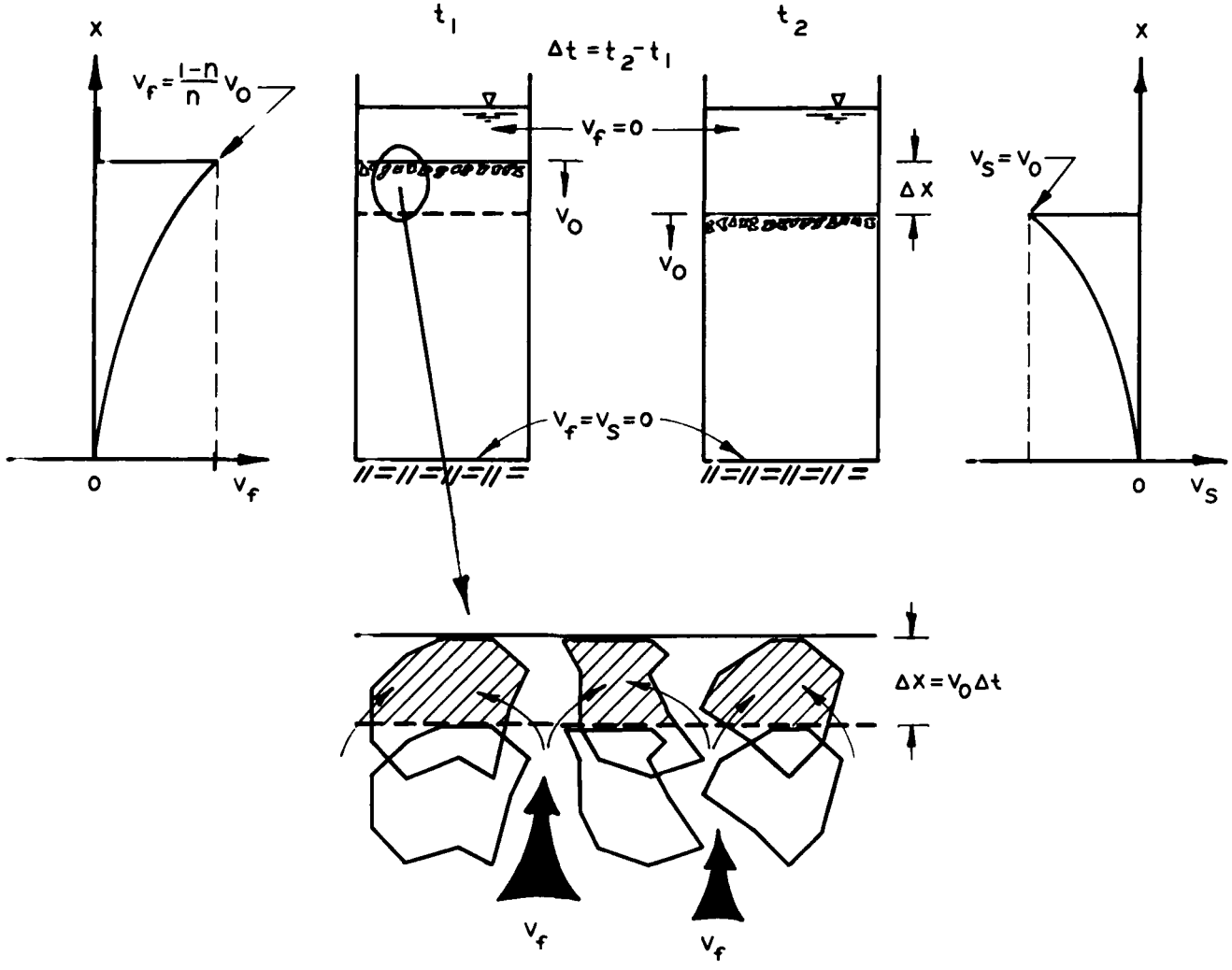

Figure 2. Boundary conditions for the singly drained consolidation test at an imposed strain rate

Now, if the boundary moves at a constant speed, over a period of time it will have traversed

$$\Delta x = v_o \, \Delta t \tag{31}$$

where

Δx = distance boundary moves

v_o = constant velocity of boundary

Δt = time interval

The volume of the voids in the element of material defined by the sample container and the incremental distance Δx is

$$V_v = n \, A \, v_o \, \Delta t \tag{32}$$

where A = cross-sectional area of container. Thus the space formerly occupied by solids can be defined by substituting Equation 32 into 30.

$$V_s = (1 - n) A \, v_o \, \Delta t \tag{33}$$

44. The velocity of fluid flowing into these spaces can be written in terms of a flow rate and area of flow or

$$v_f = Q/nA \tag{34}$$

where Q = flow rate or volume per unit time ($V_s/\Delta t$). This gives the absolute fluid velocity as

$$v_f = \frac{(1 - n)A\, v_o\, \Delta t}{\Delta t} \cdot \frac{1}{n\, A} = \frac{1 - n}{n} v_o \tag{35}$$

which is in an upward direction.

45. Since the solids at the boundary are moving downward at the same velocity as the boundary, the absolute velocity of solids is

$$v_s = v_o \tag{36}$$

Considering the directions of the absolute velocities, the relative velocity between fluid and solids at the boundary can be written as the vectoral sum of Equations 35 and 36. Thus

$$v_f - v_s = \left(\frac{1 - n}{n} + 1\right) v_o = \frac{1}{n} v_o \tag{37}$$

46. Substituting Equation 37 into 16 results in

$$\frac{\partial u}{\partial \xi} = - \frac{\gamma_w}{k} v_o \tag{38}$$

which, through Equations 19 and 3, can be written

$$\frac{\partial \sigma'}{\partial \xi} = \gamma_w \left(\frac{v_o}{k} + 1\right) - \frac{e\gamma_w + \gamma_s}{1 + e} \tag{39}$$

Through the coordinate transform of Equations 22 and 23, Equation 39 becomes

$$\frac{\partial \sigma'}{\partial z} = (\gamma_w - \gamma_s) + (1 + e) \frac{\gamma_w v_o}{k} \tag{40}$$

and, by Equation 26, becomes

$$\frac{\partial e}{\partial z} = \frac{de}{\partial \sigma'} \left[(\gamma_w - \gamma_s) + (1 + e) \frac{\gamma_w v_o}{k} \right] \tag{41}$$

which is the boundary condition for the moving permeable boundary when the opposite boundary is stationary and impermeable.

47. At the stationary impermeable boundary

$$v_f = v_s = 0 \tag{42}$$

and it can be readily shown that the boundary condition becomes

$$\frac{\partial e}{\partial z} = \frac{de}{\partial \sigma'} (\gamma_w - \gamma_s) \tag{43}$$

Two permeable boundaries

48. The controlled rate of strain test where both the moving and stationary boundaries are permeable is illustrated in Figure 3. Again there is a discontinuity in the fluid velocity at the moving boundary and now there is also a fluid velocity at the bottom of the specimen due to the permeable boundary.

49. The volume of fluid moving out of the specimen in a specified time interval is given by Equation 33 as before. However, now the fluid comes from both ends. A simple continuity equation can be written

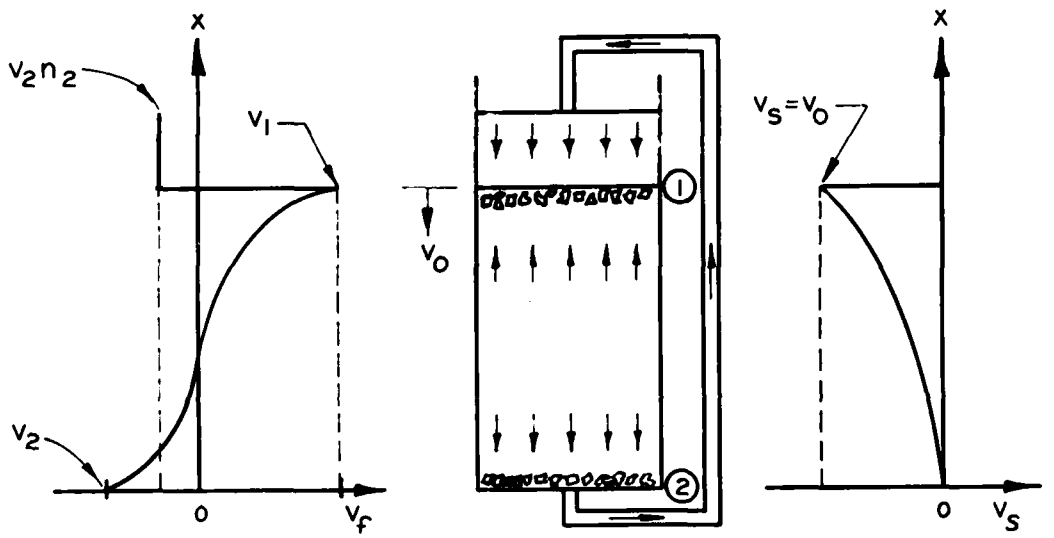

Figure 3. Boundary conditions for the doubly drained consolidation test at an imposed strain rate

$$Q_1 + Q_2 = Q = \frac{V_s}{\Delta t} = (1 - n_1)A\, v_o \tag{44}$$

where

Q_1 = flow rate at top

Q_2 = flow rate at bottom

n_1 = porosity at top

and other terms are as before. In the following subscripts 1 and 2 will indicate top and bottom of the specimen, respectively.

50. Now, in terms of actual fluid velocities,

$$Q_1 = v_1\, n_1\, A \tag{45}$$

and

$$Q_2 = v_2\, n_2\, A \tag{46}$$

Therefore,

$$v_1\, n_1 + v_2\, n_2 = (1 - n_1)v_o \tag{47a}$$

or

$$n_1(v_1 + v_o) + n_2\, v_2 = v_o \tag{47b}$$

51. The relative velocities between fluid and solids at the boundaries can now be written as their vectoral sums. At the top boundary

$$(v_f - v_s)_1 = v_1 + v_o \tag{48}$$

and at the bottom boundary

$$(v_f - v_s)_2 = v_2 \tag{49}$$

Substituting Equations 48 and 49 into 16 results in expressions for the apparent velocity, $\bar{v}$, at top and bottom

$$n_1 (v_1 + v_o) = \left(- \frac{k}{\gamma_w} \frac{\partial u}{\partial \xi} \right)_1 = \bar{v}_1 \tag{50}$$

and

$$n_2 (v_2) = \left(- \frac{k}{\gamma_w} \frac{\partial u}{\partial \xi} \right)_2 = \bar{v}_2 \tag{51}$$

where

$$\bar{v}_1 + \bar{v}_2 = v_o \tag{52}$$

by Equation 47b.

52. At this point it can be seen that the boundary conditions for two permeable boundaries are indeterminant. There are too many unknowns for the available equations. If either $\bar{v}_1$ or $\bar{v}_2$ were measured during a test, the other could be calculated. If the typical small strain theory assumptions of

no self-weight and uniform void ratios were made, the ratio $\bar{v}_1/\bar{v}_2 = 1.0$ and the problem is determinant, but may not be very realistic for very soft soils.

53. In the numerical solution of the moving boundary problem, an assumption is made (such as $\bar{v}_2 = 0$ and $\bar{v}_1 = v_o$) for the first time step, and a solution is obtained. Then, by assuming that the ratio of apparent veolocities is equal to the ratio of fluid lost through the boundaries or void ratio change

$$\frac{\bar{v}_1}{\bar{v}_2} = \frac{\Delta\bar{e}_1}{\Delta\bar{e}_2} \tag{53}$$

where $\Delta\bar{e}$ = average void ratio change during last time interval, adjustments can be made to the originally assumed values of $\bar{v}_1$ and $\bar{v}_2$. Iterating in this manner will enable an accurate description of the boundary conditions.

PART III: COMPUTER SIMULATION OF TEST

54. The LSCRS is a unique prototype apparatus for which there is no precedent to base a design. Therefore, design of equipment and procedures were based on theoretical computations. With the aid of the previously stated finite strain theory of consolidation and appropriate moving boundary conditions, various theoretical aspects of the test could be studied to determine the combinations of test conditions which offered the best chance of accurate measurement of soil consolidation properties. The principal variables considered were original sample thickness, initial conditions, boundary drainage, and strain rate. The soil modeled was considered typical of soft dredged fill material. Its effective stress-void ratio and permeability-void ratio relationships are shown in Figure 4. A specific gravity of solids of 2.70 and unit weight of water of 62.4 pcf were assumed. The zero effective stress void ratio of the material is 12.0.

The Computer Program CRST

55. Simulation of the controlled rate of strain test was accomplished with the Computer Program CRST. The program solves the finite strain consolidation governing equation by an explicit finite difference scheme as previously described by Cargill (1982). The program computes void ratios, total and effective stresses, pore water pressures, and degree of consolidation for any homogenous soft clay test specimen whose upper boundary is drained and moved at a specified rate which may change during the test, and whose bottom boundary may be drained or undrained but remains stationary. The void

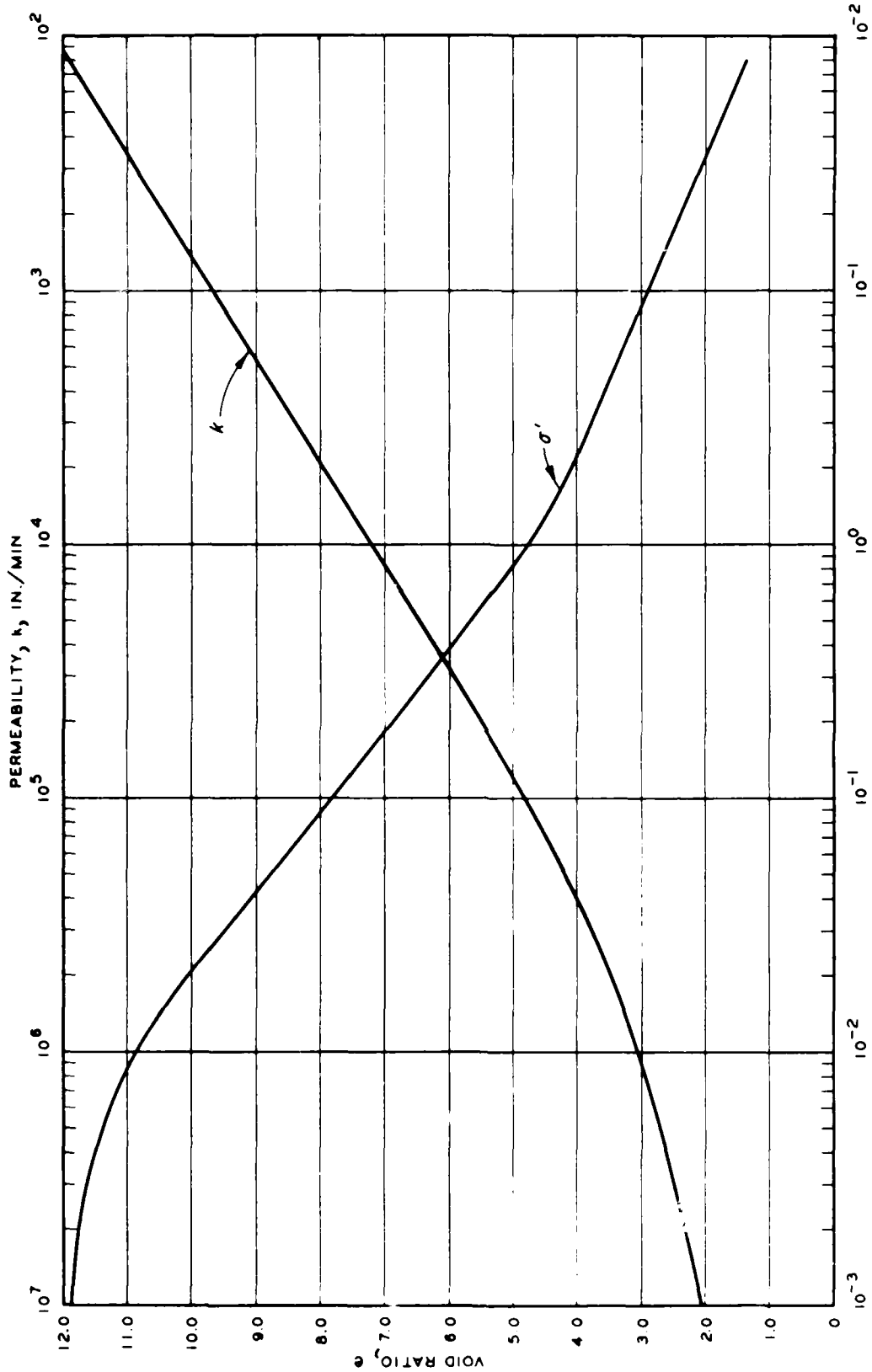

Figure 4. Void ratio-effective stress and void ratio-permeability relationships for a typical soft dredged material

ratio-effective stress and permeability relationships are input as point values and thus may assume any form.

56. A detailed user's guide describing the program CRST is contained in Appendix A and a complete program listing is reproduced in Appendix B. The program is documented in this report not only as the source of the parametric study of test variables but also for ready reference for possible future studies of consolidation testing.

Effects of Test Variables

57. As previously stated, the principal variables to be considered in this parametric study by computer simulation are original sample thickness, initial conditions, boundary drainage, and strain rates. For simplicity, the variable effects will first be compared for tests at constant strain rates to isolate the test conditions conducive to more accurate measurement of consolidation properties. Then the effects of changing the strain rate during a test will be studied with the hope of identifying the optimum test procedure.

58. Before any comparisons can be made, the basis for such comparisons must be stated. Four quantities have been chosen as indicators of test quality. The first is maximum excess pore pressure. It is felt that extraordinarily high pore pressures may lead to abnormal material behavior due to hydraulic fracturing, relative transport of solids, or other related phenomena. Therefore, the ideal test should be characterized by a steady build-up of excess pore pressure to accurately recordable levels followed by a leveling-off at moderate levels. Next is the ratio of maximum excess pore water pressure to the effective stress at the same location in the sample. Since effective stress and pore pressures are separately measured in a test,

the accuracy of subsequent calculations should be enhanced if the magnitude of the measurements is similar or their ratio close to 1.0. This requirement will also be helpful in preventing phenomena such as hydraulic fracturing. The third quantity is the ratio of minimum to maximum void ratios. The closer this quantity is to 1.0, the more uniform the sample and the more accurate are consolidation properties deduced from measured data which will tend to be averaged somewhat over the sample. The final indicator is percent consolidation during the test. The better test should exhibit an increasing or relatively high steady percent consolidation. A rapidly decreasing percent consolidation could be associated with instability and lead to abnormal test results.

Constant strain rates

59. A series of 11 simulations was accomplished as detailed in Table 1. In the table, "consolidated" means that the slurry was allowed to consolidate under its own self-weight before being strained, and "unconsolidated" means that the slurry was strained beginning at the uniform zero effective stress-void ratio. The original sample thickness is measured at the zero effective stress-void ratio. The actual sample height at the start of the test is also given in parenthesis for consolidated specimens.

60. Maximum excess pore pressures for times during each of the tests are plotted in Figure 5. As can be seen, none exhibit the ideal characteristic of a steady increase followed by a leveling off. This figure verified the fact that all constant rate of strain tests will eventually lead to infinitely large pore pressures. A strain rate must be chosen so as to delay this exponential ascension of pore pressure until after sufficient data have been collected to define the materials properties in the void ratio range of interest.

Table 1

Matrix of Computer Simulated Test Conditions at Constant Strain Rates

Simulated Test No.	Original Sample Thickness* in.	Boundary Drainage		Boundary Velocity in./min	Initial Conditions	
		Top	Bottom		Consolidated	Unconsolidated
1	6.0 (5.34)	X		1.042×10^{-3}	X	
2	6.0	X		1.042×10^{-3}		X
3	6.0 (5.34)	X	X	1.042×10^{-3}	X	
4	6.0	X	X	1.042×10^{-3}		X
5	9.0 (7.70)	X		1.562×10^{-3}	X	
6	9.0 (7.70)	X		1.042×10^{-3}	X	
7	4.0 (3.68)	X		6.944×10^{-4}	X	
8	4.0 (3.68)	X	X	1.042×10^{-3}	X	
9	6.0 (5.34)	X		6.25×10^{-4}	X	
10	6.0 (5.34)	X		3.123×10^{-3}	X	
11	9.0 (7.70)	X	X	1.042×10^{-3}	X	

* Numbers in parentheses indicate thickness of sample after consolidation under its own weight.

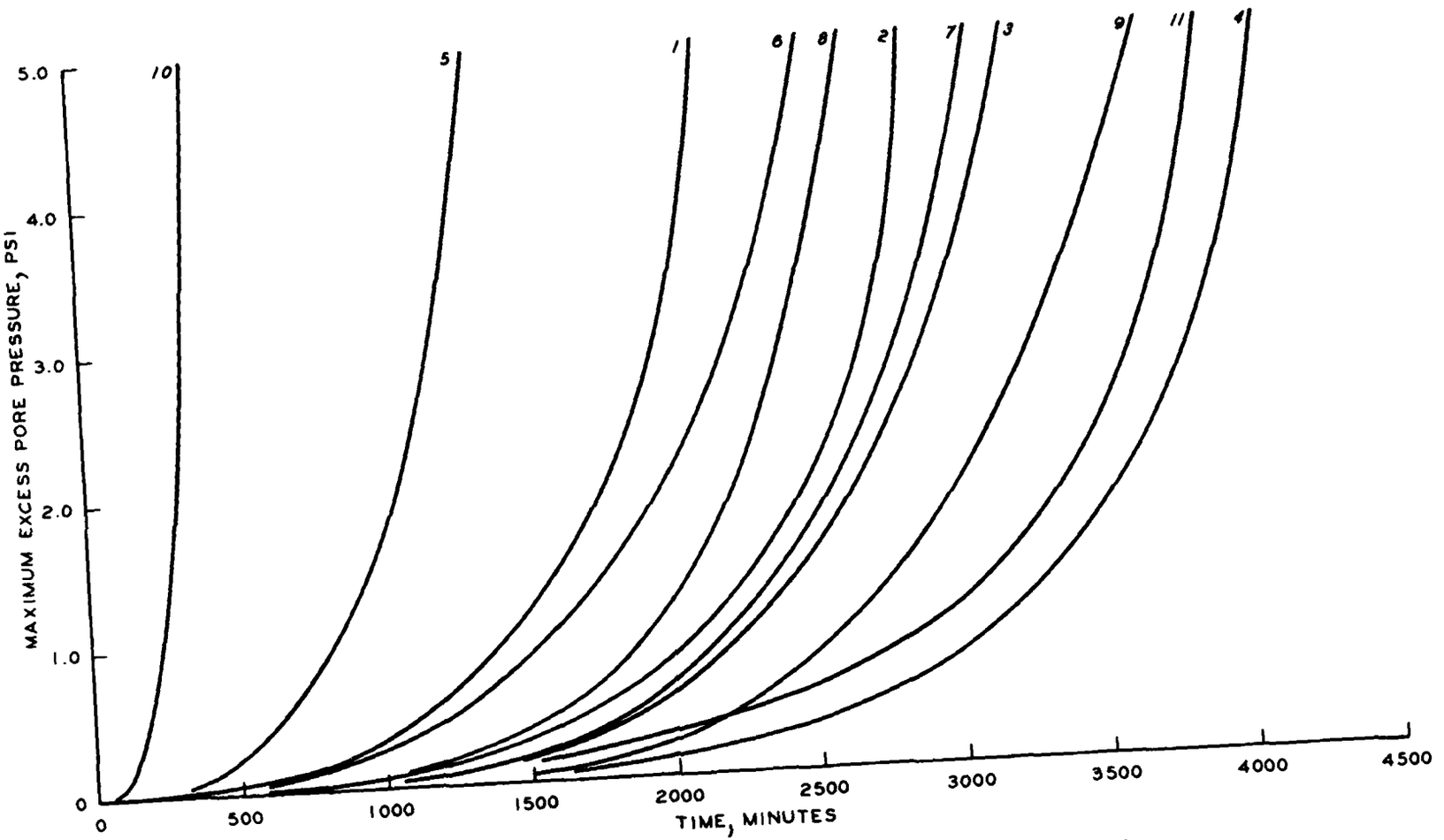

Figure 5. Excess pore pressure increase during constant strain rate consolidation tests

This suggests that the farther the curve is to the right on the figure and the flatter its slope, the better it suits the requirement concerning maximum excess pore pressures. A comparison of all tests leads to the conclusion that test numbers 5 and 10 can be judged the most unacceptable at this point.

61. Table 1 shows that tests 5 and 10 were conducted at the highest strain rates. It may be concluded that constant relatively high strain rates will cause pore pressures to increase very rapidly and thus possibly invalidate later parts of the test. However, the slower rates of tests 4, 9, and 11, while considerably delaying the rapid rise in pore pressure, go along for some time at pore pressures so small that it may be difficult to accurately record them. Thus none of these constant rate tests can be judged truely acceptable based on the criteria set for maximum excess pore pressure.

62. The ratio of maximum excess pore pressure to the corresponding effective stress at the same point in the specimen is plotted in Figure 6 for all simulated tests. As shown in the figure, tests 1, 2, 5, 6, and 10 are the least acceptable because of their ratio's very rapid rise. Tests 4 and 8 exhibit the more desirable tendency of leveling off at relatively steady ratios near unity. These comparisons indicate that drainage at both ends of the specimen promote more stable ratios between maximum excess pore pressure and corresponding effective stress.

63. Figure 7 shows the ratios of minimum to maximum void ratio for the simulated test series. Again, reference to Table 1 verifies that the better behaved tests (numbers 3, 4, 7, 8, 9, and 11 in this case) are either at the slower strain rates or doubly drained. A comparison of the tests on the basis of developed percent consolidation over the period of testing is given in Figure 8 which additionally supports previous conclusions of relative test rankings.

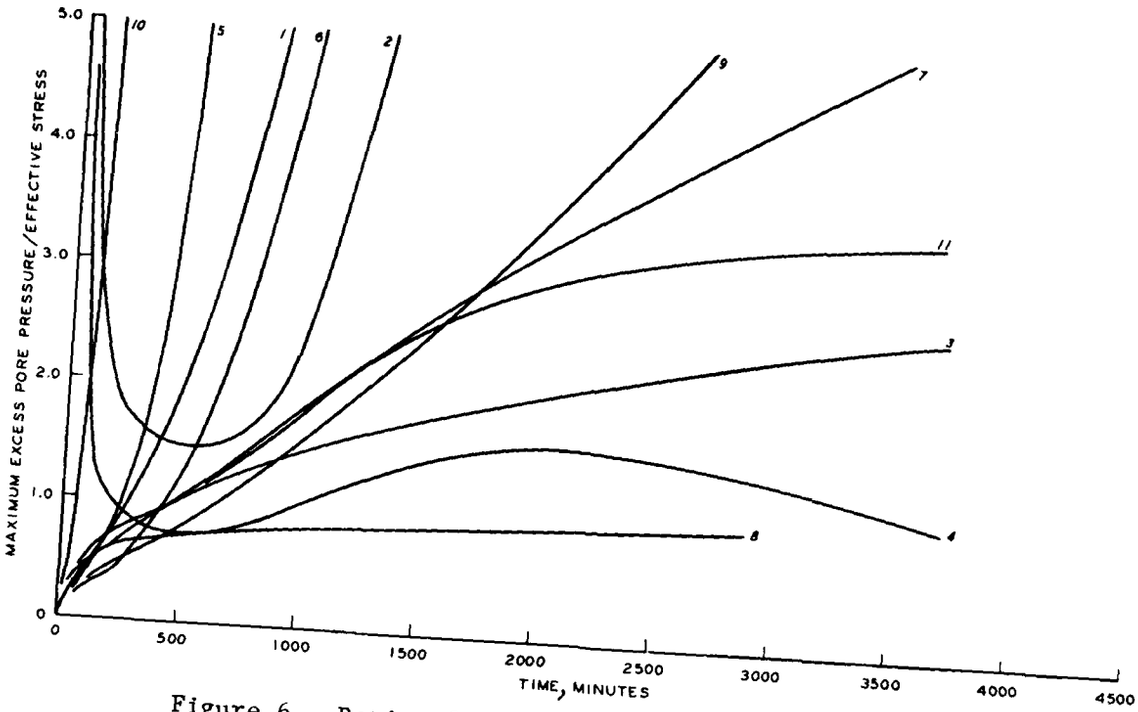

Figure 6. Ratio of maximum excess pore pressure to corresponding effective stress during constant strain rate consolidation tests

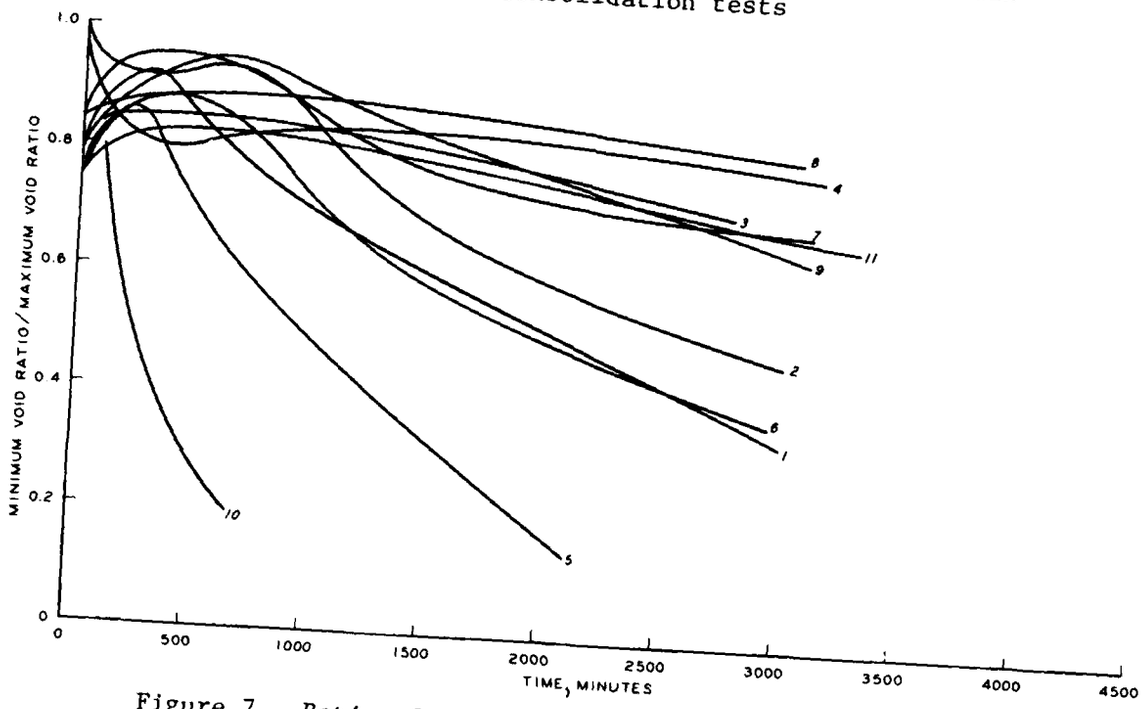

Figure 7. Ratio of minimum to maximum void ratio during constant strain rate consolidation tests

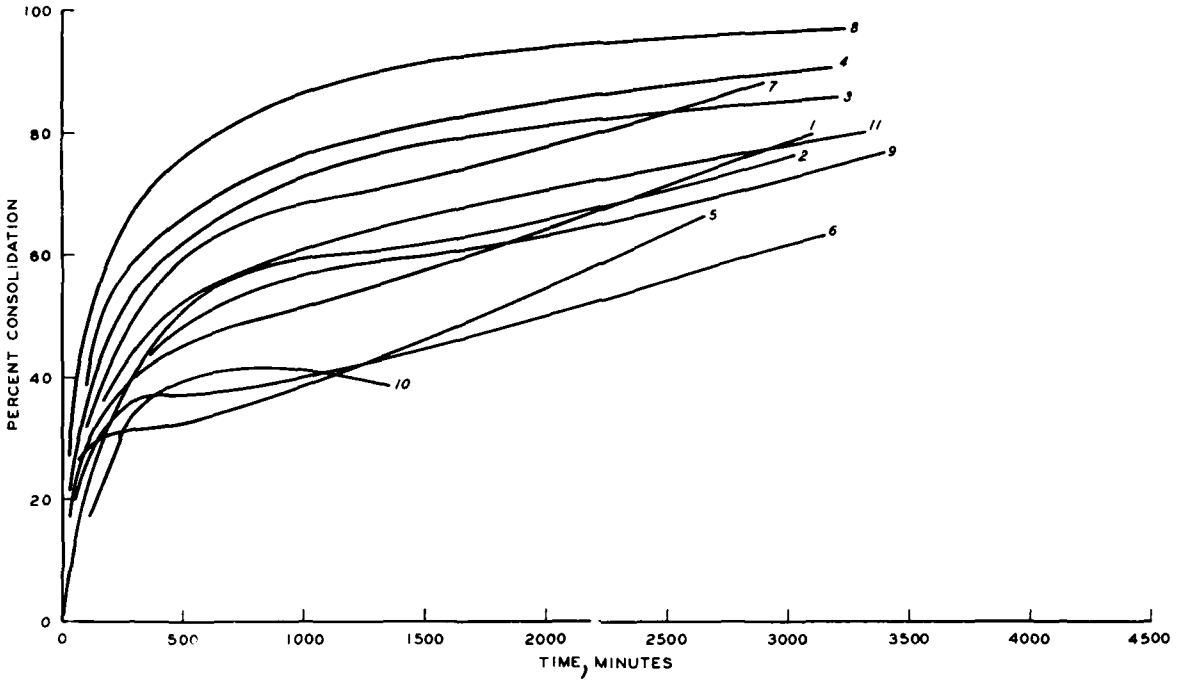

Figure 8. Percentage consolidation developed during constant strain rate consolidation tests

64. An evaluation of the importance of sample size (as determined by its original thickness) can be made by contrasting simulated tests 3, 8, and 11 which are identical in all respects except for specimen thickness. On the basis of maximum excess pore pressure, it would appear that the thicker sample offers the better chance of delaying extreme pore pressure buildup, but if these results were plotted against percent strain in the sample instead of absolute time there would be practically no difference in the curves of pore pressure rise. Thus the other factors should be given more weight in assigning relative merit of sample size. From Figures 6, 7, and 8, it is apparent that the tests should be ranked 8, 3, and 11 based on the response criterion adopted by this project. Therefore the thinner the specimen, the better are its testing attributes. While the model proposed here ignores device side friction, the thinner specimen will also make that source of error smaller.

65. It should be noted here that even though the computer simulations point toward a relatively thin sample, the sample thickness chosen for actual soil testing will be dictated by required data measurements during the test. For example, the test analysis procedure to be addressed in a later part requires measurement of the pore pressure distribution throughout the sample. Thin samples are not conducive to accurate pore pressure distribution measurements and, in fact, may also promote other test abnormalities such as drainage shortcircuiting along the side boundary. A relatively thick sample is then more advantageous if it can be given the attributes of the thin sample. This may be possible by varying the strain rate during a test.

66. The effects of sample initial conditions on test results can be seen by comparing tests 1 with 2 and 3 with 4. In all cases it would appear that the unconsolidated sample performs better in terms of the desirable

response attributes adopted than the consolidated sample. However, the disadvantages associated with testing an unconsolidated sample may outweigh the advantages shown in the figures. The greatest disadvantage is the unknown impact of the material's self-weight consolidation while it is being externally strained. It is therefore considered more reliable to test a sample after it is effectively consolidated under its own weight or at an initial uniform void ratio somewhat less than its zero effective stress void ratio.

Variable strain rates

67. The effects of changing the strain rate during a test were studied by simulation of the sample deformation histories shown in Figure 9. The three additional tests will be compared with the former test number 3 which is also illustrated in the figure. The additional test simulations were for a consolidated, doubly drained sample whose unconsolidated height was 6.0 in. Material properties conform to those shown in Figure 4 and as previously given.

68. Table 2 lists the various strain rates used during each test. These rates were chosen to give the same ultimate sample deformation but to do so by different paths. It should be noted that rates selected for the later tests were influenced by results from the previous tests. The "Percent Change" column of Table 2 represents the difference in strain rates divided by the previous strain rate.

69. Figures 10, 11, and 12 illustrate the impact of a changing strain rate on the quantities previously considered for constant strain rates. In Figure 10, it can be seen that starting with a relatively fast strain rate quickly produces easily measurable excess pore pressures, and successively decreasing the rate keeps these pressures from mimicking the rapid ascension of test number 3. From Figure 10 it would appear that test 14 gives the least

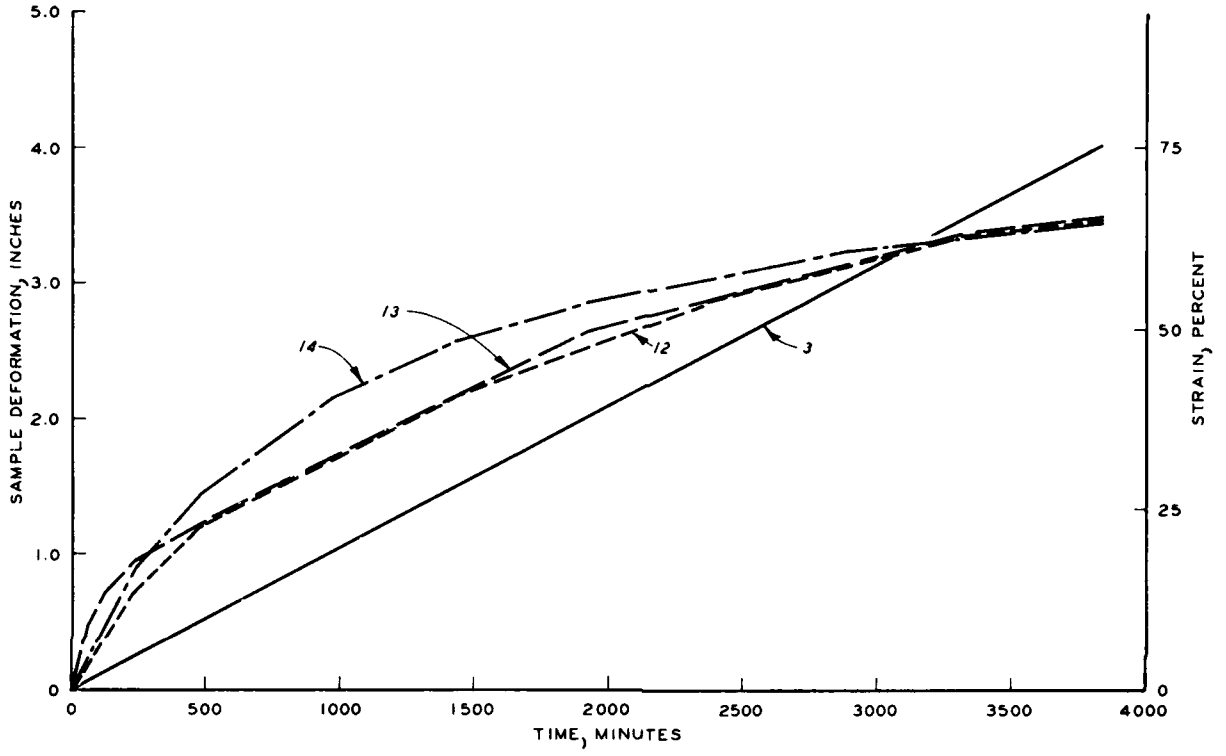

Figure 9. Sample deformation histories during variable strain rate consolidation tests

Table 2

Computer Simulated Tests at Variable Strain Rates

Simulated Test* No.	Time min	Boundary Velocity in./min	Percent Change
12	0 - 240	3.0×10^{-3}	33
	240 - 480	2.0×10^{-3}	50
	480 - 1440	1.0×10^{-3}	25
	1440 - 2400	7.5×10^{-4}	33
	2400 - 3360	5.0×10^{-4}	50
	3360 - 3840	2.5×10^{-4}	50
13	0 - 60	8.0×10^{-3}	50
	60 - 120	4.0×10^{-3}	50
	120 - 240	2.0×10^{-3}	50
	240 - 1920	1.0×10^{-3}	50
	1920 - 3360	5.0×10^{-4}	50
	3360 - 3840	2.5×10^{-4}	
14	0 - 120	4.0×10^{-3}	12
	120 - 240	3.5×10^{-3}	36
	240 - 480	2.25×10^{-3}	35
	480 - 960	1.46×10^{-3}	37
	960 - 1440	9.2×10^{-4}	37
	1440 - 1920	5.8×10^{-4}	34
	1920 - 2880	3.8×10^{-4}	34
	2880 - 3840	2.5×10^{-4}	

* All tests in this table are doubly drained samples with initial height of 6 in.

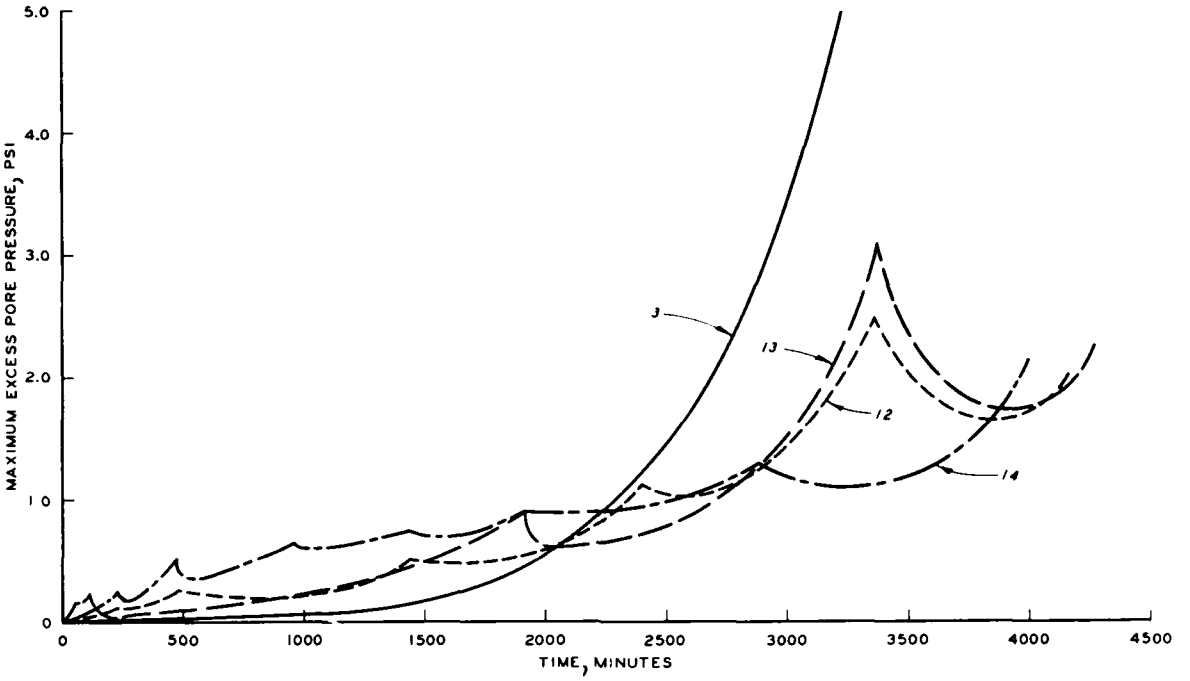

Figure 10. Excess pore pressure increase during variable strain rate consolidation tests

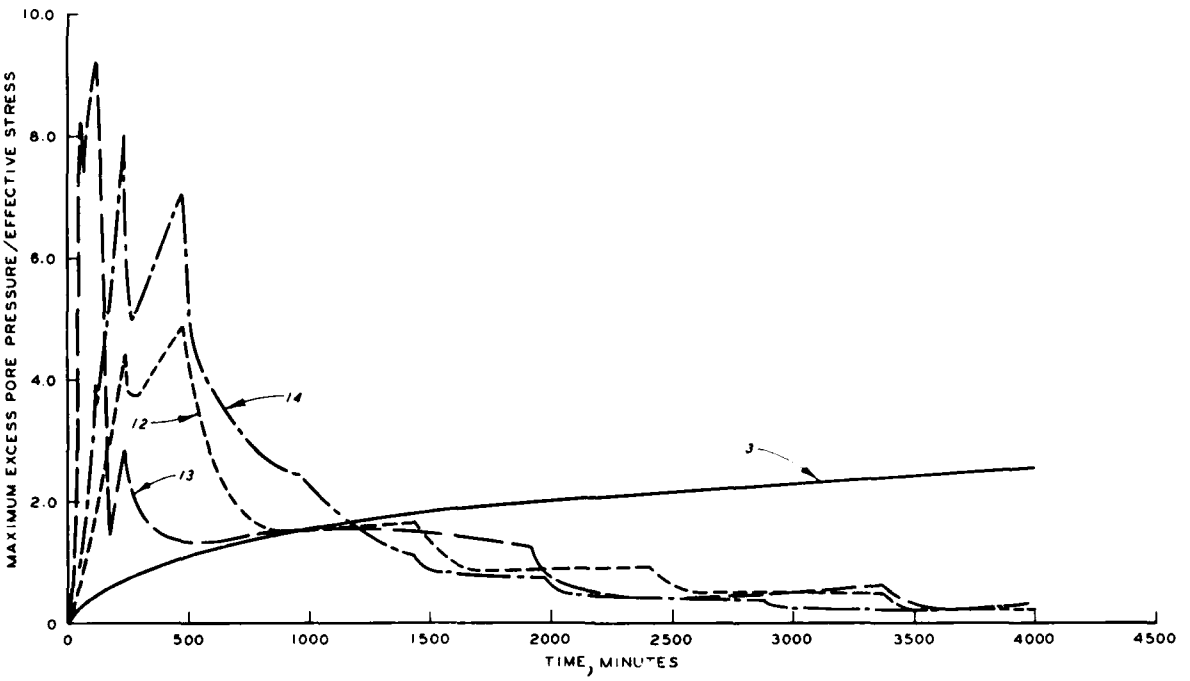

Figure 11. Ratio of maximum excess pore pressure to corresponding effective stress during variable strain rate consolidation tests

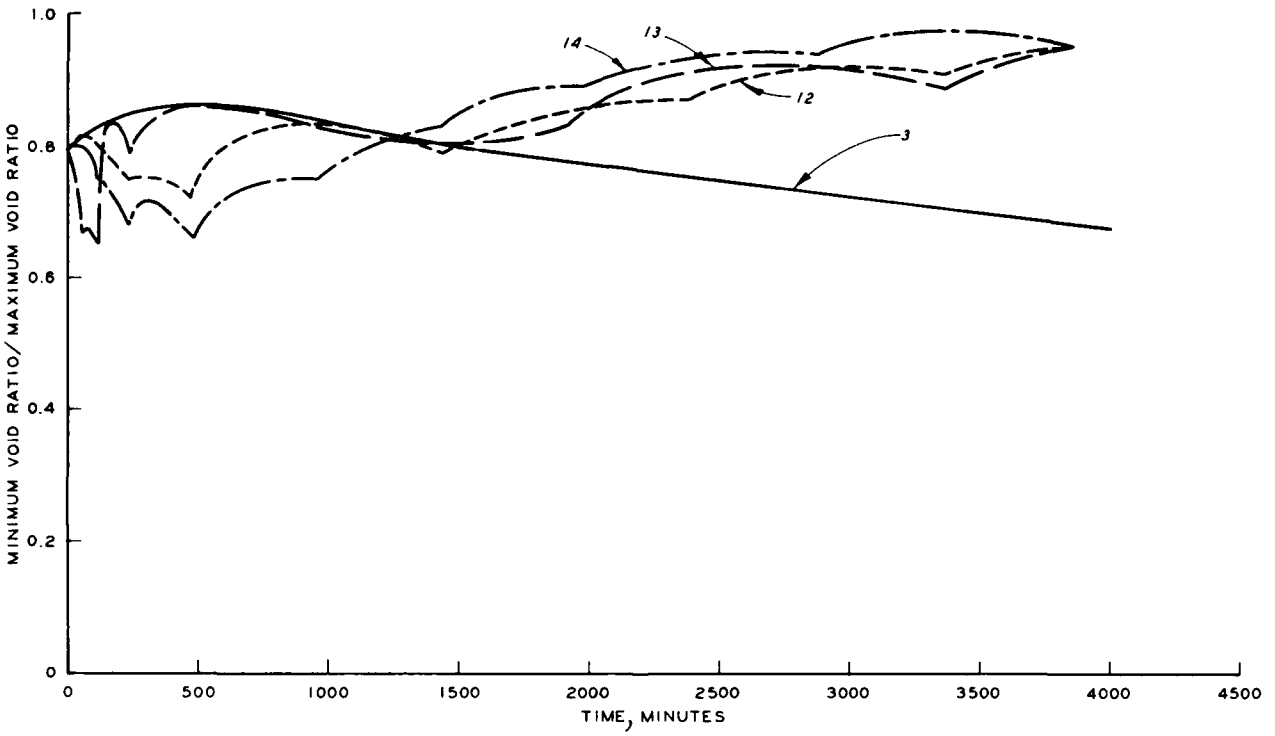

Figure 12. Ratio of minimum to maximum void ratio during variable strain rate consolidation tests

erratic or more steady rise in excess pore pressure and would be preferred above tests 12 and 13. This suggests that the smoother the transition between strain rates, the better the results of the test. Figures 11 and 12 show relatively similar and preferable characteristics after the early erratic portions of each test. In these early erratic portions it is apparent that tests at slower rates are least erratic and therefore better suited for adoption into a testing procedure.

70. Thus far, it appears that all previously identified shortcomings of the constant rate of strain test can be rectified through a controlled rate of strain test by merely decreasing the rate of sample deformation whenever the maximum excess pore pressure begins to rapidly rise. However, there is another aspect of slowing the strain rate during a test which could invalidate the results since a soil's compressibility is dependent not only on its void ratio but also on its loading history. Figure 13 shows the development of effective stress at the bottom drained boundary during the course of the variable strain rate tests as compared to the constant strain rate test. As shown, at most points of rate reduction there is a momentary decrease in effective stress and the curves are very similar to the maximum excess pore pressure curves.

71. Any reduction in effective stress as calculated by the Computer Program CRST is a direct result of an increase in void ratio calculated by the program. Thus where effective stresses decrease, the material is undergoing rebound. In CRST there is a unique effective stress associated with each void ratio, whereas in an actual material the void ratio associated with a particular effective stress depends on whether the material has been loaded monotonically or is rebounding. Even though the simulated test may not correctly model an actual material quantitatively, it can and does represent general

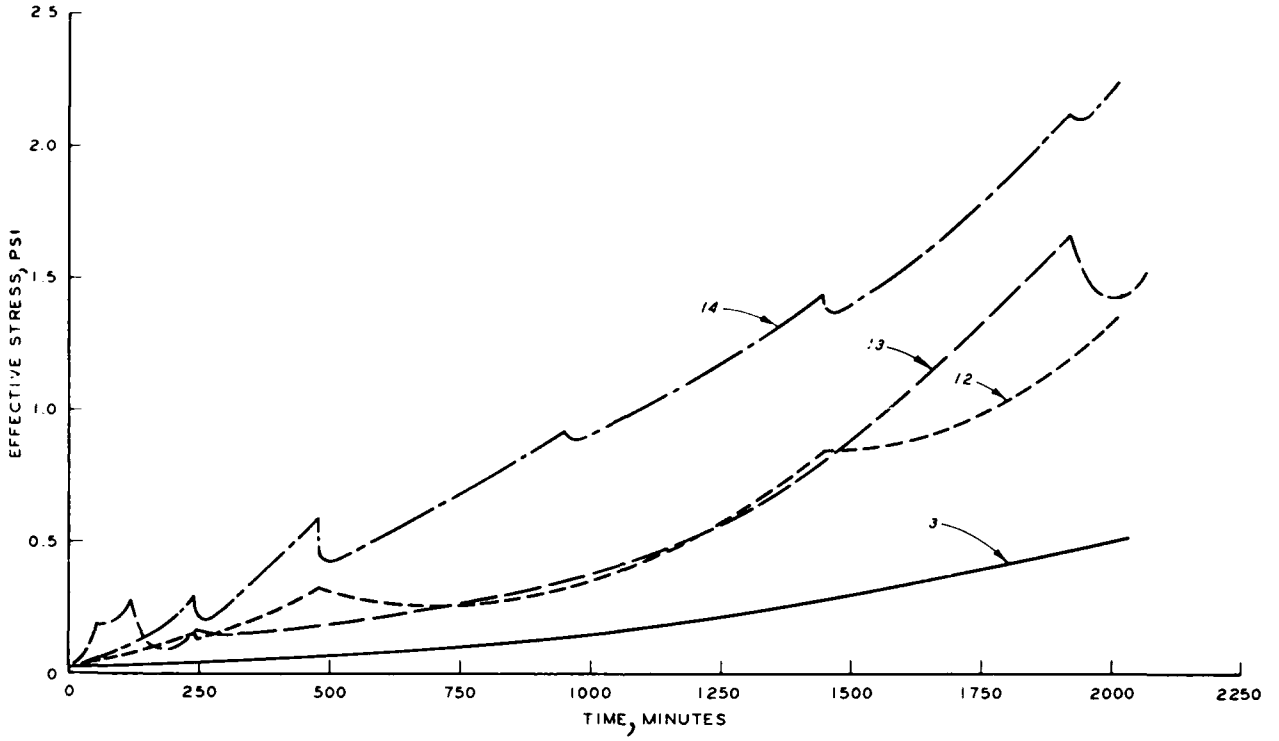

Figure 13. Effective stress increase at drained boundary for variable strain rate consolidation tests and constant strain rate test

material behavior. Therefore it is imperative that during an actual soil test in the LSCRS device, effective stresses must be closely monitored so that strain rates are adjusted without reducing them.

The Idealized Test

72. Based on the above-described experience with simulated test results, it should now be possible to specify an appropriate series of strain rates which will result in a monotonic sample loading while also preserving the other desirable test attributes. A portion of such a test was, in fact, simulated by CRST and the effective stress plot indicated by the simulation is shown in Figure 14 where strain rates and percent change in strain rates are also noted. The key to successful large strain, controlled rate of strain tests appears to be in making several small rate changes as opposed to one larger change or in maintaining the percentage change at 10-15 percent or less. The 10-15 percent is probably material dependent and in actual soil tests, the effective stress should be closely monitored as stated previously.

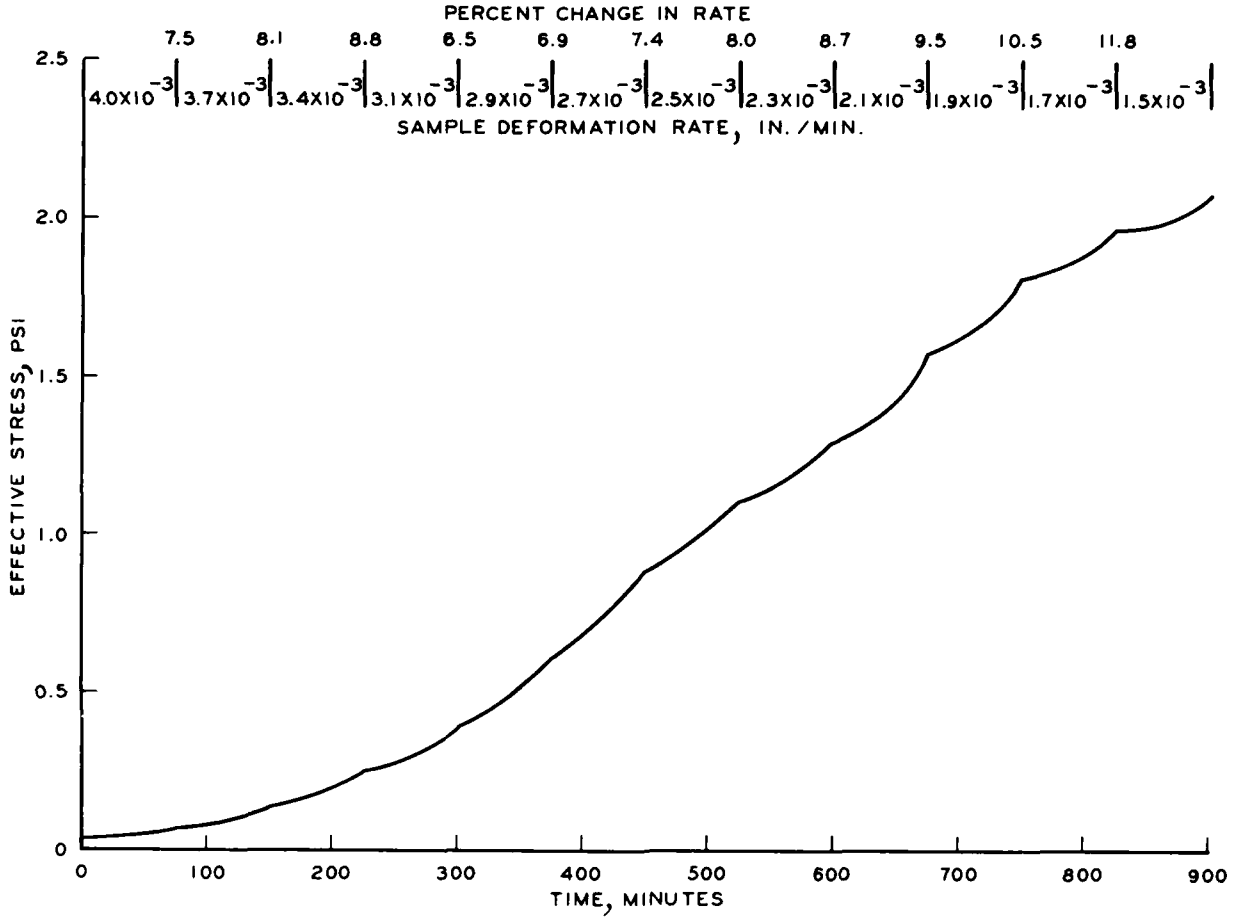

Figure 14. Effective stress increase at drained boundary for idealized variable strain rate test

PART IV: THE LSCRS TEST DEVICE

73. In this part, the physical equipment comprising the LSCRS test device will be described. Principal topics will include the test chamber auxiliary equipment to include the loading bellofrom and equipment layout. An auxiliary device for determination of initial test conditions is also covered.

74. The objective of the test is to track changes in the stress state of the material as it undergoes an imposed and controlled rate of deformation. The equipment is designed to accomplish this objective in as straightforward a manner as possible. Deformation measurements are made with dial gages, stress measurements with load cells isolated from device friction, and pore pressure measurements with differential transducers. These measurements form the basis for deducing the material's consolidation properties and will be covered in later sections.

Test Chamber

75. The principal equipment item of the LSCRS test device is the chamber shown in Figure 15. All metal parts are machined from stainless steel and the fittings are brass to avoid corrosion problems from salt water samples tested. The test chamber is constructed to hold a cylindrical sample of soft, fine-grained material 6 in. in diameter and initially 9 in. high. The piston loading rod is configured to allow 6.5 in. of sample deformation. A new rod allowing more deformation could easily be substituted for testing thinner samples.

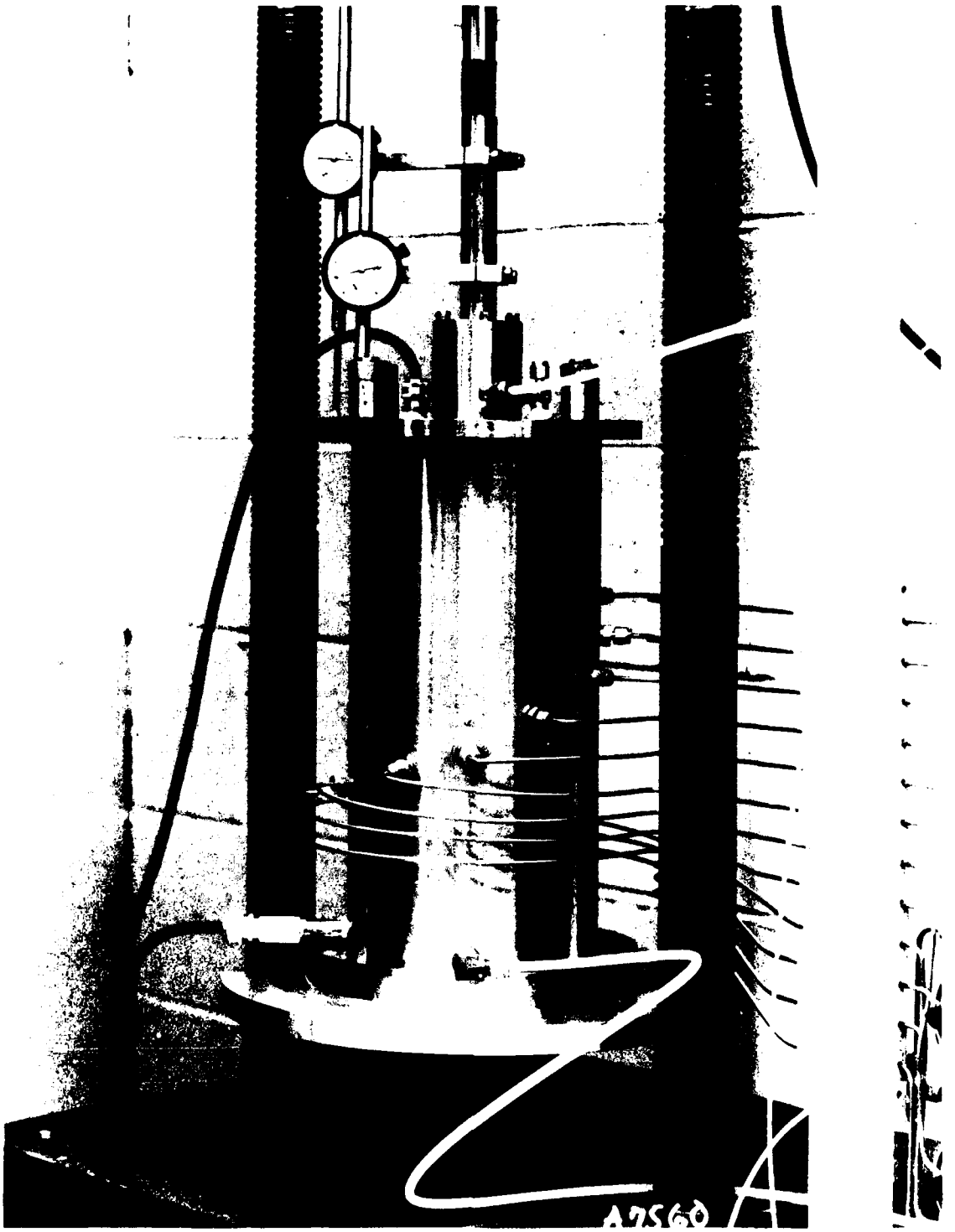

Figure 15. The LSCRS test chamber

76. Components of the test chamber are shown in the exploded view of Figure 16. The material sample is situated between the top and bottom stainless steel porous stones. The chamber is sealed with "O" rings top and bottom as are the ball bushing housing and the pressure port fittings. Water ports at the top and bottom of the chamber make it possible to conduct tests with either the top boundary drained or both boundaries drained. Load cell cables enter through fluid-tight connectors.

77. Load cells are mounted inside the chamber to eliminate the inclusion of frictional resistance due to pressure seals and piston movement in load measurements. Of course, side wall friction has not been eliminated. Once the bottom load cell has been zeroed to account for the buoyant weight of the bottom stone, the only force it feels comes from the material's self-weight and what is added by the external force applied to the loading piston. The top load cell is attached to the loading piston and moves with it in such a manner that it only feels force from the resistance of the soil to deformation. The top stone is hung from four bolts through the piston so that it is free to move upward into contact with the upper load cell. Therefore, the total load exerted on the top of the material sample will equal the buoyant weight of the stone and hanger bolts plus whatever is registered by the load cell.

78. The tight fit of the loading piston "O" rings supports the weight of the piston, rod, load cell, and stone so that it will move only with application of an external force. This insures positive control of the rate of sample deformation and eliminates the need to account for any extraneous surcharges on the sample except for the buoyant weight of top stone and hanger. The rate of application of this surcharge can be interpolated from measured loading rates.

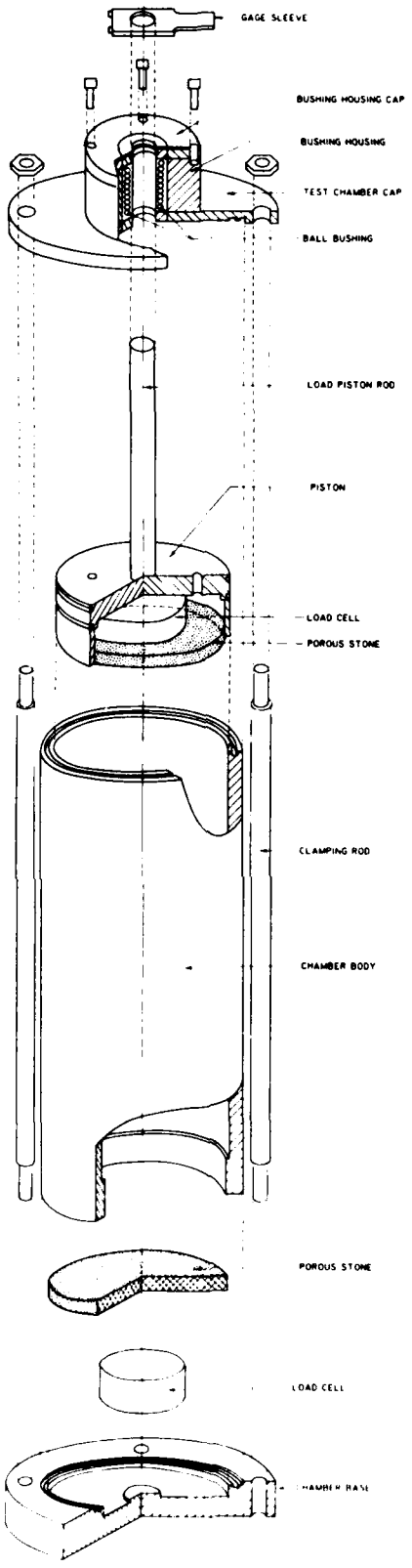

Figure 16. Exploded view of the LSCRS test chamber

79. There are 12 peripheral pore pressure measurement ports spaced 30 deg apart around the circumference of the test chamber. The ports have a 1/8-in.-diam stainless steel porous filter set on the interior side of the chamber wall. They are placed spiraling around the chamber rather than in a vertical line to reduce the tendency for drainage short circuits between the ports and hopefully provide a good average vertical pore pressure distribution measurement. The lower six ports are spaced vertically every 1/2 in. rather than the 1-in. vertical spacing of the upper six ports to provide greater detail during the later stages of material sample compression.

80. A layout of the test chamber and components is shown in Figure 17.

Auxiliary Equipment

81. The main part of the LSCRS loading/deformation system is a converted diaphragm air cylinder mounted on a loading frame as shown in Figure 18. Instead of air, silicon oil is forced behind the cylinder's diaphragm at a known rate which, in turn, causes the cylinder's ram to move at a rate proportional to the oil flow rate. The principle of operation is illustrated in Figure 19. The quantity of oil flowing through the micrometer needle valve is governed by the valve setting and the drop in pressure across the valve. The relay is a spring biased regulator which supplies air pressure totalling the signal pressure plus a preset differential amount. This relay is used for maintaining a constant pressure difference across the valve and thus a steady flow rate through the valve. A calibration chart relating ram movement rates with valve setting and pressure drop across the valve was developed for the system and is shown in Figure 20.

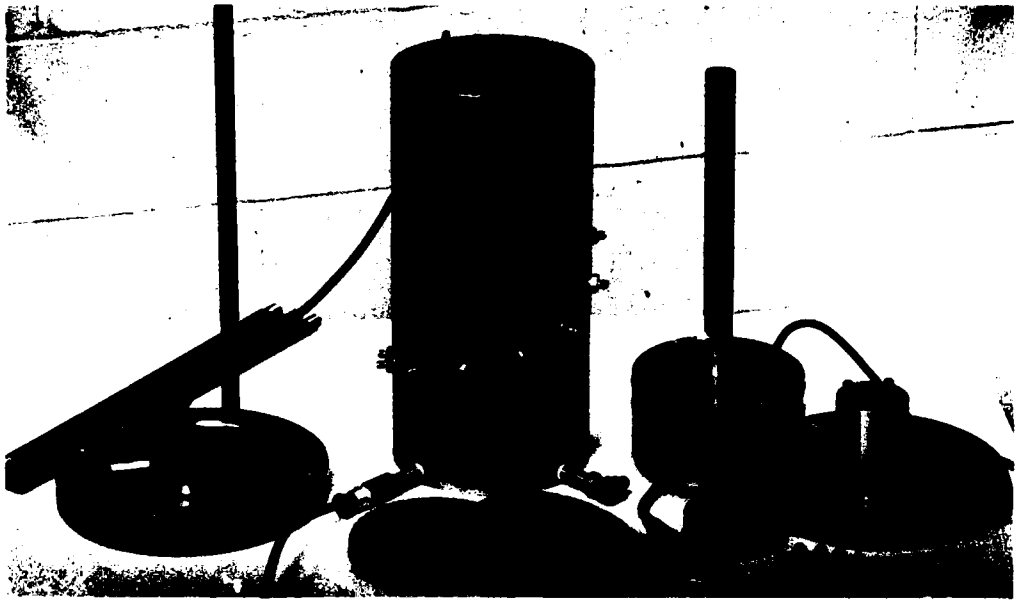

Figure 17. Components of the LSCRS test chamber

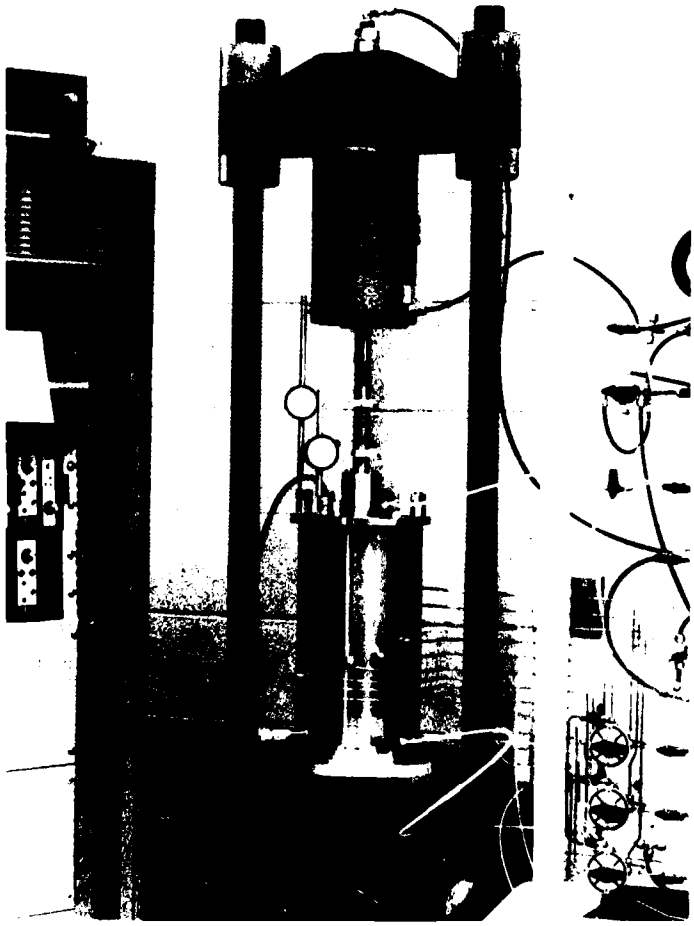

Figure 18. The LSCRS loading/deformation system

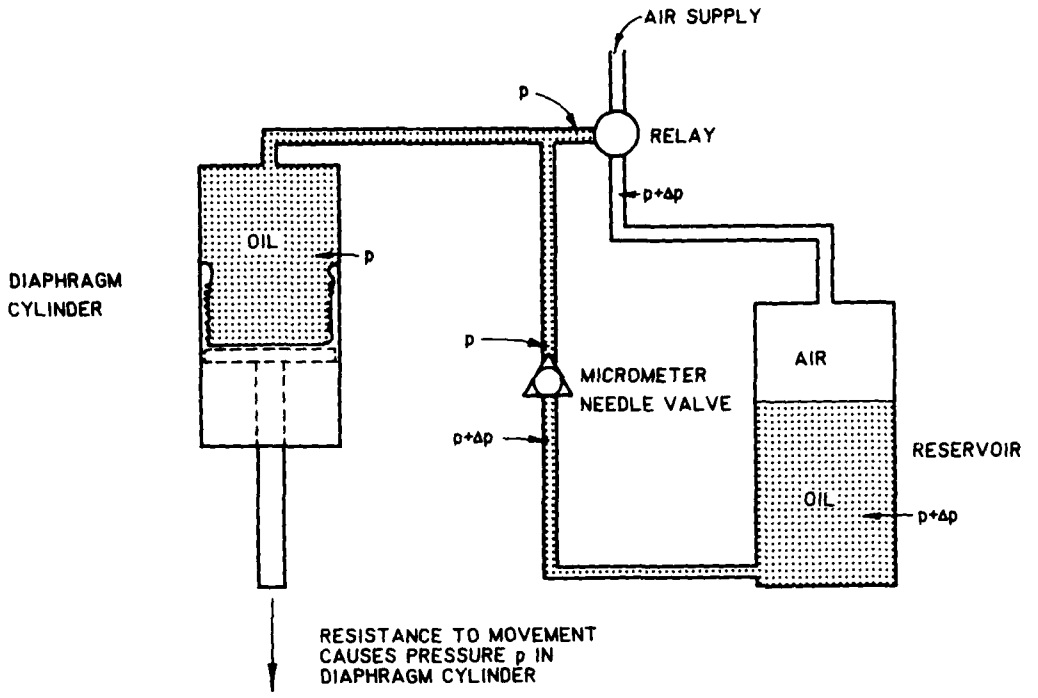

Figure 19. Principle of operation of the loading/deformation system

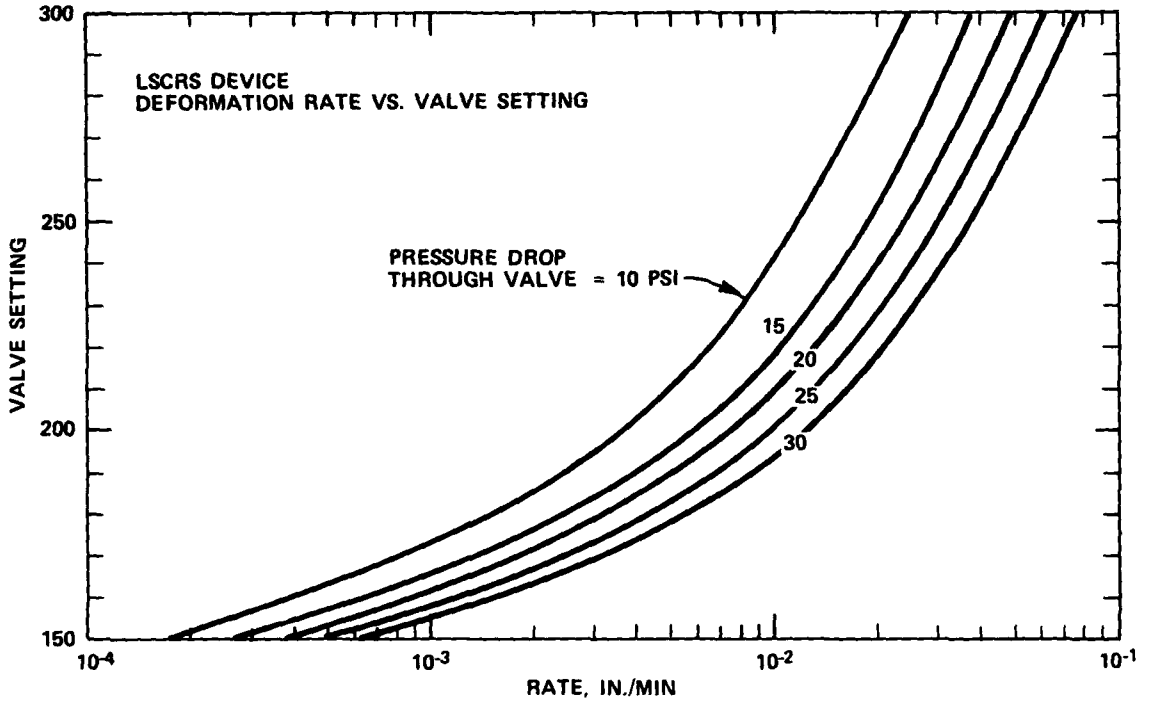

Figure 20. Calibration chart relating deformation rate to valve setting and pressure drop across valve

82. The diaphragm cylinder bore measures 6.3 in. and has a stroke of 5.4 in. The system is limited to a 30 psi pressure in the cylinder which means approximately 900 lb of force can be generated by the ram during normal operation.

83. Load cells in the test chamber are sealed for underwater use and compensated up to a back pressure of 50 psi. Their range is 0-500 lb, which means that the material sample can be loaded to an effective stress of approximately 19.25 psi or 1.38 tsf (assumes sample is loaded over 5.75-in. diam). Through signal conditioning and amplification, load cell output can be read to the nearest 0.1 lb which is an effective stress of 3.85 by 10-3 psi or 2.77 by 10-4 tsf.

84. There are three differential transducers for monitoring pore pressures from the 12 ports spiraling around the test chamber. The range of these transducers is 0-50 psi, and through signal conditioning and amplification can be read to the nearest 0.01 psi or within about 0.28 in. of water.

85. Output from both load cells and transducers is scanned and read by a digital voltmeter with integral timer and printer. Thus readings can be taken and recorded automatically every 5, 10, 15, 30, or 60 min. Alternatively, data from the five channels can be manually scanned and printed at any time.

86. All regulators, valves, and gages used in plumbing and control of the LSCRS device are standard manufacturer's items. The function of the various components is given with the following descriptions where numbers correspond to those shown in the photograph of the control panel (Figure 21):

(1) On-off valve: main air supply control for water subsystem.

(2) On-off valve: main air supply control for oil subsystem.

(3) On-off valve: auxiliary water supply control.

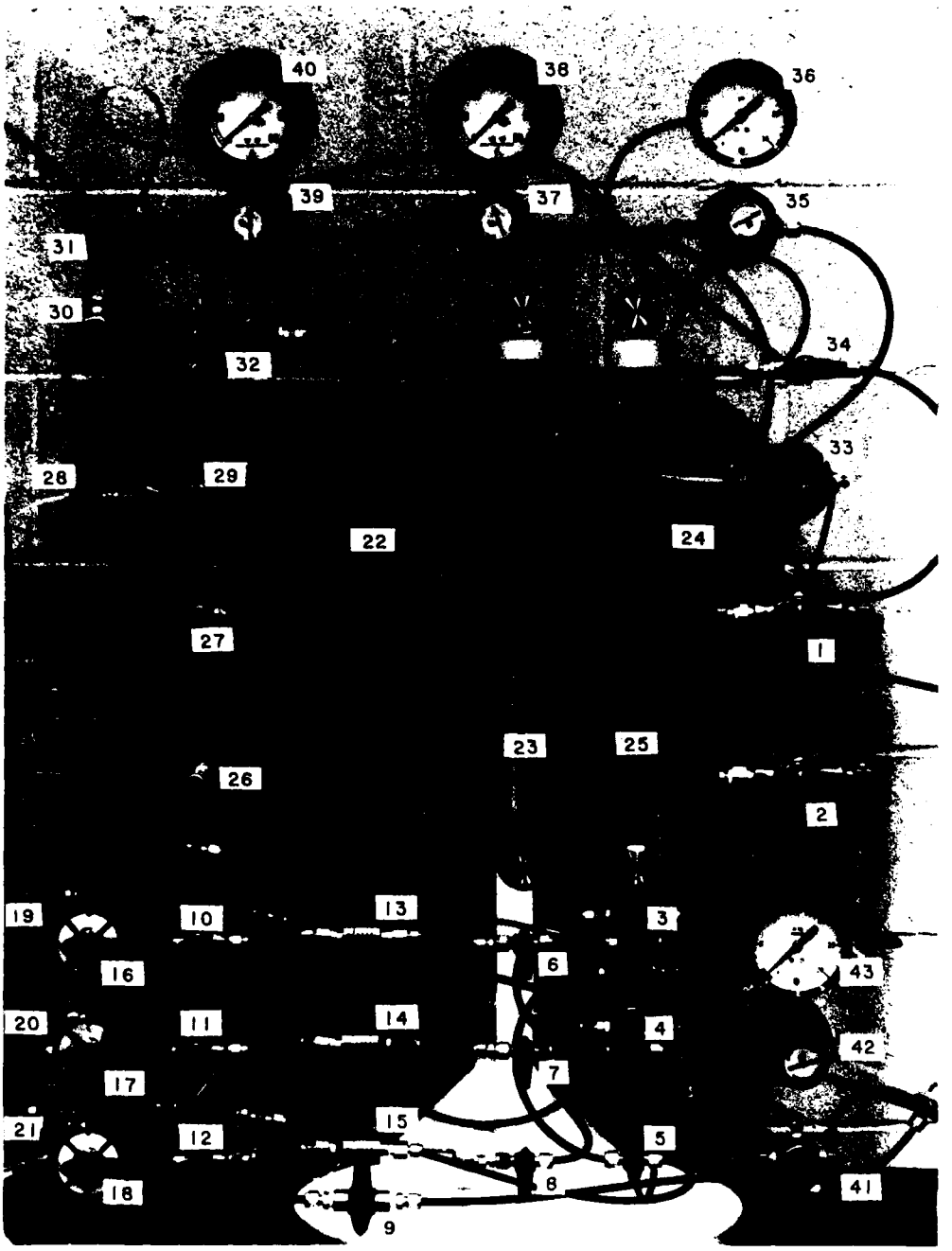

Figure 21. LSCRS device control panel

(4) On-off valve: control on water line to top of test chamber.

(5) On-off valve: control on water line to bottom of test chamber and reservoir drain.

(6) On-off valve: control on water line to back pressure side of pressure transducer No. 1.

(7) On-off valve: control on water line to back pressure side of pressure transducer No. 2.

(8) On-off valve: control on water line to back pressure side of pressure transducer No. 3.

(9) On-off valve: control on water line used to drain test chamber and/or water reservoir.

(10) Three-way valve: for switching between pore pressure ports on chamber and water line to top of chamber. Common to transducer No. 1.

(11) Three-way valve: for switching between pore pressure ports on chamber and water reservoir. Common to transducer No. 2.

(12) Three-way valve: for switching between pore pressure ports on chamber and water line to bottom of chamber. Common to transducer No. 3.

(13) Differential pressure transducer No. 1: for measuring pressure at ports 1, 4, 7, and 10 or top of chamber in reference to system back pressure.

(14) Differential pressure transducer No. 2: for measuring pressure at ports 2, 5, 8, and 11 or reservoir in reference to system back pressure.

(15) Differential pressure transducer No. 3: for measuring pressure at ports 3, 6, 9, and 12 or bottom of test chamber in reference to system back pressure.

(16) Five-way valve: for switching between pore pressure ports 1, 4, 7, and 10 on test chamber. Common to three-way valve 10.

(17) Five-way valve: for switching between pore pressure ports 2, 5, 8, and 11 on test chamber. Common to three-way valve 11.

(18) Five-way valve: for switching between pore pressure ports 3, 6, 9, and 12 on test chamber. Common to three-way valve 12.

(19) On-off valve: control for purging pore pressure ports 1, 4, 7, and 10 with deaired water.

(20) On-off valve: control for purging pore pressure ports 2, 5, 8, and 11 with deaired water.

(21) On-off valve: control for purging pore pressure ports 3, 6, 9, and 12 with deaired water.

(22) Reservoir: for storing silicon oil and providing air-oil interface.

(23) Sightglass: for monitoring level in silicon oil reservoir.

(24) Reservoir: for storing system water and providing air-water interface.

(25) Sightglass: for monitoring level in water reservoir.

(26) Micrometer needle valve: for controlling rate of oil flow into diaphragm cylinder.

(27) Three-way valve: for bypassing needle valve in returning oil to reservoir. Common to top of diaphragm cylinder.

(28) On-off valve: control for bleeding air from top of test chamber.

(29) Three-way valve: for switching between on-off valve 28 and four-way valve 30. Common to top of test chamber.

(30) Four-way valve: for switching between pressure and vacuum (for deairing) in the oil reservoir and providing pressure or vacuum to the top of the test chamber.

(31) Three-way valve: for switching between atmosphere and air pressure. Used to force oil out of diaphragm cylinder and back into reservoir. Common to bottom of diaphragm cylinder.

(32) Three-way valve: for switching between air line on inflow and outflow side of relay 39. Common to three-way valve 34.

(33) Air regulator: for controlling air pressure on purging water line or other auxiliary lines.

(34) Three-way valve: for switching between three-way valve 32 and air regulator 33. Common to pressure gage 38.

(35) Air regulator: for controlling air pressure in water reservoir.

(36) Pressure gage: for monitoring air pressure in water reservoir.

(37) Air regulator: for controlling maximum air pressure available to relay 39 and oil subsystem.

(38) Pressure gage: for monitoring maximum air pressure available air pressure in oil reservoir, and air pressure on purging water line.

(39) Relay-air regulator: for sensing oil pressure in diaphragm cylinder and supplying that plus a preset amount to the oil reservoir.

(40) Pressure gage: for monitoring oil pressure in diaphragm cylinder.

(41) Four-way valve: for switching between pressure and vacuum (for de-airing) in the water reservoir and providing an auxiliary line of vacuum or pressure.

(42) Vacuum regulator: for controlling vacuum.

(43) Vacuum gage: for monitoring vacuum.

87. An overall view of the LSCRS device with control panel and data acquisition unit is shown in Figure 22. A 4-in. and a 2-in. dial gage are provided for tracking the piston movement relative to the chamber body throughout the entire range of possible sample deformation.

Self-Weight Consolidation Device

88. Test data interpretation, to be covered in detail in a later section, requires knowledge of the initial conditions in the test chamber at the time the imposed deformation rate is begun as well as an initial or starter relationship between void ratio and effective stress. Therefore, an auxiliary device to allow incremental sampling of a 6-in.-diam specimen which has undergone self-weight consolidation was designed and constructed. Figure 23 is an exploded view of the device.

89. As the outer cylinder is lowered exposing each inner ring in turn, the inner ring is slid off exposing material of the specimen in 1/2-in. increments. Each increment of material is sampled for water content measurement, and from this measurement a relationship between void ratio and vertical position in the sample can be obtained. The device is very useful in defining a material's effective stress-void relationship at the highest void ratios sustainable by the material when consolidated from a slurry. Calculation of

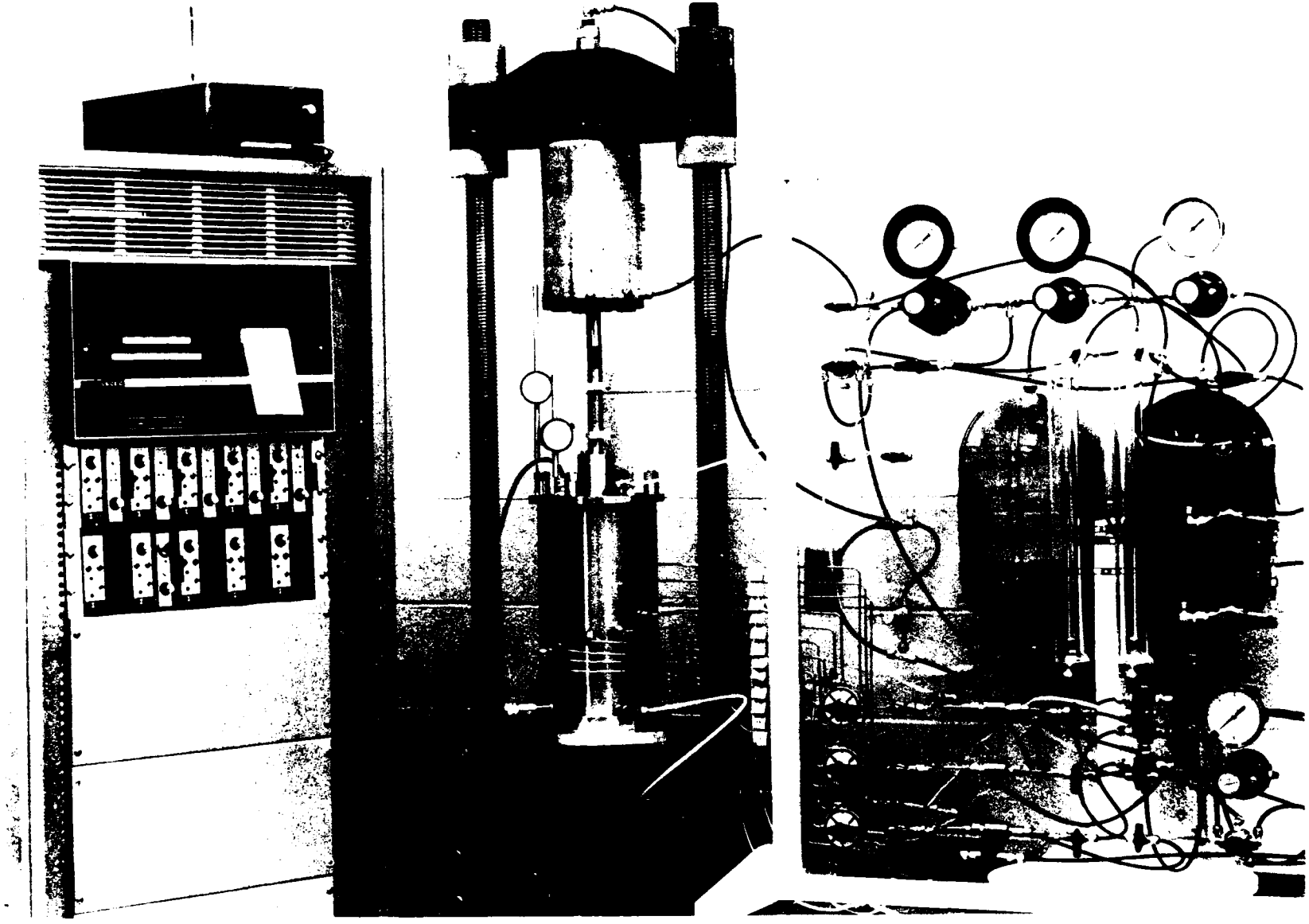

Figure 22. Overall view of LSCRS device, control panel, and data acquisition unit

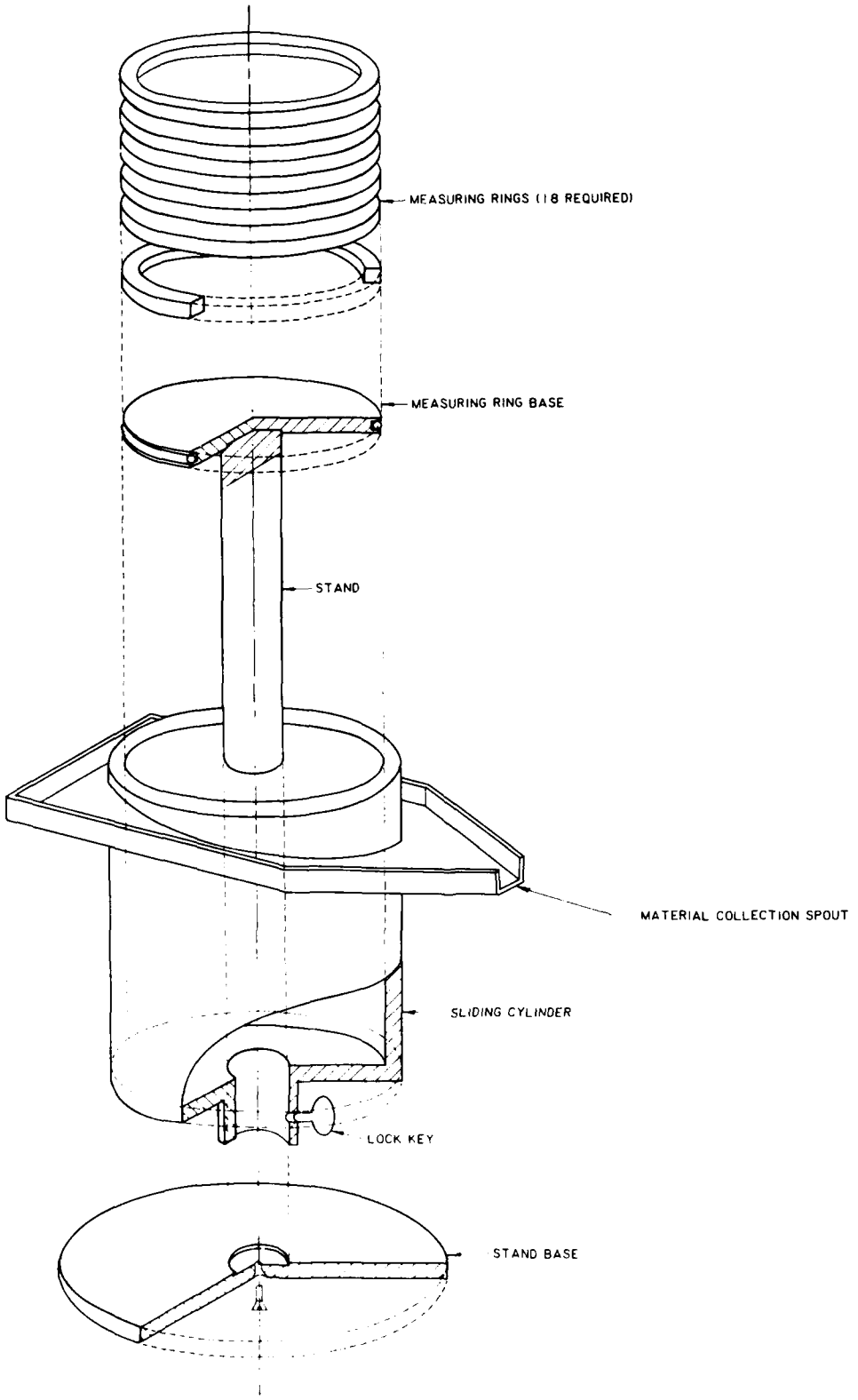

Figure 23. Exploded view of self-weight consolidation device

effective stress in the sample is discussed in a later section. Figure 24 shows the device with outer cylinder lowered.

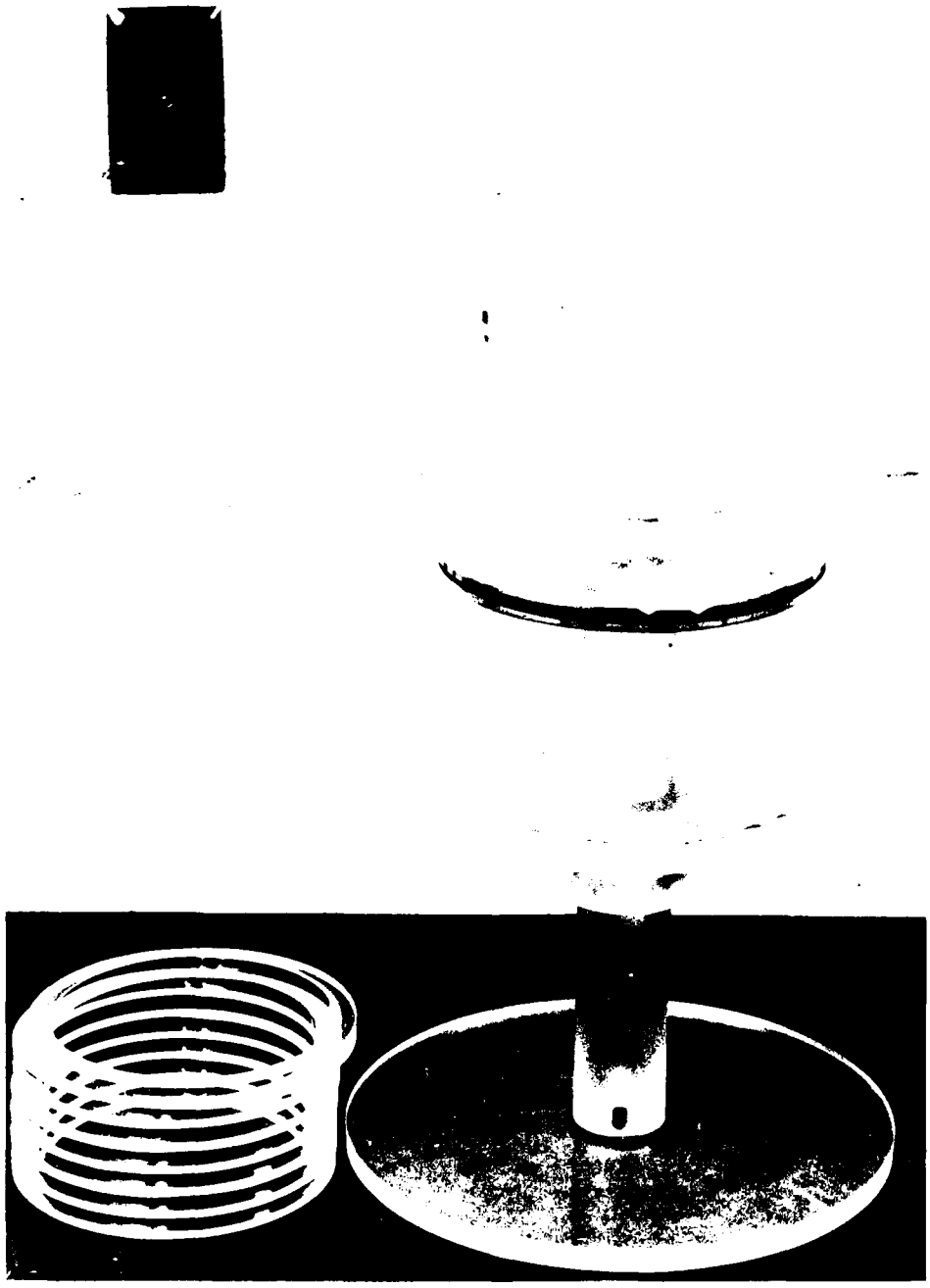

Figure 24. The self-weight consolidation device

PART V: TEST PROCEDURES

90. The LSCRS test is a relatively simple procedure once the purpose of the test and its objectives are thoroughly understood. As previously set forth, the purpose of the LSCRS test is to define the consolidation properties of a very soft, fine-grained soil over the full range of void ratios which it may undergo during initial self-weight or later surcharged consolidation in the field. More specifically, the purpose is to define the relationships between void ratio and effective stress and void ratio and permeability for the material between its zero effective stress or slurried condition and its condition under the maximum effective stress foreseen in the field.

91. Simply stated, the test consists of straining or deforming a soil specimen at a known rate. The specific objectives of the test are to record effective stresses at the top and bottom boundaries of the soil specimen and to record excess pore pressures within the specimen in sufficient detail to accurately determine the excess pore pressure distribution over its full length. With these measurements, the required consolidation properties can be calculated as will be detailed in the next part of this report.

General

92. It was originally thought that the LSCRS test should only be conducted on samples fully consolidated under their own self weight. However, this often lengthy wait can be eliminated by some preliminary self-weight consolidation testing. For materials whose self-weight consolidation characteristics at the highest possible void ratios have been previously well defined in the self-weight consolidation test, there is no need to delay LSCRS testing

until full self-weight consolidation is achieved. The LSCRS test can proceed immediately after deposition of the material on the assumption that the specimen exists at a uniform initial void ratio which can be made equal to but preferably something less than the previously determined zero effective stress-void ratio.

93. The procedures described here assume that no prior information on the material to be tested is available. It is therefore necessary to perform a self-weight consolidation test on a specimen initially at a void ratio higher than its zero effective stress-void ratio before a specimen is placed in the LSCRS device so that initial conditions in the device and a starter relationship between void ratio and effective stress are known.

94. It is expected that as more experience is gained in conducting the LSCRS test, some modification to the procedures outlined here may be in order. Of particular interest should be ways in which the time required for self-weight consolidation tests can be reduced. Perhaps a system of interior drainage could be devised which eliminates the excess water faster but does not affect the final void ratio distribution.

Device Preparation

95. The self-weight consolidation device is prepared for testing by simply assemblying the device to the height of the slurry to be tested plus about 1/2-in. freeboard. As previously shown in Figures 23 and 24, the device is composed of an outer cylinder and up to 18 interior rings, each 1/2 in. high. In assembly, the outer ring should be moved up in 1/2-in. increments between which an interior ring is installed. The bottom surface of each interior ring is lightly but uniformly coated with a silicon grease to make

the joint between rings watertight. After assembly, the watertightness of the joints should be tested by filling the device with water. Small leaks have been found to be self-sealing when the slurry is placed, but any observable leak should be repaired with an additional coating of grease before the slurry is placed.

96. In readying the LSCRS device for testing, it is important to first de-air both the silicon oil and water reservoirs. To do so, valves 3 through 6 and micrometer valve 26 should be closed. The 3-way valve, valve 27, is set to close the bypass, and 4-way valves 30 and 41 are turned to the vertical position. This isolates the reservoirs from all other plumbing, regulators, and gages, and connects them with the vacuum system. Opening the vacuum regulator 42 now simultaneously applies the vacuum read on gage 43 to both reservoirs. It is suggested that a maximum vacuum be maintained at least overnight to aid in the de-airing of the reservoirs.

97. De-airing is required to assure responsiveness of the loading system because its design is based on the assumption that fluid pumped into the cylinder is incompressible. If the oil supply contains dissolved air, this air will likely come out of solution as the oil undergoes the pressure drop through micrometer valve 26 to form air bubbles which may cause the ram movement through the diaphragm cylinder to become erratic. De-airing is also required to assure responsiveness of the pore pressure system. Air bubbles in the lines between the test chamber and pressure transducers will cause a sluggish or inaccurate output by the transducers. Thus a freshly de-aired water supply is used to fill and/or flush all lines to the test chamber.

98. Provisions have been made to flush the lines between the 5-way valves and the test chamber with de-aired water to help remove any trapped air bubbles. With the 4-way valves 30 and 41 in the horizontal position, an air

pressure can be applied to the reservoirs. The line downstream of valve 3 can then be used as a supply of de-aired water to the common line feeding valves 19, 20, and 21 which control access to the 12 pore pressure lines connected to the test chamber. To assist in de-airing these lines and water in the test chamber a vacuum can also be applied to a fully assembled test chamber through 3-way valve 29.

99. De-aired water should also be maintained between the 5-way valves and the pressure transducers. The transducer itself is initially filled with de-aired water from a syringe and thin flexible tubing before assembly. It is then assembled in such a manner to ensure air is not allowed into the transducer or the lines feeding it.

100. Once all lines are de-aired, the test chamber should be fully assembled and filled with water. All air should be drained out the top of the chamber through the 3-way valve 29 by opening valve 28 and by loosening the plate sealing the load piston ram to allow the air trapped in the ball bushing housing to escape. With the system thus filled, the back pressure to be used during the test should be applied so that load cells and transducers can be zeroed and recalibrated. During this step, valves 4 through 8 should be open, and 3-way valves 10, 11, and 12 should be set open to the test chamber.

101. After satisfactory de-airing and electronics calibration, the system is depressurized and made ready for sample placement. Valves 4 and 5 are closed and then the top plate of the test chamber and loading piston are removed. Valve 9 is opened and water drained from the test chamber until it is within 1 in. of the bottom porous stone. Next, a 6-in.-diam filter paper is placed to cover the bottom stone and inner ridge of the test chamber. The water is again drained until it is level with the bottom porous stone and is at but not above the filter paper. During this drainage of cell water,

ensure that no air bubbles become trapped below the filter paper. The device is now ready for placement of the sample.

Sample Preparation and Placement

102. Preparation of the sample for both the self-weight consolidation test and testing in the LSCRS device is similar. The main aspects of the material tested is that it is completely remolded (as is the actual site material after being dredged and pumped through pipelines) and is comprised only of the fine-grained portion of the sample (a similar segregation also occurs at the site after hydraulic placement of the material). Thus field material is washed through a No. 40 sieve with liberal amounts of water also from the site. The material retained on the sieve may be useful in determining the gross percentages of fines and coarser particles if it is representative of the entire site to be dredged. However, it has no use in the testing described herein. The void ratio of this slurry should be adjusted to approximate the field placement void ratio by either adding water or decanting water after some period of quiescent settling.

103. Once the void ratio approximating its field placement condition is obtained, the mixture should be thoroughly agitated and mechanically mixed to obtain a uniform mixture of solids and constant void ratio throughout but not to entrain undue amounts of air. The mixture can then be split into approximately 1-gal quantities through a device such as shown in Figure 25 to obtain similar samples for the self-weight and LSCRS devices. The material should be sampled midway through the splitting process to determine its void ratio. If an LSCRS test is to be conducted on a sample fully consolidated

Figure 25. Method for splitting a slurry sample

under its own self-weight, modifications to the sample described in the next paragraph are not applicable.

104. The ideal uniform void ratio at which to start an LSCRS test is somewhat less than the zero effective stress-void ratio, but this is an initial unknown. Therefore, it is suggested that the initial void ratio of the slurry be based on material appearance after about three days of quiescent settling. If the material is at or above its zero effective stress-void ratio, large amounts of free water will appear at the top. Most of this water should be decanted and the remaining material remixed. If very little free water appears at the top within about one day, the slurry may be well below the zero effective stress-void ratio. In this case, some water should be added and mixed and the material observed through an additional period of quiescent settling.

105. At this point, the testing procedure can proceed in either of two ways. If testing time is not critical, both the self-weight and LSCRS devices are filled with material at its field placement void ratio to the same heights. Figure 26 shows the self-weight device after filling. The material is then allowed to fully consolidate under its own self weight before LSCRS testing is started. If testing is to be accomplished in the shortest possible time, the self-weight device is only half filled to reduce the time required for self-weight consolidation and the determination of a "starter" relationship between void ratio and effective stress. The void ratio of the sample for the LSCRS device is adjusted as described in paragraph 104 above and then placed in the LSCRS for immediate testing at the predetermined uniform initial void ratio.

106. Regardless of which procedure is followed, the material should again be well mixed before placement in a device. It should be poured slowly

Figure 26. Self-weight consolidation device after filling

and continuously so as not to entrap air bubbles and to provide a uniform material in the devices. After half the material has been placed in the LSCRS device, a sample of the material should be taken for a void ratio check.

Conduct of the Test

107. The self-weight consolidation test is self-conducting. Once material is placed in the device, it should be set aside and left undisturbed, except for periodic measurements to the material surface, until the process of primary consolidation is complete as determined from a semilogrithmic plot of material settlement versus time. Keeping the device covered with a piece of plastic during the consolidation period has been found helpful in preventing evaporation. Figure 27 shows excess water being removed from the top of a completed self-weight consolidation test. The same stainless steel tube with plastic locking collar pictured is used for making periodic measurements of the material surface during the self-weight consolidation phase.

108. After material is carefully placed in the LSCRS, the distance from the top of the device to the top surface of the test material is immediately measured. Each pore pressure port is then purged of any air that might have collected on its porous stone filter between the time they were de-aired and the time the sample was placed. This is accomplished by reconnecting the translucent plastic tube from valve 3 to the output of regulator 33 and applying a pressure to the water in the line. Then by slightly opening and rapidly closing valves 19, 20, and 21 in succession, a very small amount of water (the water interface in the translucent line should move no further than about 1/4 in. for each port) can be forced through each of the pore pressure ports in turn. The amount of water introduced to the sample in this manner is insignificant

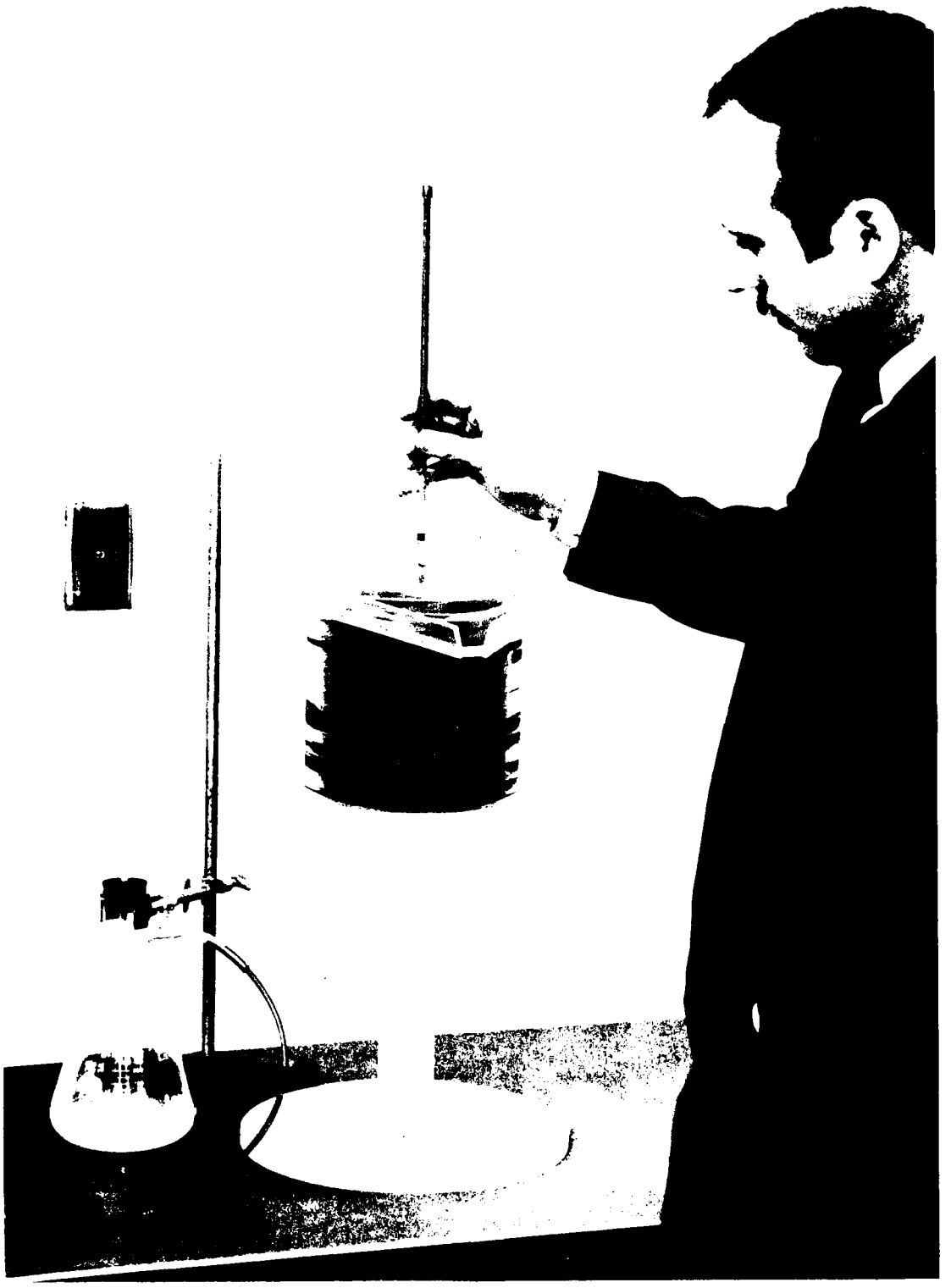

Figure 27. The removal of excess water on completion of the self-weight consolidation test

compared with the total volume of water in the sample. This purging procedure is also useful during the loading phase of the test to restore responsiveness to a port which may have become clogged with material.

109. The next step depends on whether a fully consolidated or unconsolidated sample is to be tested. If the sample is to be consolidated under its own weight, the test chamber should be covered with a plastic sheet to prevent excessive evaporation. Measurements of the material surface are periodically made as in the self-weight device test. After primary consolidation is complete, the test proceeds in the same manner as it would for an unconsolidated sample.

110. If the sample is to be tested from the uniform initial void ratio or unconsolidated state, a filter paper is carefully placed on its top surface and the test chamber is completely filled with water so as not to disturb this top surface. The loading piston, complete with its load cell and porous stone, is then slowly pushed into the test chamber. This will cause some water to overflow the chamber, but that is necessary to ensure that the space between the inner wall of the chamber and the outer wall of the piston below its "0" ring seal is completely filled with water. The piston should be slowly moved down the chamber until it is within 1/4 in. of the sample top surface. The top plate of the chamber should next be installed and its headspace de-aired by opening valve 4 and allowing air to escape through valve 28 and the top plate of the roller bushing housing. Dial gages are then attached to the load piston ram in a position convenient for reading and in a manner that permits coverage of anticipated piston movement.

111. With the test chamber thus fully assembled and de-aired, valve 5 is also opened and the system slowly back pressured. Back pressure is introduced through regulator 35 and read on gage 36. A back pressure of 15 psi has bee

found to work well in testing materials thus far. It should be gradually applied over a period of about 30 min. During backpressure application, the tendency for water to move through the pressure ports and possibly clog them with material can be eliminated by backpressuring both sides of the stones simultaneously by connection of valve 3 to valves 19, 20, and 21. A 15-psi back pressure should not be sufficient to cause the loading piston to move upward, but the diaphragm cylinder ram should be positioned in contact with the piston ram to eliminate any tendency for upward movement.

112. The top load cell zero and calibration can be rechecked at this time. However, the bottom load cell should be feeling the self-weight of the sample and, if zeroed, this fact should be noted. Zero and calibration of the transducers can be rechecked also by setting 3-way valves 10, 11, and 12 open to the reservoir manifold.

113. It is recommended that 5-way valves 16, 17, and 18 be set to monitor the first and second ports below the sample top surface and the port nearest the sample center during the test. When the top boundary of the sample has been deformed past a particular port, the valve should be adjusted to another port. When adjustment is made to a new port, it is recommended that it be purged with a small amount of water as previously described. Regulator 33 should be set to a pressure about 5 psi greater than the sum of the back pressure plus the maximum excess pressure in the sample.

114. With the micrometer valve 26 closed and 3-way valve 27 open to it, a maximum oil system pressure of 30 psi plus the preselected amount of pressure drop is set with regulator 37. The relay-air regulator 39 is then set to the oil reservoir pressure at the preselected amount higher than the pressure registered on gage 40.

115. To start the loading piston moving down at a controlled and known rate, the micrometer valve is opened to the setting corresponding to that rate and preselected pressure drop from Figure 20. From this point onward, the test consists of constantly monitoring the load measured by the bottom load cell so that subsequent adjustments in the deformation rate do not cause load rebound, adjusting the micrometer valve to maintain a steady and slow rise in the measured load by periodically slowing the deformation rate, and collecting and recording data from the load cell's, pressure transducers, and dial gages.

116. There are no set rules for adjusting the deformation rate. The objective is to deform a sample about 3.0 in. over about an 8-hr period if possible. During this period, it is desirable that the boundary load steadily increase from zero to about 400 lb. A typical advance plan for accomplishing this objective based on the calibration curves of Figure 20, a 10-psi pressure drop across the micrometer valve, and an "idealized" plot of load increase and deformation versus time is shown in Figure 28. Of course, such a plan must be continuously adjusted to account for the particular material tested. How well those adjustments are made will depend on the experience of the person conducting the test.

117. The sample deformation plot in Figure 28 is based on the staircased micrometer valve setting schedule also shown in the figure. Such drastic changes in the deformation rate will assuredly cause rebound of the load applied to the sample. Therefore, a more gradual and continuous valve setting schedule typified by the dashed line in the figure is recommended. Maintaining the load growth and rate of deformation suggested in the figure simultaneously will generally not be possible. Whenever conflict arises, consideration to maintaining a steadily increasing load similar to that shown

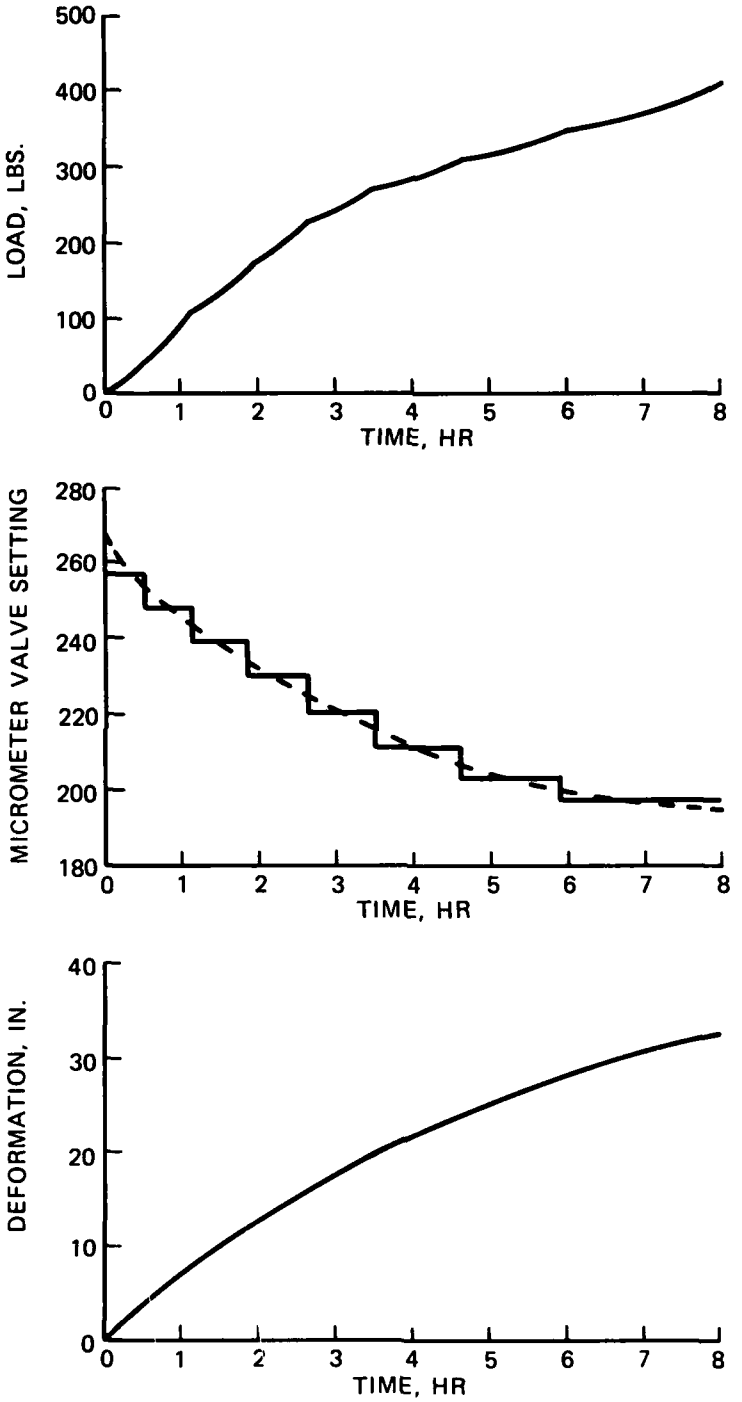

Figure 28. Typical advance plan for conducting the LSCRS test

should be given priority. If this should mean that the testing time is significantly increased, then so be it. Figure 29 is a plot of the maximum excess pore pressure in the sample interior (which also corresponds to the effective stress at the drained boundaries) and deformation history of the first sample tested in the LSCRS. As can be seen, very minor changes in the deformation rate can cause considerable load rebound. Experience gained from this test led to a much more uniform load increase in later tests which will be illustrated in Part VII.

Data Collection

118. Data collected during the self-weight consolidation test is limited to surface settlement measurements with time. The results of these measurements are to be plotted on a logrithmic time scale and therefore more frequent measurements are required during the earlier stages of the test. At the conclusion of the self-weight test when primary consolidation is complete the specimen is sampled at 1/2-in. intervals through its full depth.

119. The sequence in Figure 30 shows the process. First, the exposed material surface is sampled to a depth less than 1/4 in. by removing material with a flat spatula and depositing it into a tare can for later water content (void ratio) determination. Then the outer cylinder of the device is lowered about 1/2 in. and the next inner ring is removed by sliding it horizontally and allowing the removed material to spill into a collection container. The newly exposed surface is sampled as before and the process repeated until the entire specimen depth has been sampled.

120. Collection of data during the LSCRS test is primarily accomplished with the digital voltmeter and integral timer and printer. At times when

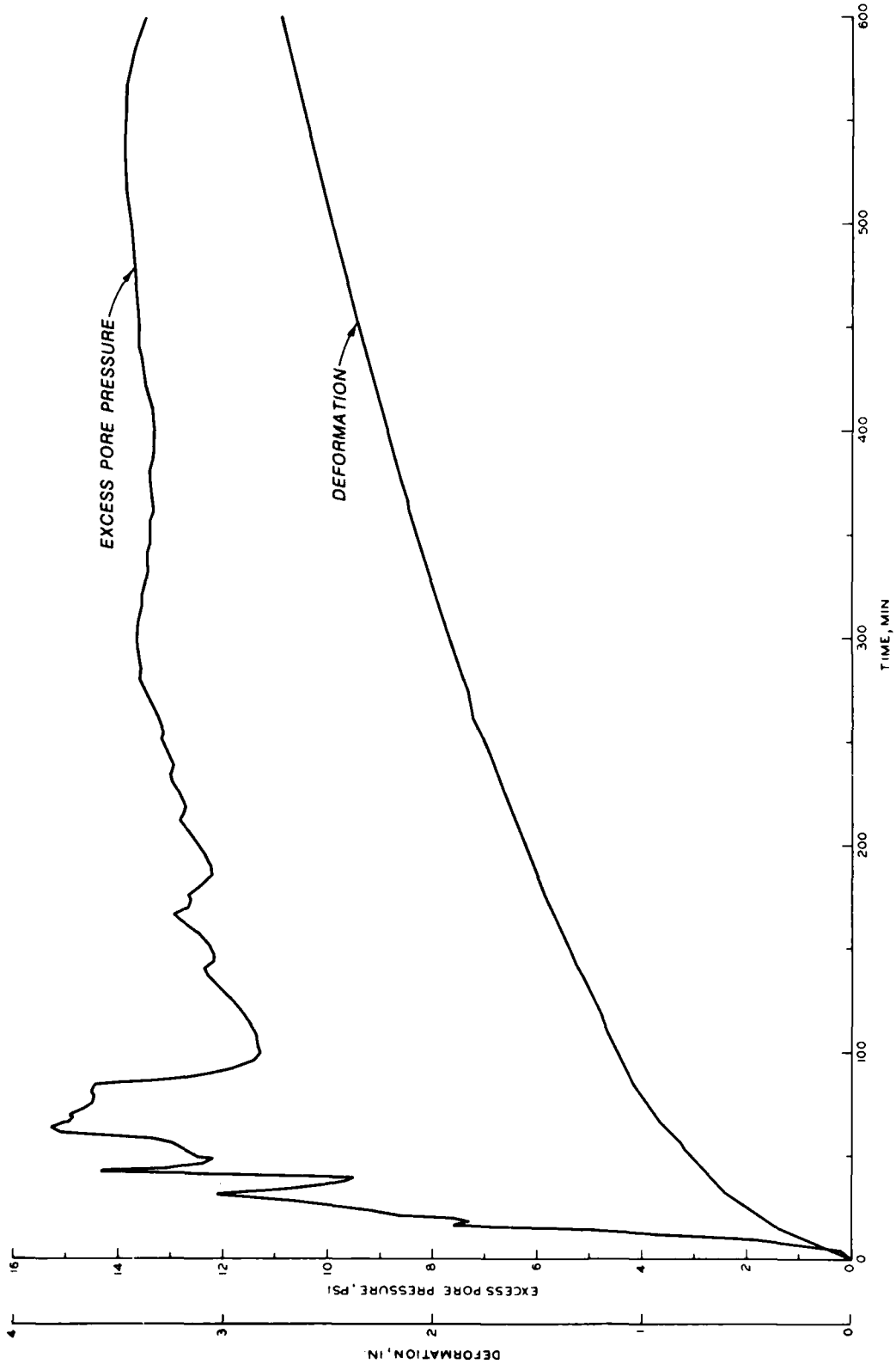

Figure 29. Maximum excess pore pressure and deformation during the first test in the LSCRS device

a. Exposed material surface is sampled

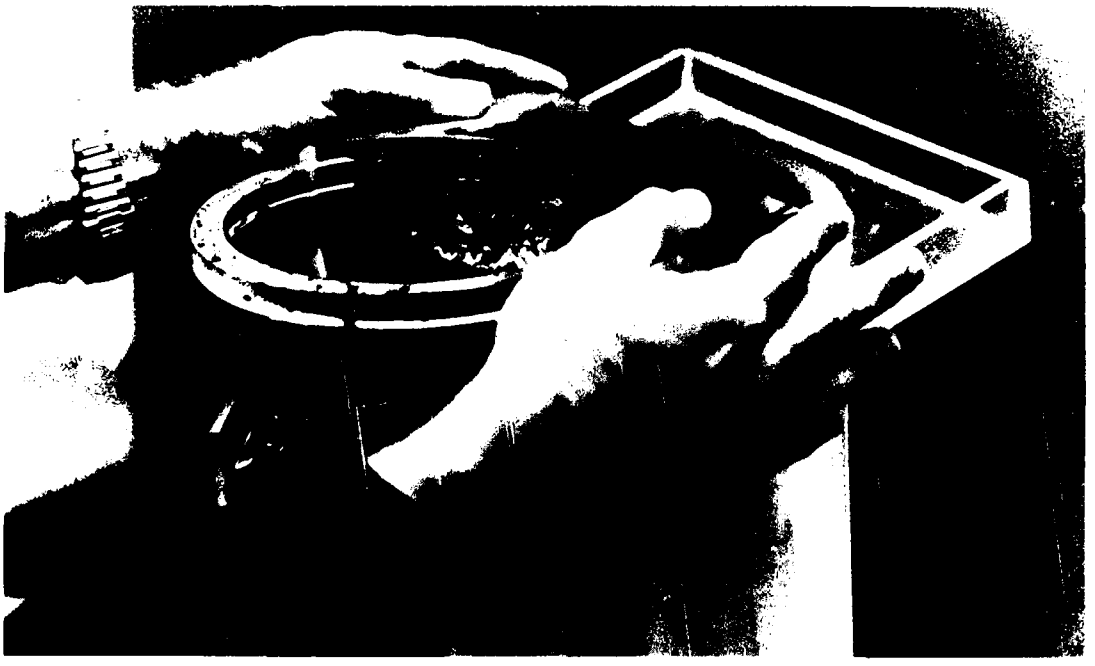

b. Inner ring is removed allowing the removed material to spill into a collection container

Figure 30. The sequence in sampling material for determination of void ratio with depth in the self-weight consolidation device (Continued)

c. The newly exposed surface is sampled as before and the process repeated

Figure 30. (Concluded)

rapid changes are occurring in either the boundary loads or measured pore pressures due to the boundary nearing or passing a port, the electronic data should be collected every 30 sec to 1 min. A typical data set is shown in Figure 31 where it can also be seen that the time of reading is also recorded. During later stages of the test when changes are occurring more slowly, data should be printed every 1 to 5 min.

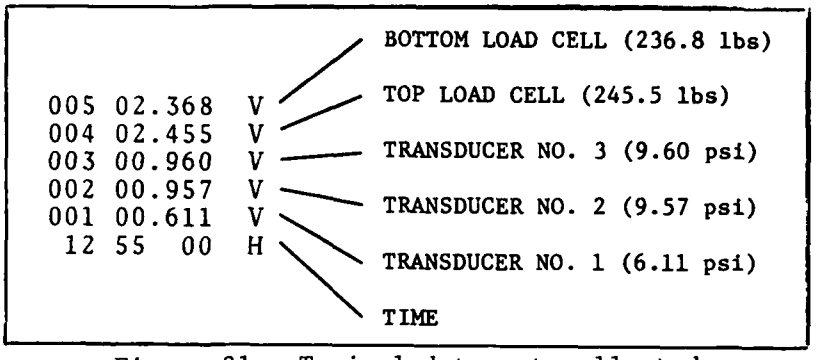

Figure 31. Typical data set collected during an LSCRS test

121. Sample deformation must also be closely monitored during the test. It is preferred that the dial gage be read and recorded each time load cells and pressure transducers are scanned plus whenever a change is made in the micrometer valve setting. However, during early stages of the test when the valve is adjusted almost continuously, it may be only feasible to read and record the dial gages at intervals of about 1 min. Later in the test, this time interval should be stretched to about 5 min.

122. At the conclusion of the test, load is removed from the LSCRS test specimen and it is permitted to rebound to full equilibrium before the device is disassembled. After device disassembly, the final rebound height of the specimen is measured. The specimen is then incrementally sampled to determine the after-test void ratio distribution which will be compared to the predicted final void ratio.

Sources of Testing Error

123. As in all laboratory soil testing procedures, the self-weight consolidation and LSCRS tests offer opportunities for experimental errors. In addition to those sources of error normally associated with water content

determination, specific gravity measurement, void ratio calculation, and conventional consolidation testing (US Army Corps of Engineers, 1980, "Laboratory Soils Testing"), there are several additional sources peculiar to the test described here.

124. The simplicity of the self-weight test gives it the advantage of avoiding the many possible error sources of a more sophisticated test. However, the accuracy of the test remains highly dependent on the homogeneity of the material tested. Special care must be taken to ensure a homogeneous sample by thoroughly mixing the material near its zero effective stress void ratio. A heterogeneous mixture will lead to an unnatural segregation during consolidation and may show up as a discontinuity in the otherwise smooth curve defining the relationship between void ratio and effective stress.

125. A second possible source of error in the self-weight test is the effect of container side friction. An indicator of the degree of the effect is in the unevenness of the material's top surface during consolidation. Final calculation errors resulting from container side friction can be minimized by measuring the top surface fall at the same representative spot during consolidation and by sampling the material away from the container edges in each 1/2-in. segment after full consolidation.

126. The primary source of possible error in the LSCRS test lies in its sophisticated loading and pore pressure measurement system. Besides the obvious potential problems with electronic calibrations, there remains the question of whether the devices are actually measuring what they were intended to measure. Confidence in the recorded values can be raised by comparing the measurement of one device with another similar or different device. For example, maximum excess pore pressure measured by one transducer near the middle of the sample during a test can be compared with another transducer which is

also near the sample center. They should favorably compare with each other and also the calculated maximum interior excess pore pressure produced by the measured load at the sample drained boundaries. Thus the load cell can be used to check the pressure transducers.

127. Air trapped within the pore pressure measuring system of the LSCRS will also lead to possible calculation errors, especially where accurate knowledge of pore pressure change with time is required. If air is in the system, a volume change in the air is necessary to induce a pressure change. This volume change is only possible with a movement of water. The low permeability of the material usually tested inhibits water movement and therefore pore pressure changes are registered slower than they actually occur, if at all. These sluggish measurements are usually easily detected when plotted with correct measurements from other transducers and should be disregarded.

128. Other possible sources of error in the LSCRS test include an erratic load application allowing material rebound, a too fast load application causing material to cake at the drained boundaries, and friction between the material and container sidewalls. The ill effects of rebound and caking can be minimized by slowing the rate of load application. The relative magnitude of side friction can be estimated from the measured load at top and bottom drained boundaries. Theoretically, the load felt by the bottom cell should equal the load of the top cell plus material self-weight. Measurements not according to theory may indicate the quantity of material side friction.

PART VI: TEST DATA INTERPRETATION

129. The interpretation of data generated during laboratory testing of soft fine-grained soils in the self-weight and LSCRS devices is accomplished mainly by the equations of material equilibrium, equation of continuity, and Darcy's Law. Only in calculating a permeability value based on the self-weight test is there any need to invoke the theoretical equation governing the consolidation process.

Void Ratio-Effective Stress Relationship

130. At the completion of the self-weight consolidation test and material sampling, the determination of the relationship between void ratio and effective stress is a straightforward exercise of matching the void ratio determined at selected points in the material with the effective weight of material above those points.

131. First, a plot of the void ratio distribution through the consolidated material should be constructed. Figure 32 shows such a plot from a typical soft material consolidated under its own weight from an initial height of 8.84 in. and an initial void ratio of 12.48. Next, the material is divided into increments for calculation purposes and an average void ratio, $\bar{e}_i$, is assigned to each increment based a plot such as Figure 32. The amount of solids in each increment is determined from

$$\ell_i = \frac{\xi_i}{1 + \bar{e}_i} \tag{54}$$

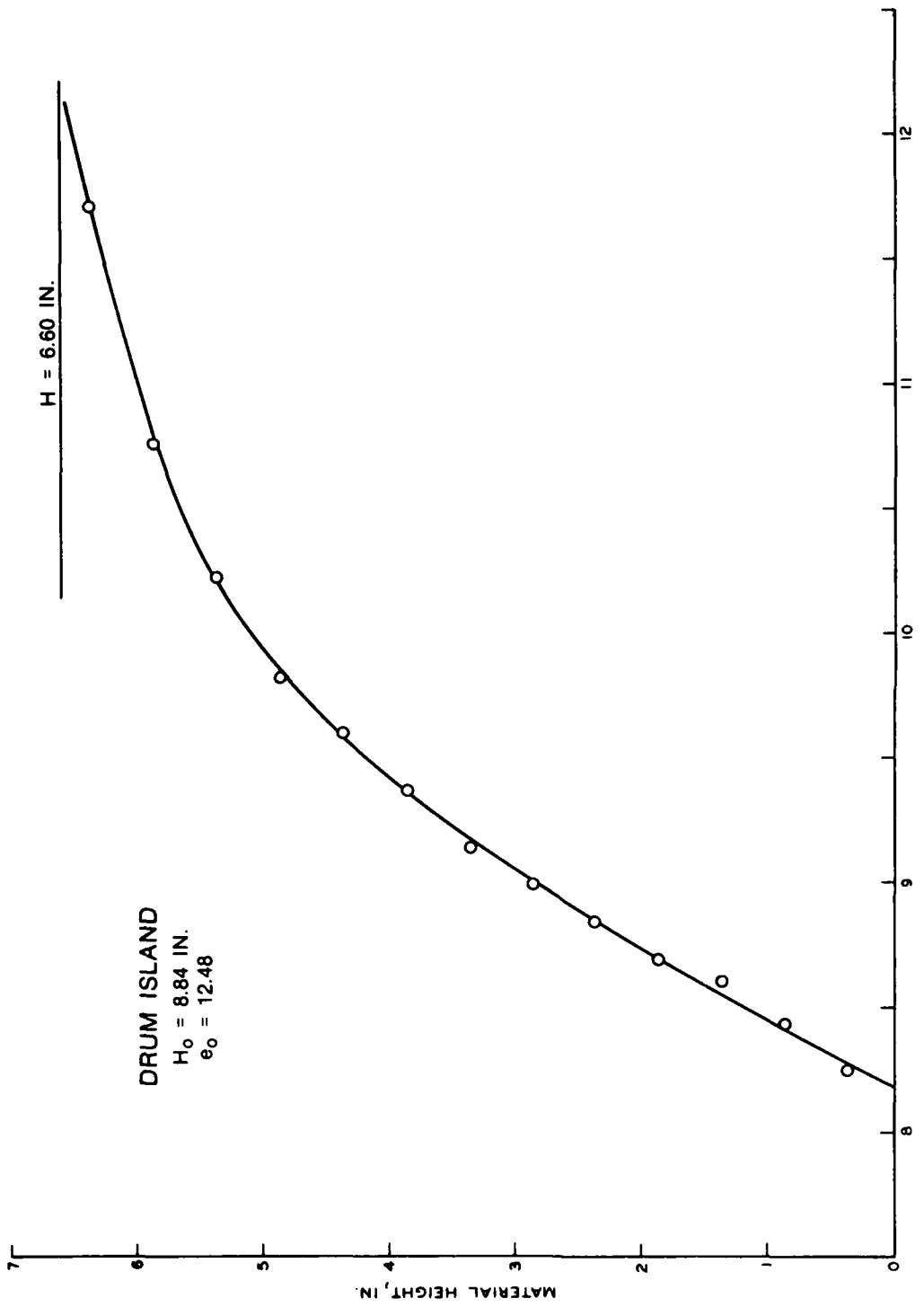

Figure 32. Final void ratio distribution after self-weight consolidation test of Drum Island material, e_o = 12.48

where

ℓ_i = volume of solids per unit area in the increment

ξ_i = actual thickness of increment

The effective weight per unit area of each increment can then be determined by

$$W_i' = \gamma_w(G_s - 1)\ell_i \tag{55}$$

The void ratio at the bottom of each increment is plotted with the effective weight per unit area of all increments above to give the relationship between void ratio and effective stress at these very low effective stresses.

132. Definition of the void ratio-effective stress relationship at higher effective stresses comes from interpretation of data generated in the LSCRS test. The analysis begins with the calculation of the void ratio distribution in the LSCRS specimen at a particular time from the measured effective stress distribution and an extension of the $e - \log \sigma'$ curve determined in the self-weight test. This calculated void ratio distribution is next adjusted to a distribution of roughly the same shape as the calculated distribution and so that the total volume of solids determined from the new distribution equals the known volume of solids in the test specimen. After the adjustment, the $e - \log \sigma'$ curve is extended using the average void ratio and average effective stress next to the moving boundary as the next point on the $e - \log \sigma'$ curve. By repeating this procedure with measured data at increasing test loads, a complete void ratio-effective stress relationship can be defined for the material.

133. The LSCRS test data analysis procedure involves considerable trial and error calculations. Therefore it has been programmed for computer

AD-A171 591 THE LARGE STRAIN CONTROLLED RATE OF STRAIN (LSCRS) 2/2
DEVICE FOR CONSOLIDATI.. (U) ARMY ENGINEER WATERWAYS
EXPERIMENT STATION VICKSBURG MS GEOTE.. K W CARGILL
UNCLASSIFIED JUL 86 WES/TR/GL-86-13 F/G 8/13 NL

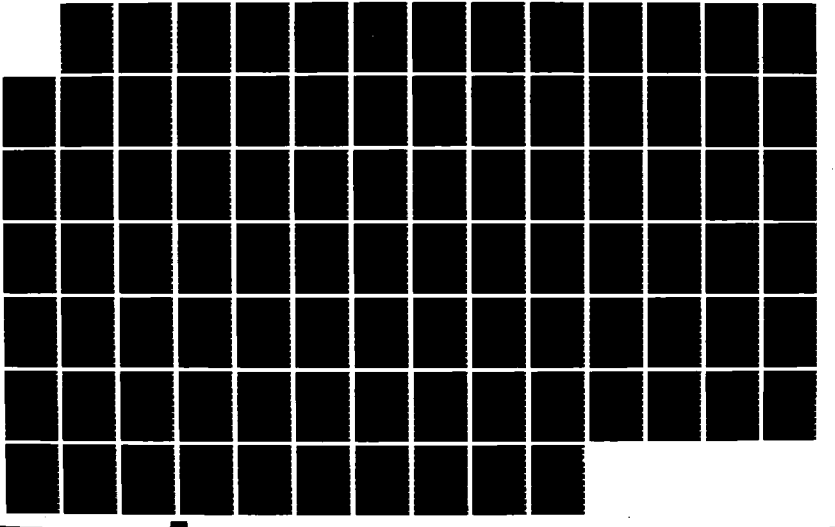

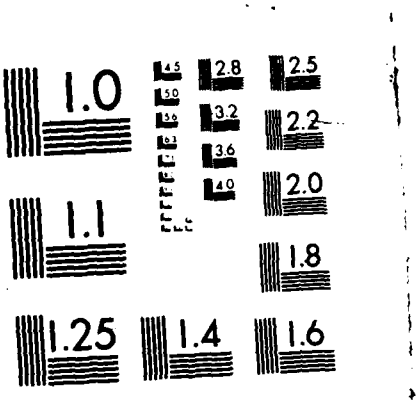
1.0
1.1
1.25
1.4
1.6
1.8
2.0
2.2
2.5
2.8
3.2
3.6
4.0
4.5
5.0
5.6

solution. A Users Manual for the program is included as Appendix C and a listing is found in Appendix D. In the program, effective stresses for points between the boundaries are calculated by the familiar effective stress principle. The first estimate of void ratio is made through the equation

$$e_i = e_{ref} - C_c \log \frac{\sigma'_i}{\sigma'_{ref}} \tag{56}$$

where

e_{ref} = reference void ratio on the previously determined $e - \log \sigma'$ curve

C_c = compression index or slope of $e - \log \sigma'$ curve through e_{ref}

σ'_i = effective stress for which e_i is being calculated

σ'_{ref} = value of effective stress at e_{ref}

The volume of solids is then computed by Equation 54 for each increment in the test specimen.

134. After adjustment of the calculated volumes in each increment, an average void ratio within a specified distance of the top drained boundary is computed from

$$\bar{e} = \frac{\Sigma \xi_i}{\Sigma \ell_i} - 1 \tag{57}$$

where

$\Sigma\ \xi_i$ = sum of increment thicknesses within a specified distance of the drained boundary

$\Sigma\ \ell_i$ = sum of volume of solids per unit area

An average effective stress associated with this average void ratio is calculated from

$$\bar{\sigma}' = \frac{\Sigma\left(\ell_i \cdot \bar{\sigma}_i'\right)}{\Sigma\ \ell_i} \tag{58}$$

where $\bar{\sigma}_i'$ = one-half of the sum of the effective stresses at the top and bottom of the increment. The compression index of the extended portion of the $e - \log \sigma'$ curve is then

$$C_c = \frac{\bar{e} - e_{ref}}{\log(\sigma'_{ref}) - \log(\bar{\sigma}')} \tag{59}$$

where

e_{ref} = void ratio at last point on previously defined $e - \log \sigma'$ curve

σ'_{ref} = effective stress of last point on previously defined $e - \log \sigma'$ curve

135. The e - log σ' curve generated in this manner by the computer program LSCRS gives a reasonable estimate of the true relationship between void ratio and effective stress so long as the calculations remain stable and convergent. Signs of probable instability in the calculations include an abrupt and increasingly downward trend of the calculated curve or a flattening of the calculated curve at abnormally high void ratios. The first is caused by calculated void ratios at low effective stresses being above their true values and the latter is due to calculated void ratios at the low effective stresses being below their true values.

136. If an analysis presents a stability problem, input data should be carefully rechecked to assure its consistency with measurements. If input data are correct, the starter e - log σ' curve should be adjusted and extended to compensate for the unstable tendency. For example, if the curve shows an increasing downward trend at higher effective stresses, the slope of the starter curve should be adjusted to give lower void ratios at the lower effective stresses. If the calculated curve shows a premature flattening at abnormally high void ratios, the slope of the starter curve should be adjusted to give higher void ratios at the lower effective stresses.

137. A calculated e - log σ' curve that slowly flattens at the higher effective stresses and provides estimates of a void ratio distribution giving a close correspondence to the known solids volume at all test analysis times is a good estimate of the true relationship between void ratio and effective stress in the material. The program has been used to calculate the e - log σ' curve from four different tests that are compared with results of other testing in Part VII.

Void Ratio-Permeability Relationship

138. A plot of the sample deformation during the self-weight consolidation test results in a familiar time-consolidation curve as shown in Figure 33. Utilizing the linear version of the finite strain consolidation theory (Gibson, Schiffman, and Cargill 1981) and a plot relating percent consolidation to a dimensionless time factor (Cargill 1983), an estimate of permeability at an average void ratio during the test can be obtained. Applicable equations are given here but the reader is referred to the cited references for details of the theoretical basis.

139. Once sample deformation is plotted as in Figure 33, the time of 50 percent consolidation is determined in the usual way corresponding to 50 percent deformation. This time is related to a dimensionless time factor at 50 percent consolidation from Figure 34 by the equation

$$T_{f.s.} = \frac{gt}{\ell^2} \tag{60}$$

where

$T_{f.s.}$ = dimensionless finite strain theory time factor

g = finite strain theory coefficient of consolidation

t = real time

ℓ = total depth of solids in sample as previously described

140. Exactly which of the family of curves from Figure 34 is to be used is determined by the equation

$$N = \lambda \ \ell(\gamma_s - \gamma_w) \tag{61}$$

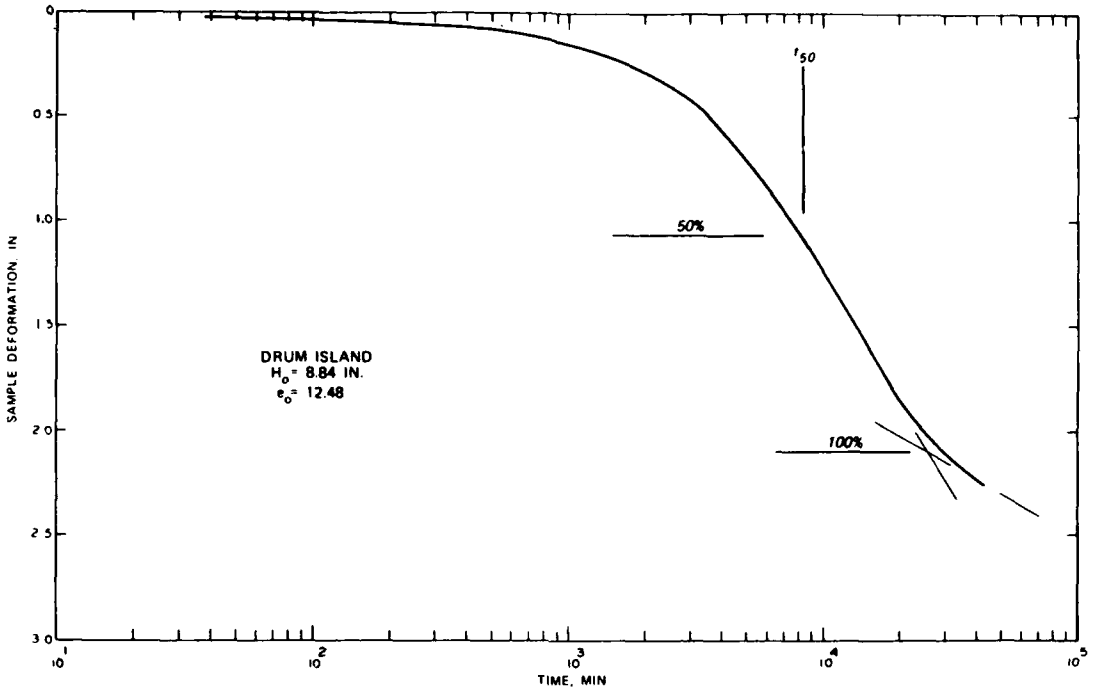

Figure 33. Sample deformation during self-weight consolidation test of Drum Island material, e_o = 12.48

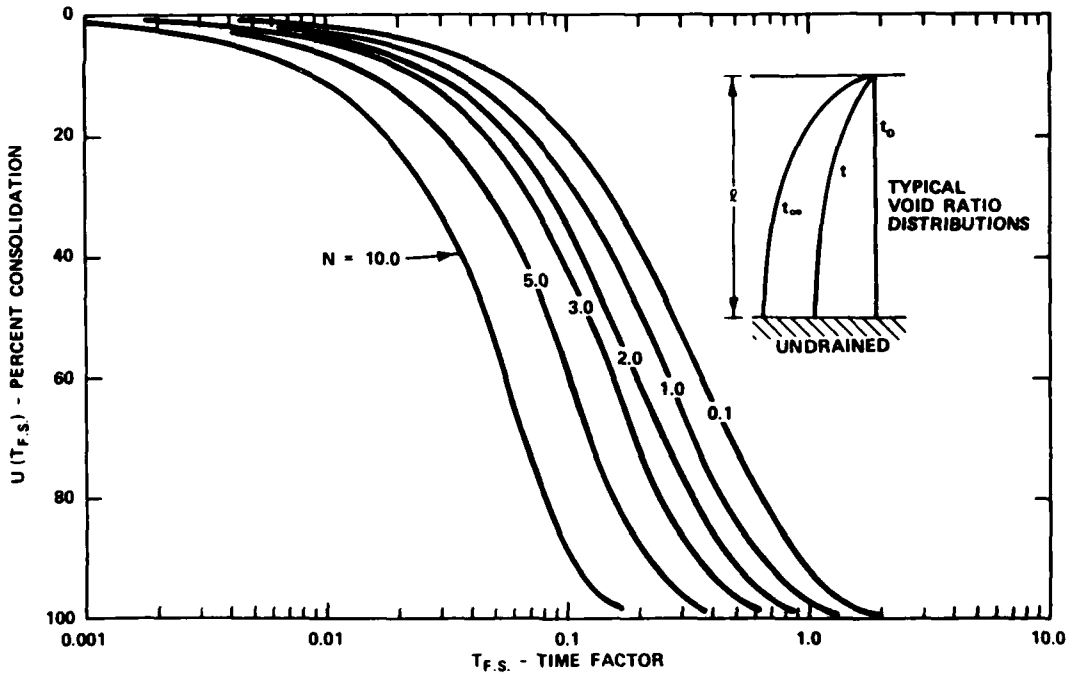

Figure 34. Degree of consolidation as a function of the time factor for dredged material, singly drained layers by linear finite strain theory

where λ = linearization constant describing the soils compressibility and other terms are as previously given.

141. A value for the linearization constant λ is found by matching a curve of

$$e = (e_{oo} - e_{\infty})\exp(-\lambda\sigma') + e_{\infty} \tag{62}$$

where

e_{oo} = void ratio at zero effective stress

e_{∞} = ultimate void ratio

with the $e - \sigma'$ relationship determined from the self-weight consolidation test as in Figure 35. The constants e_{oo}, e_{∞}, and λ are chosen to give the best curve fit.

142. With the values of λ, N, and $T_{f.s.}$ thus determined in turn, the value of the finite strain theory coefficient of consolidation can be calculated from Equation 60. Now,

$$g = -\frac{k}{\gamma_w(1 + e)}\frac{d\sigma'}{de} \tag{63}$$

where

k = permeability

$\frac{d\sigma'}{de}$ = the inverse of the coefficient of compressibility

e = void ratio

Substituting an average void ratio at 50 percent consolidation, a compressibility coefficient calculated at the average void ratio from the $e - \sigma'$ relationship determined in the self-weight test, the value determined for g,

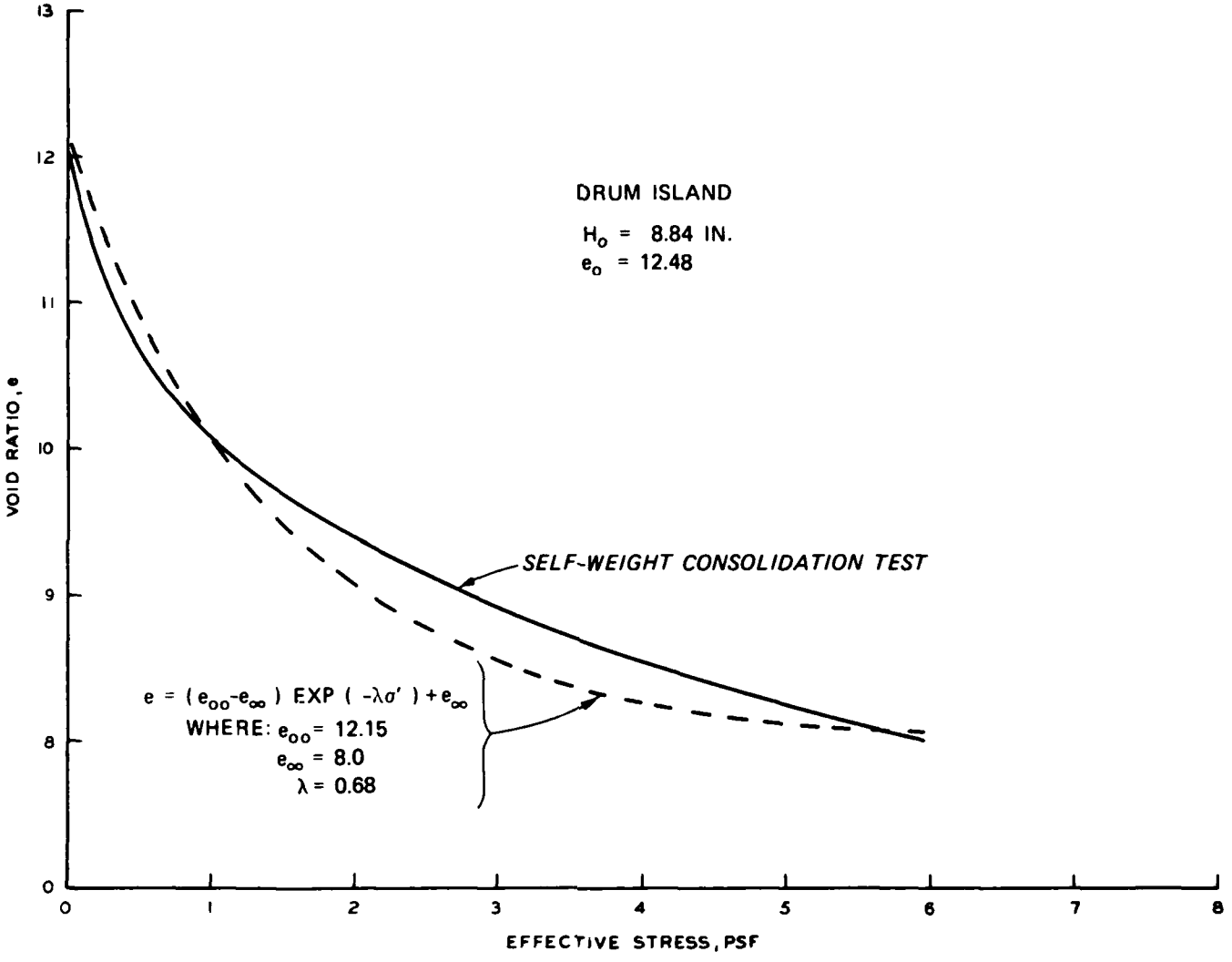

Figure 35. Exponential relationship between void ratio and effective stress chosen to represent results of self-weight consolidation test on Drum Island material, e_o = 12.48

and a value for γ_w enables one to calculate a permeability value which can be associated with the average void ratio.

143. In the computer program LSCRS, permeabilities at the drained boundaries are calculated directly from Darcy's law

$$k = - \frac{\bar{v} \gamma_w}{\frac{du}{d\xi}} \tag{64}$$

where

v = apparent fluid velocity at the boundary

$\frac{du}{d\xi}$ = excess pore pressure gradient at the boundary

In the case of a single drained test, the apparent fluid velocity is equal to the velocity of boundary movement. For doubly drained tests, Equations 52 and 53 are used to estimate the apparent velocities at top and bottom.

144. It is important here to note that calculations in the program LSCRS are at points in the sample. It is incorrect to assume the values of effective stress or permeability calculated for that point to be the true values. Rather, the point calculated values should be considered the extreme values for the average void ratio of the interval between the points.

145. In order to obtain values for permeability at interior points, an estimate of the apparent fluid velocity at those points is necessary. The excess pore pressure gradient is calculated from test measurements. Using the equation of fluid continuity (Equation 15), an appropriate difference equation relating the change in apparent velocity over a material increment to the change in void ratio with time can be written as

$$\Delta\bar{v} = \frac{\Delta\xi}{1 + \bar{e}} \frac{\Delta\bar{e}}{\Delta t} \tag{65}$$

where

$\Delta\xi$ = distance between calculation points

$\bar{e}$ = average void ratio in $\Delta\xi$

$\Delta\bar{e}$ = change in average void ratio over Δt

Δt = time increment

Thus the apparent velocity at an adjacent point is

$$\bar{v}_{i+1} = \bar{v}_i + \Delta\bar{v} \tag{66}$$

and permeability can be calculated for the point on the opposite side of an increment.

Input Data for the Computer Program LSCRS

146. The computer program LSCRS uses the equations of material equilibrium, equation of continuity, and Darcy's Law to estimate the probable relationships between void ratio and effective stress and void ratio and permeability in a soft fine-grained material. The performance of this task requires very accurate measurements of the excess pore pressure distribution within the sample, effective stresses at the boundaries, and the rate of sample deformation. The measurements of deformation rate and boundary effective stresses are straightforward, but determination of excess pore pressure distribution to the required accuracy involves some interpretation.

147. The excess pore pressure distribution within the sample can be determined from discrete measurements taken at ports which are set 1/2 or 1 in. apart by tracking the excess pore pressure decrease at a port as the top boundary moves past the port. Examples of some measured pressure histories are given in the next part. With a continuous plot of excess pore pressure decrease as the boundary approaches, the characteristic curves of normalized pressure versus distance from boundary illustrated in Figure 36 can be developed at average times during the test. Each curve is developed from the information generated at one port. These curves can then be used to estimate the excess pore pressure distribution in the sample at most other times from the measured maximum pressure only. As noted in Figure 36, u_{max} is approached asymptotically. In arriving at the appropriate distribution to use as input for LSCRS, it is recommended that the distance between 99 percent u_{max} and 100 percent u_{max} be set at about the same distance between 0 percent and 99 percent.

148. The pore pressure distribution within the sample near the bottom boundary of a doubly drained sample cannot be scanned continuously using the procedure described above. However, the only reason for there being a difference between pore pressure dissipation at the top and bottom boundaries is the material's buoyant self-weight which is generally less than the lowest reliable pressure which can be measured. Therefore, a mirror image of the top pressure distribution curve is assumed for the lower parts of the sample during doubly drained tests.

149. Specific details of the required input for computer program LSCRS is contained in Appendix C along with an example.

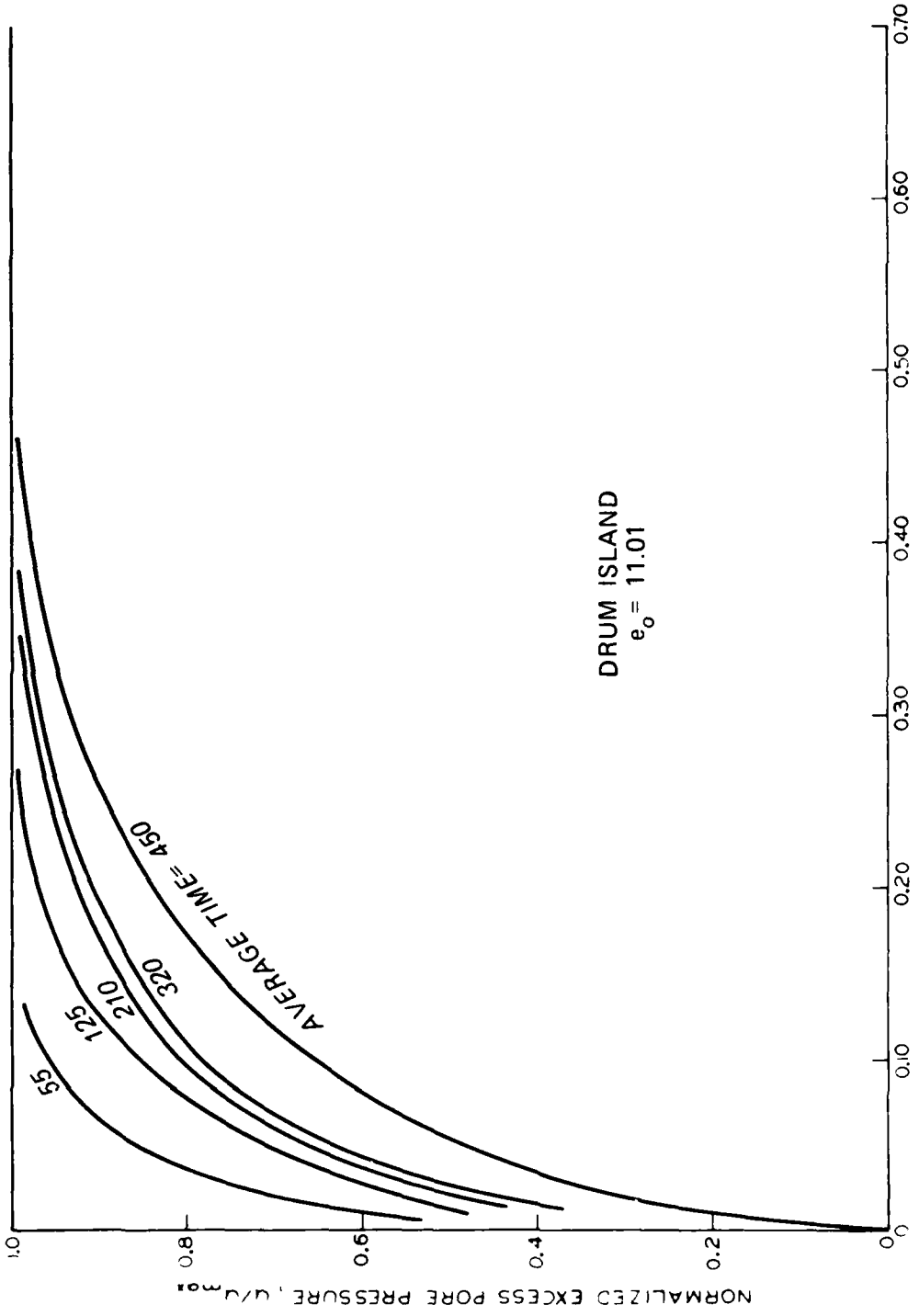

Figure 36. Plot of normalized excess pore pressure near the moving boundary of the LSCRS test on Drum Island material, e_o = 11.01

PART VII: TESTING OF TYPICAL SOFT SOILS

150. In this part, the results of a validation testing program using soils from three different areas are documented. These soils were taken from existing dredged material disposal sites designated Canaveral Harbor, Drum Island, and Craney Island which are near the cities of Port Canaveral, Fla., Charleston, S. C., and Norfolk, Va., respectively. All materials were reconstituted into slurries using water from the navigation channel adjacent to the sites.

151. The results of laboratory testing for basic material characteristics for samples previously taken from these areas are shown in Table 3.

Self-Weight Consolidation Tests

152. Eight separate self-weight consolidation tests were conducted with the soils described above. Figures depicting the time-deformation relationship, final void ratio distribution, and exponential approximation of the void ratio-effective stress relationship for each test, except the one used as an example in Figures 32, 33, and 35, are included in Appendix E. Table 4 summarizes the self-weight testing program and tabulates data used in the calculation of permeabilities corresponding to the given average void ratios.

153. The relationships derived between void ratio and effective stress from this testing are given later along with the results of LSCRS testing.

Table 3

Basic Material Characteristics

Material Location	G_s	LL	PI	Unified Soil Classification
Canaveral Harbor	2.70	143	103	CH
Drum Island	2.60	152	101	CH
Craney Island	2.75	127	88	CH

Table 4

Summary of Self-Weight Consolidation Tests

Material Location	Initial Void Ratio e_o	Initial Height H_o in.	Permeability Calculation Data						Permeability
			t_{50} min	ℓ in.	λ psf^{-1}	N	$\frac{de}{d\sigma'}$	$\bar{e}$	k ft/min
Canaveral Harbor	11.12	4.20	4100	0.35	0.60	1.80	3.26	9.70	6.82×10^{-5}
	9.92	8.90	8800	0.81	0.52	3.68	1.26	9.02	4.37×10^{-5}
	9.79	4.39	3650	0.41	0.80	2.69	1.80	9.24	4.42×10^{-5}
Drum Island	13.62	4.17	2950	0.29	0.95	2.68	4.44	12.10	6.75×10^{-5}
	12.48	8.84	8300	0.66	0.68	3.68	1.85	10.98	5.38×10^{-5}
	12.30	4.28	3300	0.32	1.30	3.79	3.95	10.66	6.19×10^{-5}
Craney Island	12.38	4.34	2000	0.32	1.40	4.07	2.17	10.44	5.50×10^{-5}
	9.26	8.81	5900	0.86	0.45	3.38	1.18	8.35	6.98×10^{-5}

LSCRS Tests

154. In this section, the results of four tests conducted with the subject soils will be described. Table 5 summarizes the LSCRS testing program and gives basic sample conditions. Due to time limitations, all testing was conducted on unconsolidated samples. Later figures will show histories of excess pore pressure measured at various ports in the LSCRS device. Figure 37 shows the location of these ports relative to the lower stationary boundary of the sample.

155. Figures 38-41 show the plots of sample deformation, maximum excess pore pressure, and the decrease in pore pressure as the top boundary passes a port for the various tests. The number by the excess pressure curve indicates at which port the measurement was taken. The broken lines in the figures represent the best estimate of average pressure conditions across a horizontal plane in the sample as it nears the location of the measurement port. Since each pore pressure port is 1/8 in. in diameter, it is impossible to accurately record average pressures at a point as the boundary passes. The velocity of the moving boundary is merely the slope of the deformation-time curve. As can be seen, this velocity is steadily decreasing during the test.

156. Using the digital data from which the above figures were constructed, the variation in normalized excess pore pressure as the boundary passes a port can be graphically depicted as shown in Figures 42, 43, and 44. The results of testing Drum Island material was previously given as Figure 36. As can be seen, these curves are somewhat regular and permit accurate estimation of intermediate times. The excess pore pressure distributions developed from these curves and used in the computer program LSCRS are included in Appendix F.

Table 5

Summary of LSCRS Tests

Material Location	Initial Void Ratio e_o	Initial Height H_o in.	Total Deformation δ in.	Total Time of test t min
Canaveral Harbor	10.55	5.05	2.64	550
	7.56	4.95	2.03	600
Drum Island	11.01	5.12	2.70	555
Craney Island	9.75	5.09	2.71	425

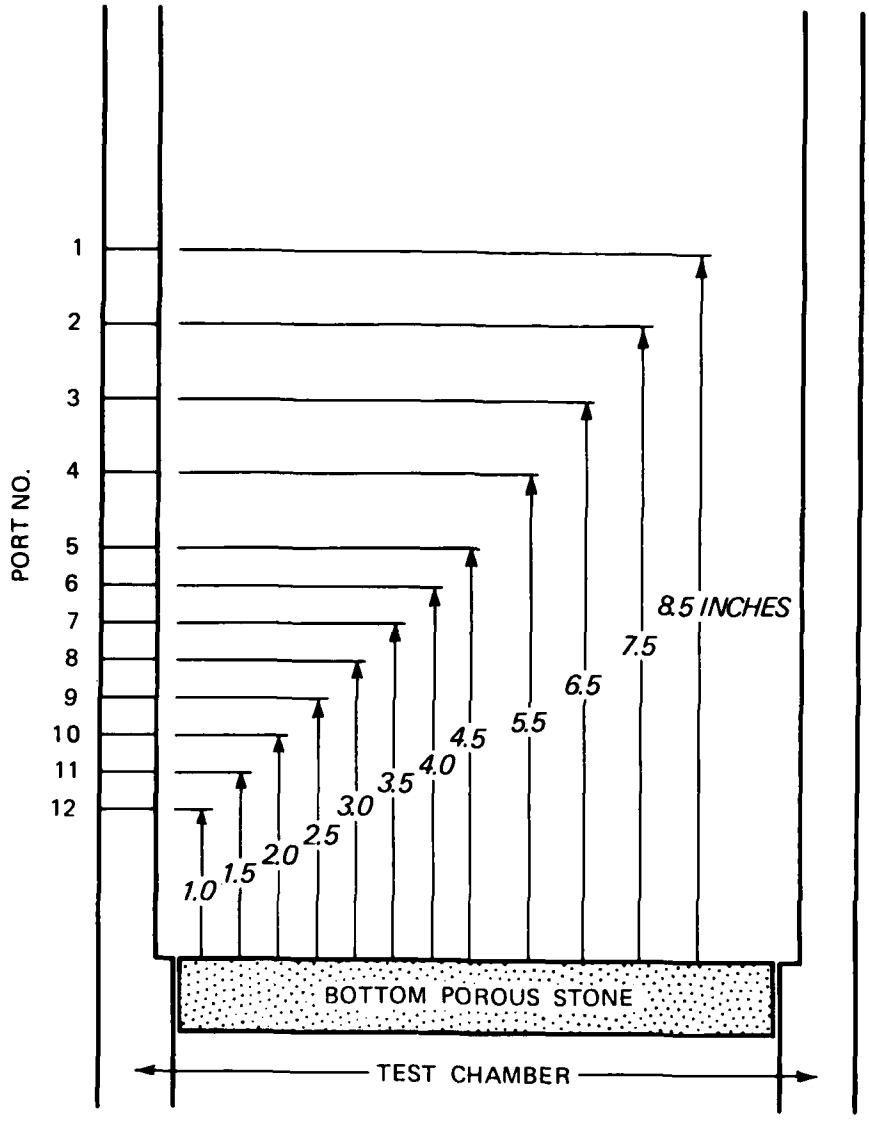

Figure 37. Location of pore pressure measurement ports relative to the bottom sample boundary

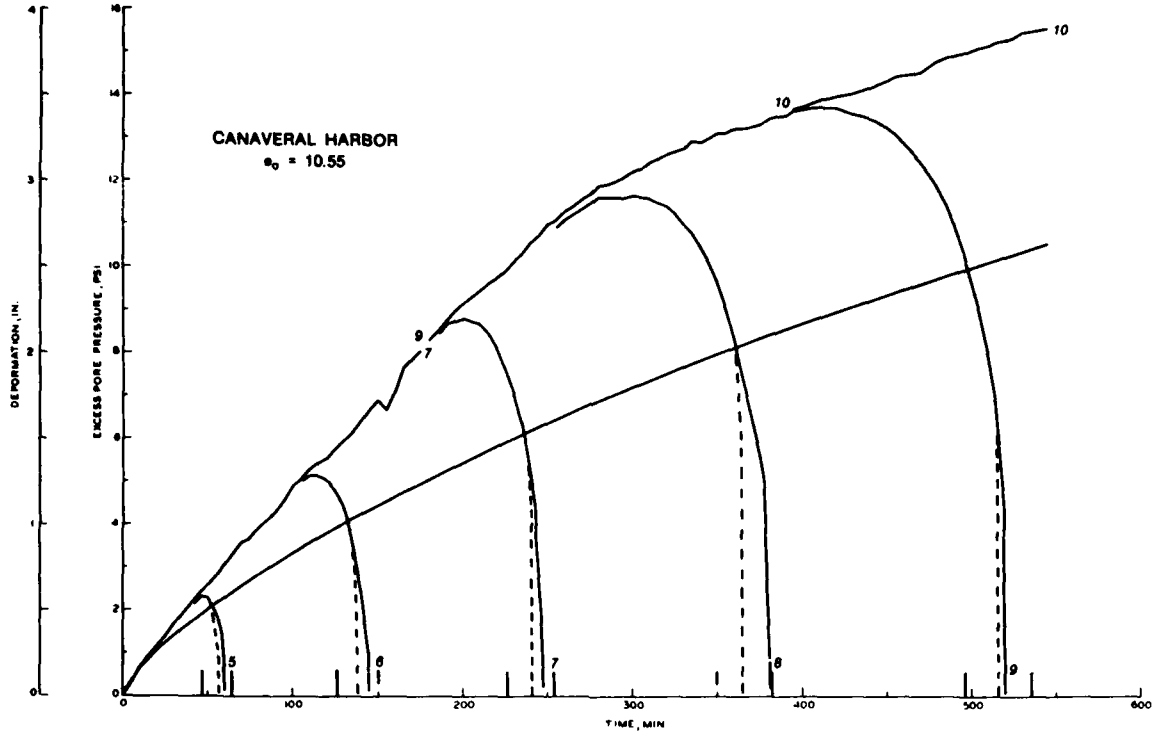

Figure 38. Excess pore pressure and deformation measurement during the LSCRS test on Canaveral Harbor material, e_o = 10.55

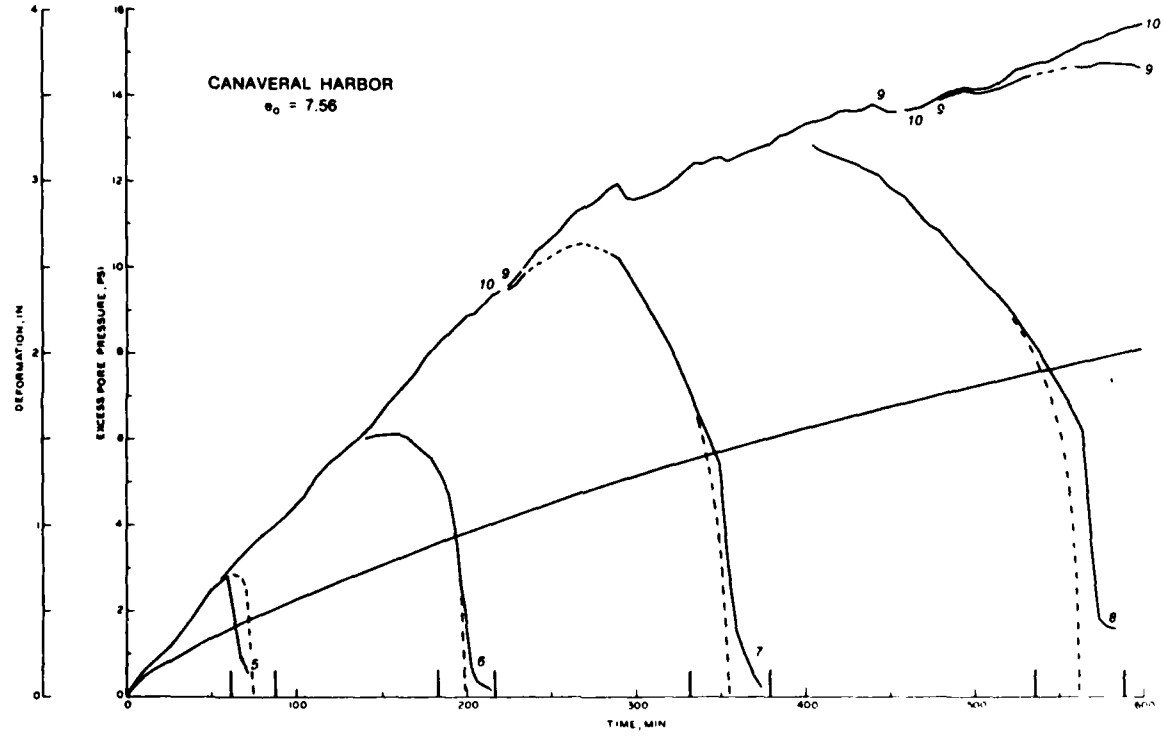

Figure 39. Excess pore pressure and deformation measurement during the LSCRS test on Canaveral Harbor material, e_o = 7.56

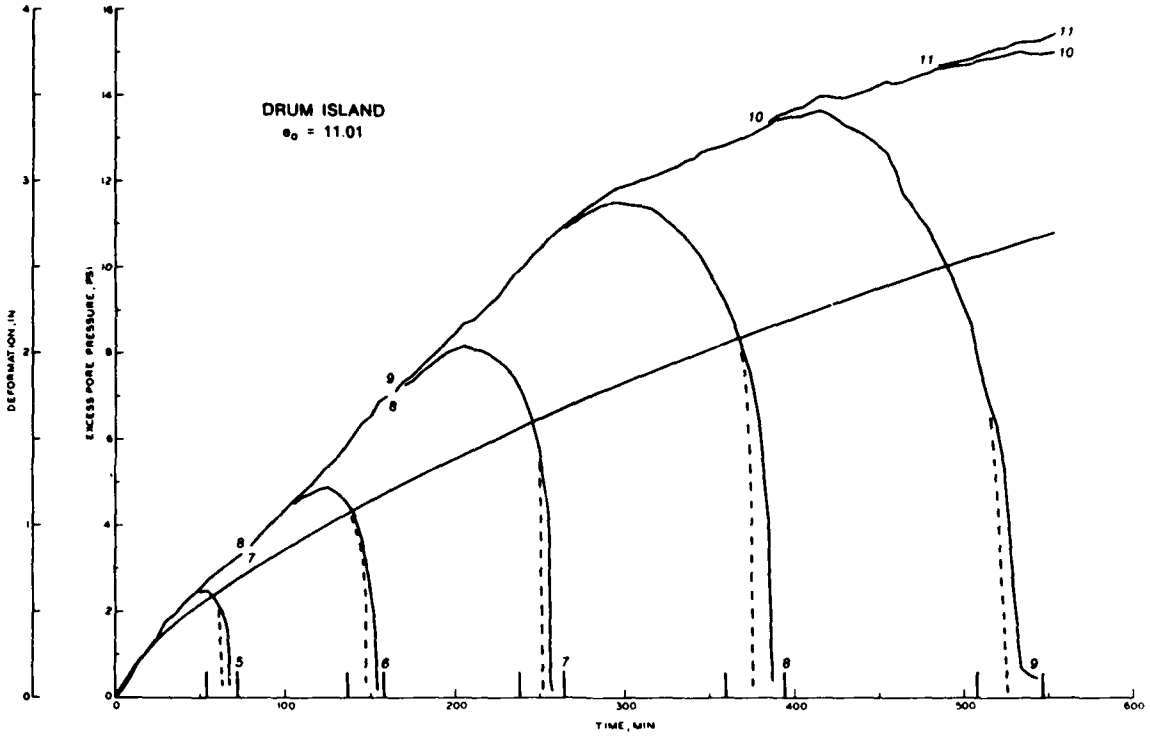

Figure 40. Excess pore pressure and deformation measurement during the LSCRS test on Drum Island material, e_o = 11.01

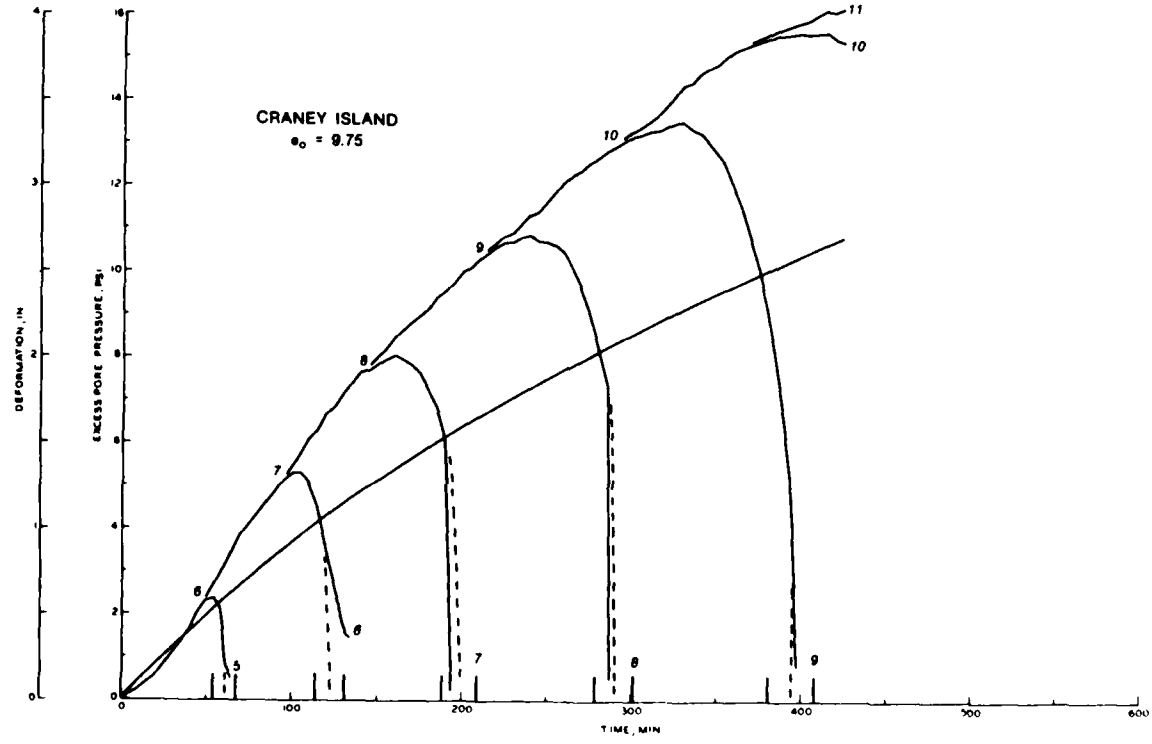

Figure 41. Excess pore pressure and deformation measurement during the LSCRS test on Craney Island material, e_o = 9.75

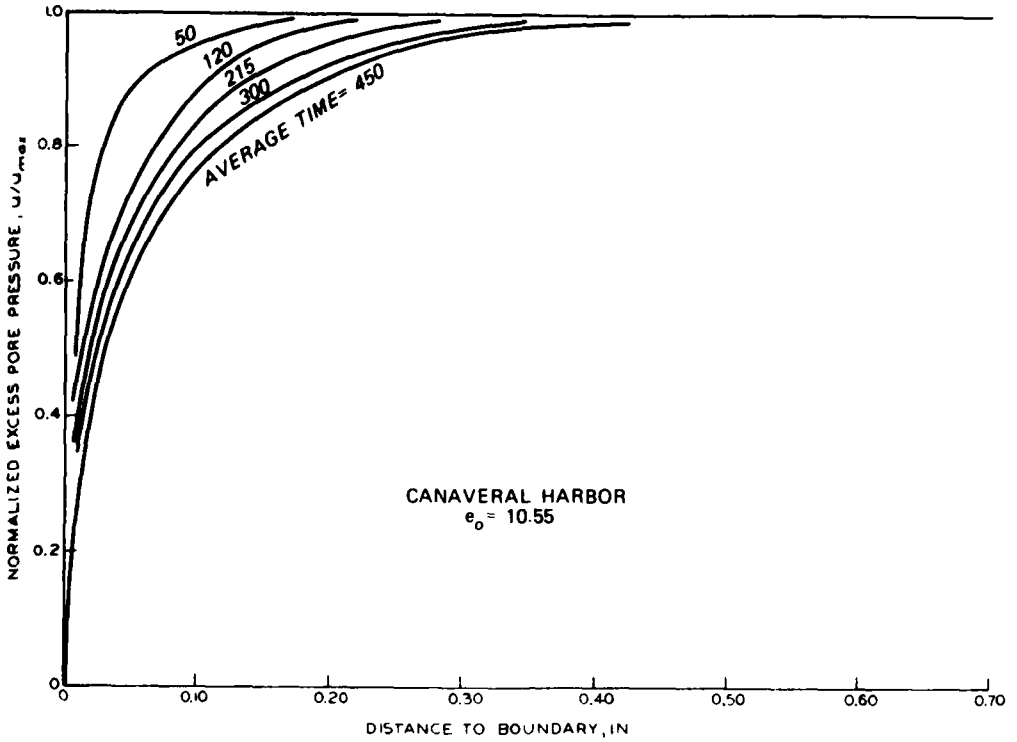

Figure 42. Plot of normalized excess pore pressure near the moving boundary of the LSCRS test on Canaveral Harbor material, e_o = 10.55

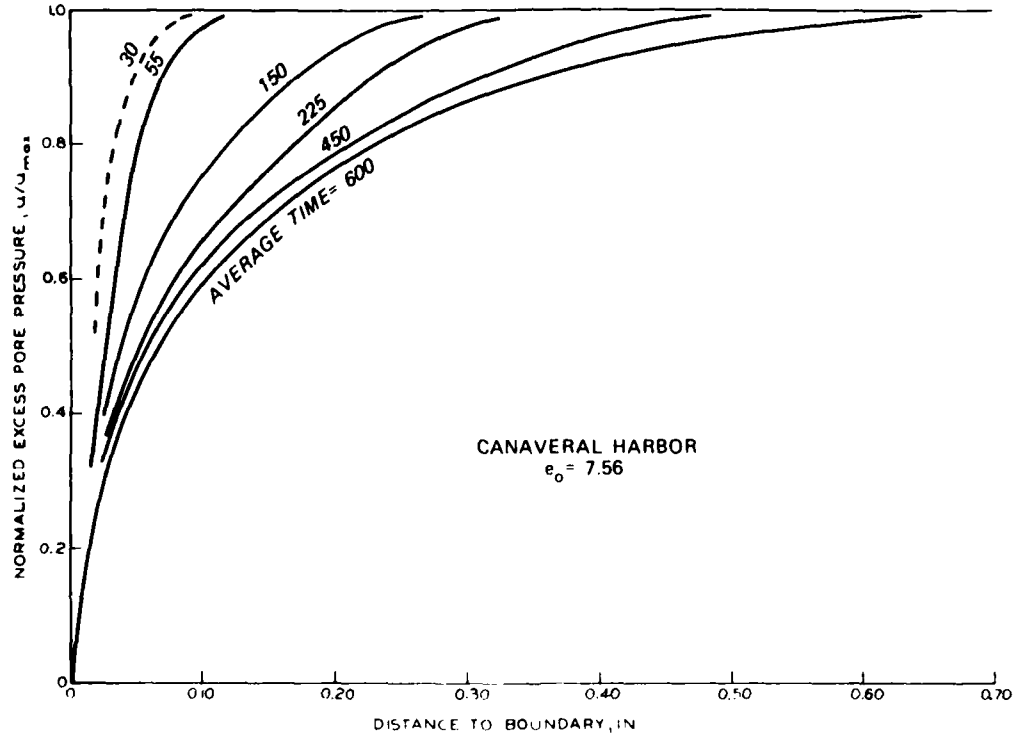

Figure 43. Plot of normalized excess pore pressure near the moving boundary of the LSCRS test on Canaveral Harbor material, e_o = 7.56

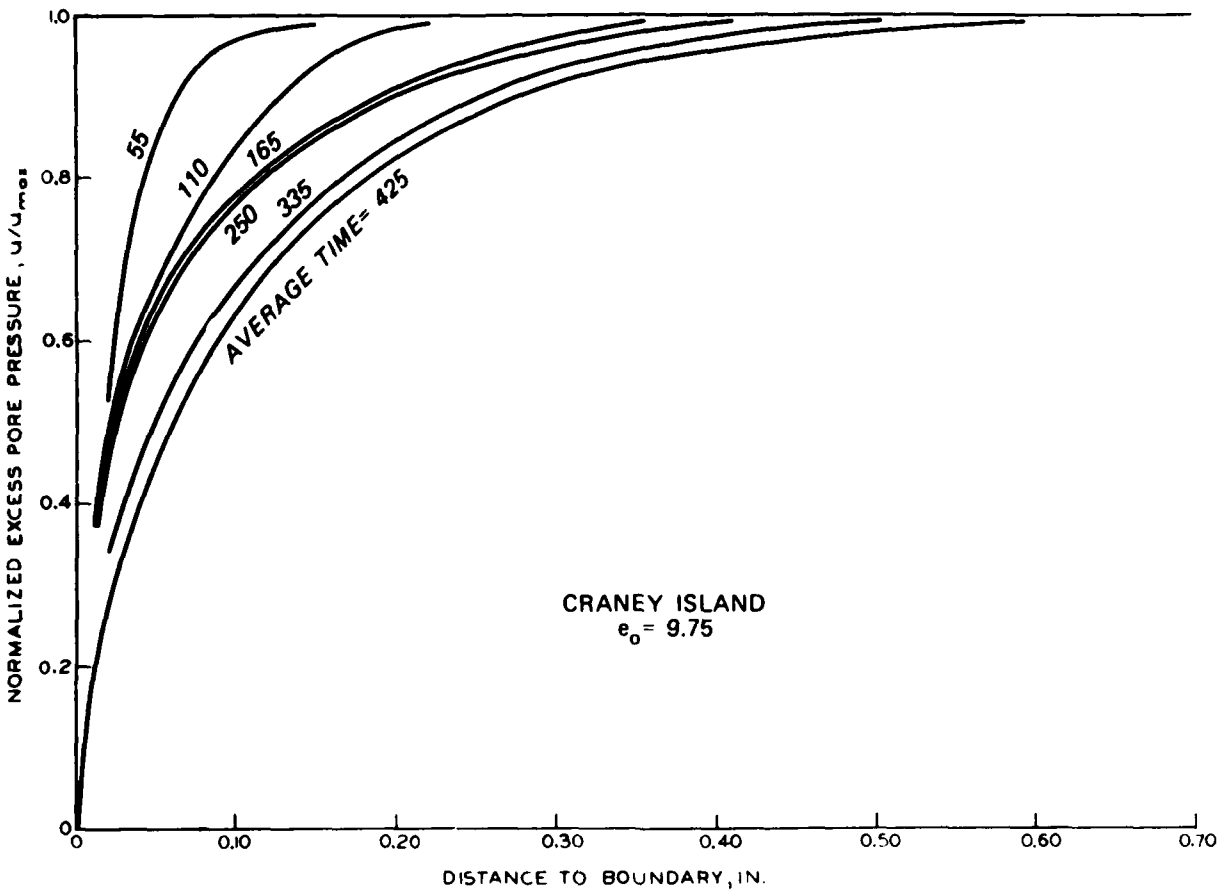

Figure 44. Plot of normalized excess pore pressure near the moving boundary of the LSCRS test on Craney Island material, e_o = 9.75

Relationships

157. The relationships between void ratio and effective stress and void ratio and permeability developed from the preceding self-weight consolidation testing and LSCRS testing are shown in Figures 45 through 50 for the subject materials. Also shown for comparison are these relationships developed from previous conventional oedometer testing of material from the same areas.

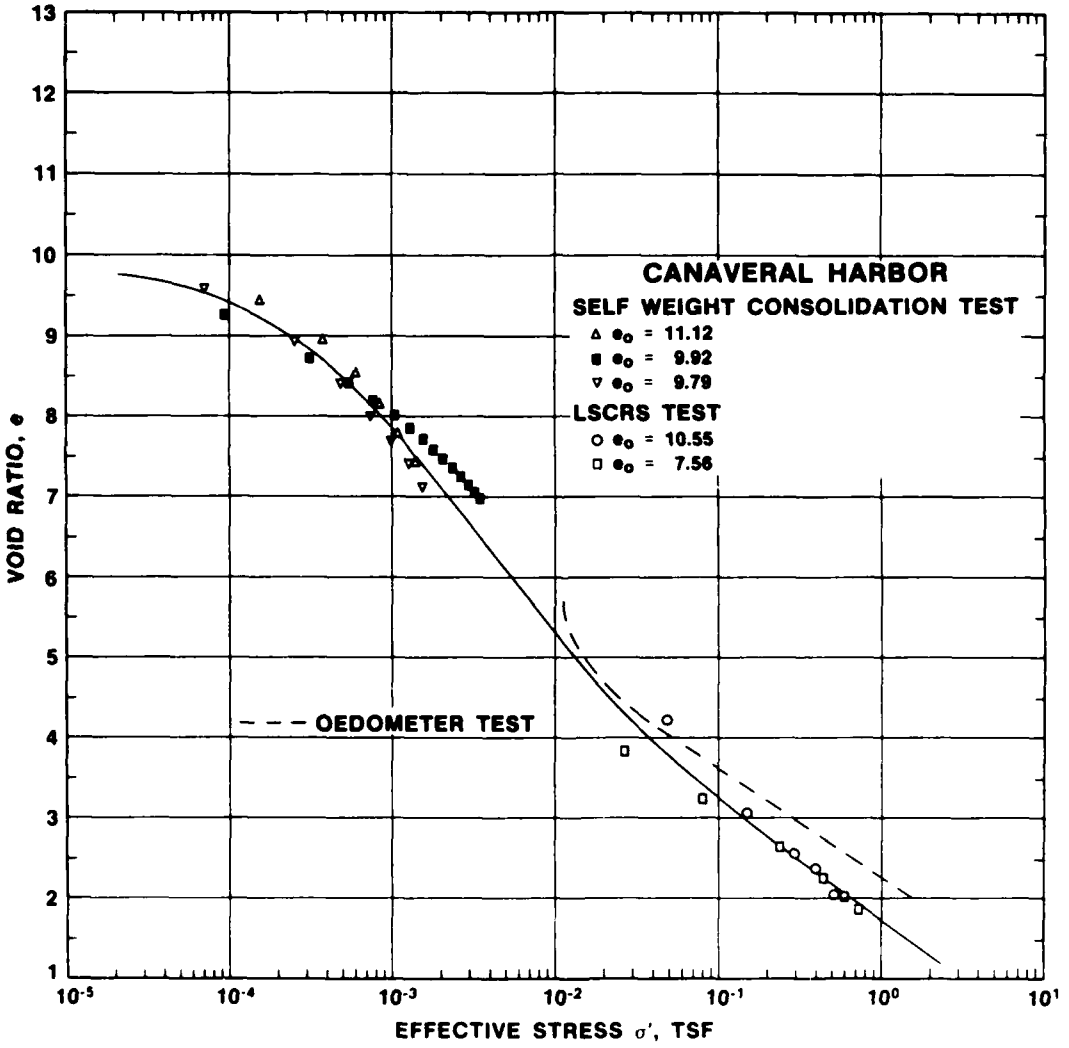

Figure 45. Void ratio-effective stress relationship from self-weight consolidation and LSCRS testing on Canaveral Harbor material

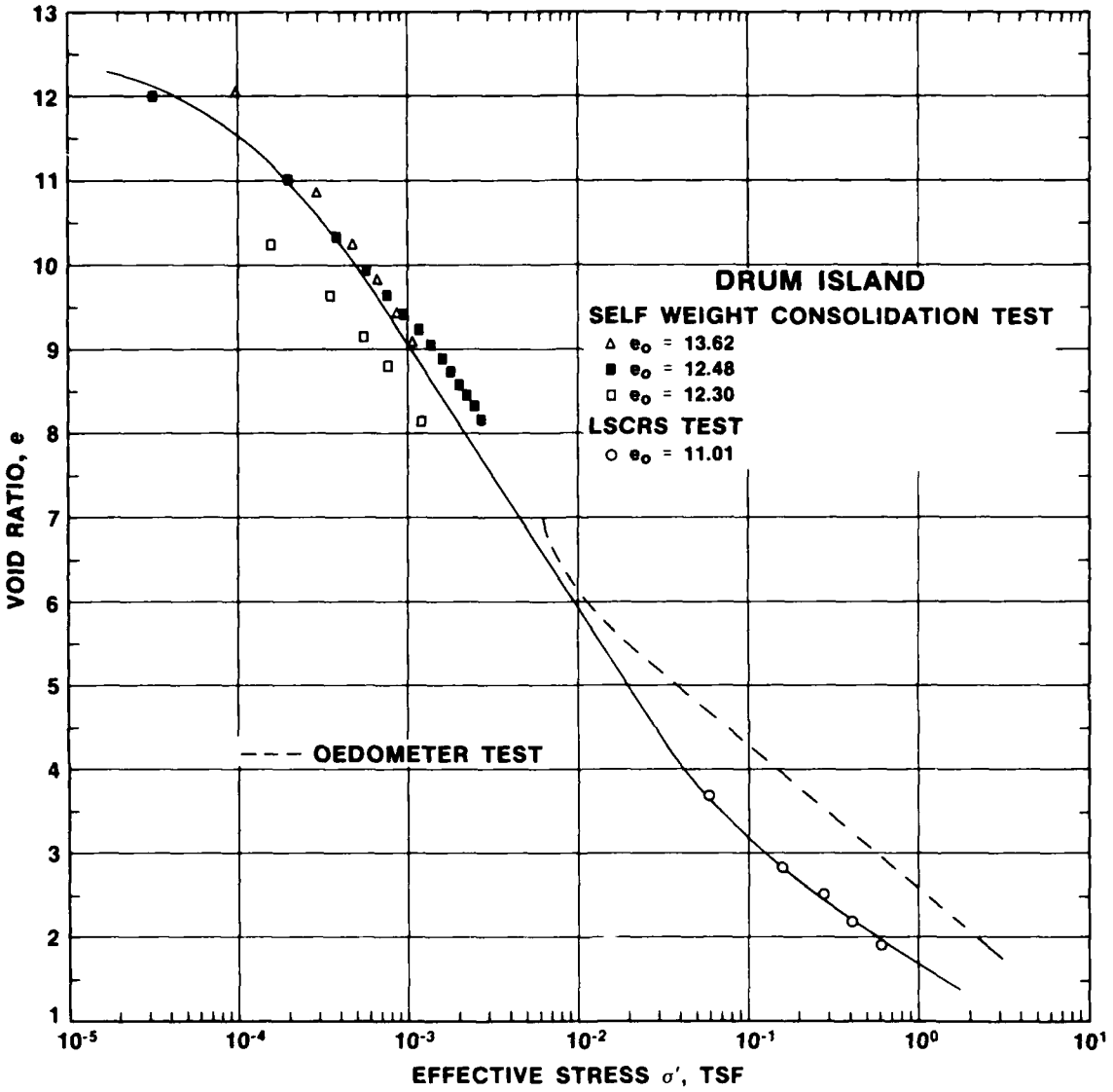

Figure 46. Void ratio-effective stress relationship from self-weight consolidation and LSCRS testing on Drum Island material

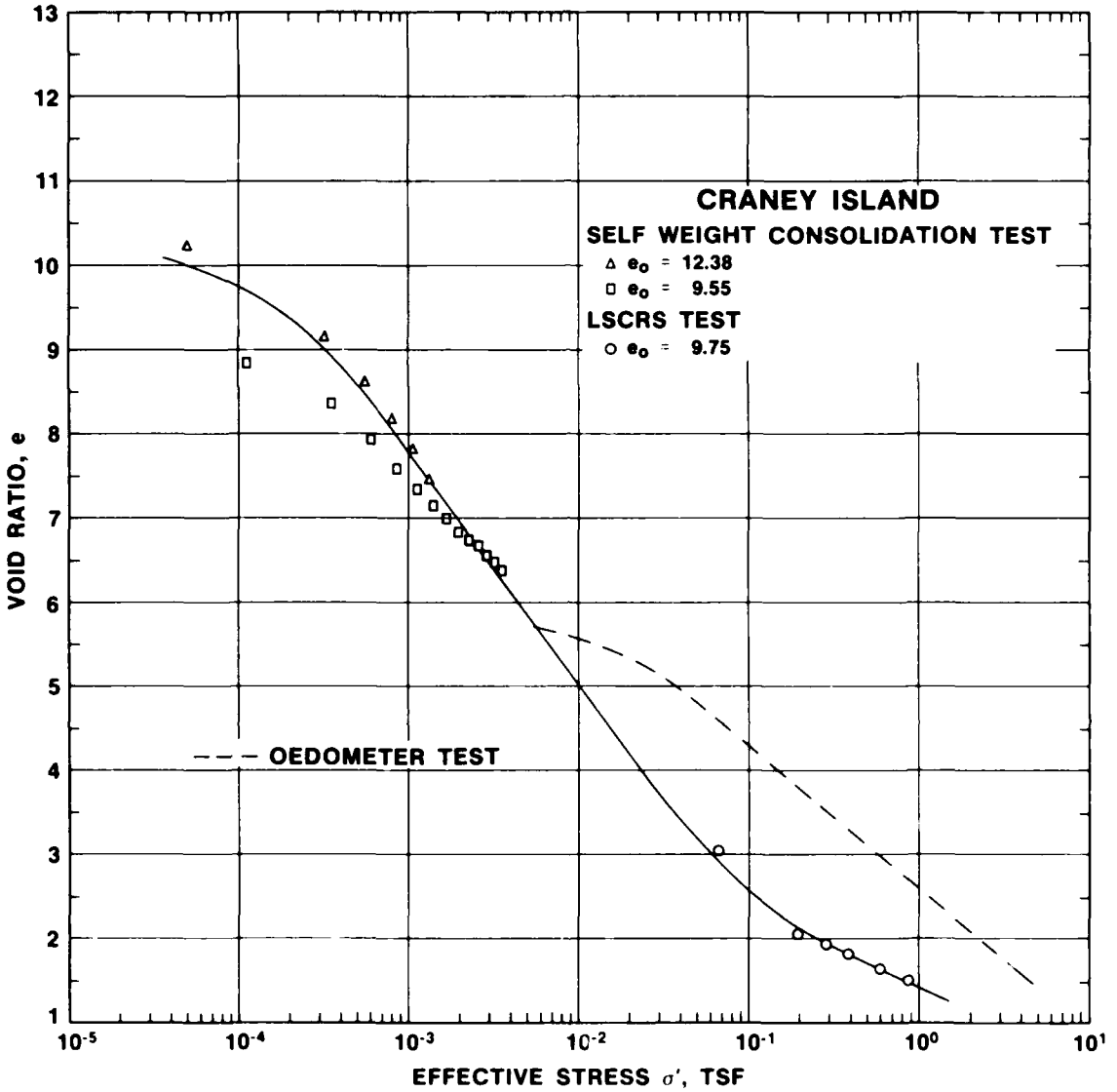

Figure 47. Void ratio-effective stress relationship from self-weight consolidation and LSCRS testing on Craney Island material

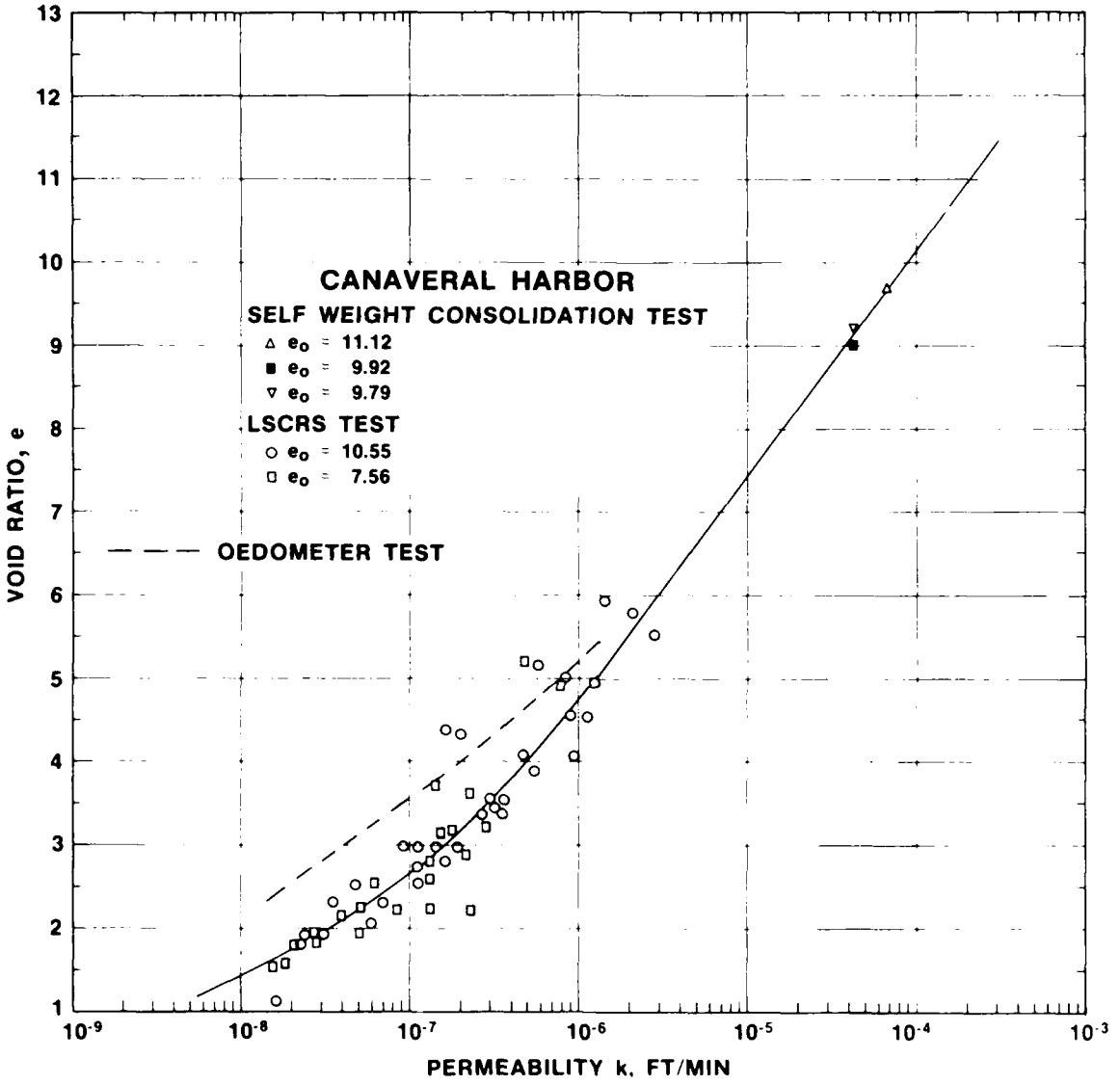

Figure 48. Void ratio-permeability stress relationship from self-weight consolidation and LSCRS testing on Canaveral Harbor material

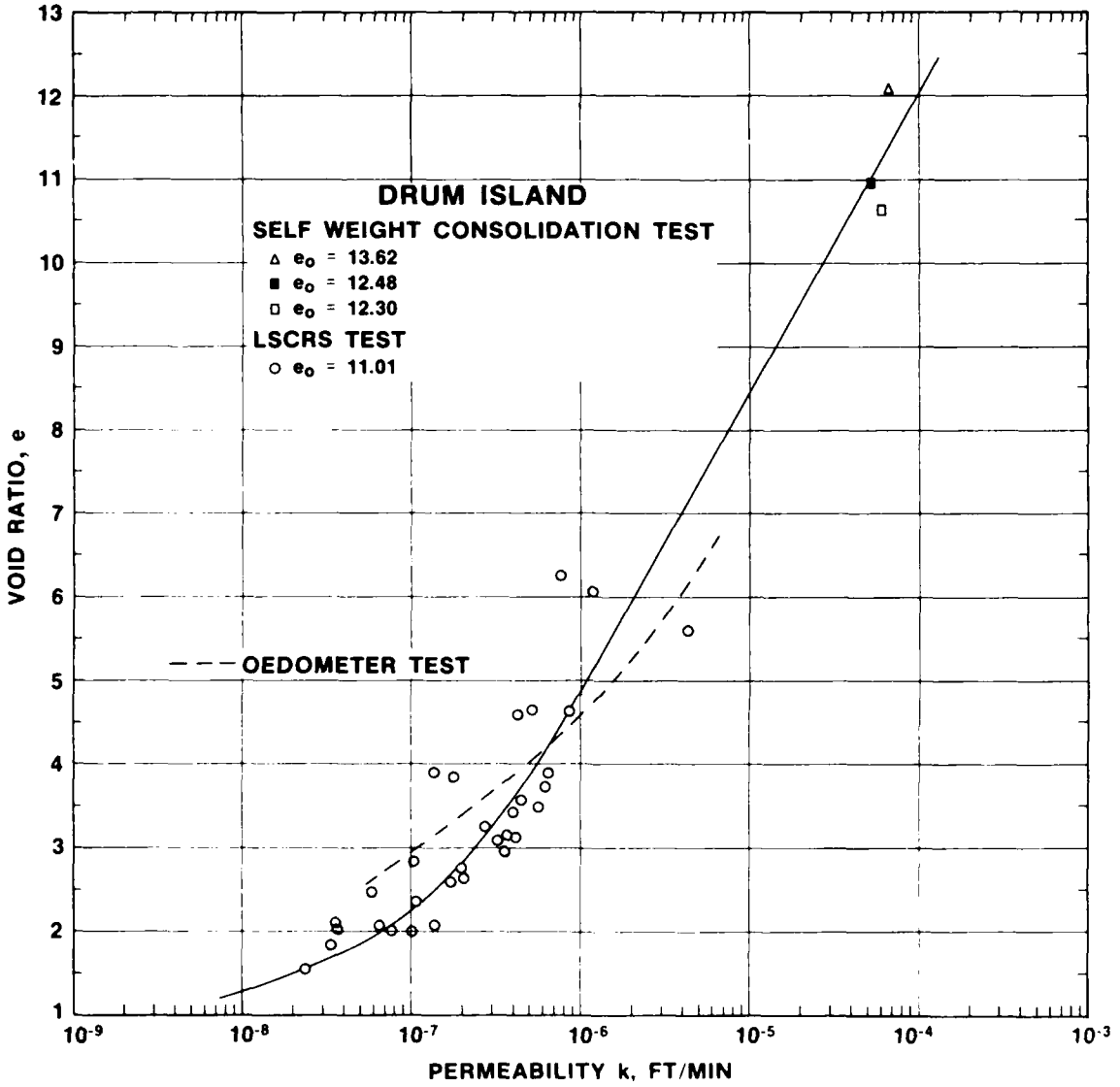

Figure 49. Void ratio-permeability stress relationship from self-weight consolidation and LSCRS testing on Drum Island material

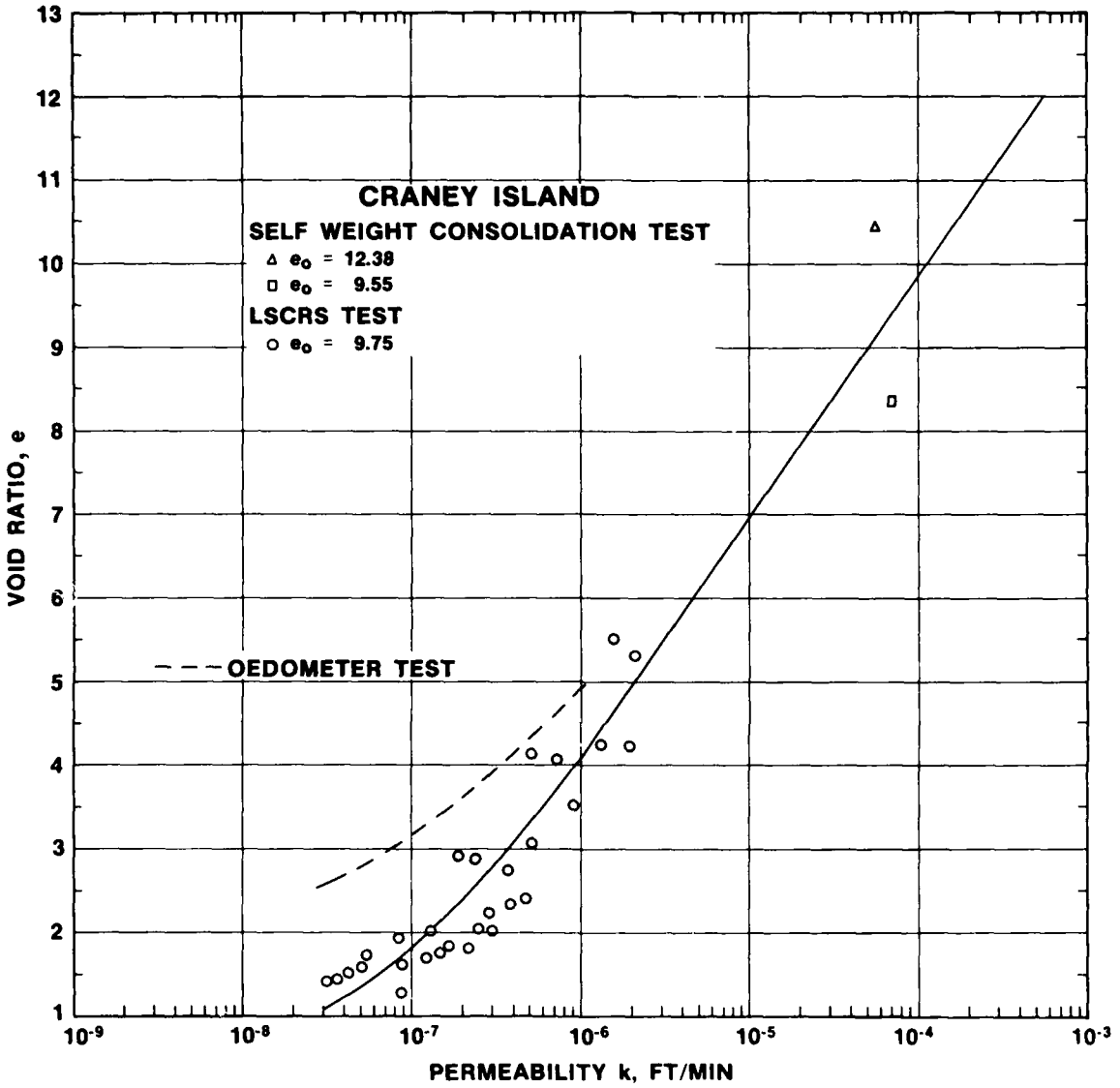

Figure 50. Void ratio-permeability stress relationship from self-weight consolidation and LSCRS testing on Craney Island material

PART VIII: SUMMARY, CONCLUSIONS, AND RECOMMENDATIONS

158. This report has documented the development of a large strain, controlled rate of strain device for consolidation testing of very soft fine-grain materials. The development of a self-weight consolidation device to cover effective stress ranges too small to measure in the LSCRS device has also been included.

159. In consonance with report objectives, the mathematical model of the test to include a governing equation based on finite strain consolidation theory, initial conditions for consolidated or unconsolidated specimen, and boundary conditions for the cases of single or double drainage has been detailed. A parametric study of the consolidation test was conducted to gain insight into the effects of several test variables including strain rates, initial conditions, and boundary conditions. The hardware for conducting LSCRS and self-weight consolidation testing has been fully described along with all required test procedures from sample preparation to data collection. Procedures for interpretation of test measurements to determine soil consolidation properties are provided, and finally the capabilities of the devices are illustrated through a program of typical soft soil testing.

160. Based on the research documented in this report, it is concluded that large strain, controlled rate of strain consolidation testing of very soft soils is a feasible alternative to conventional consolidation testing methods and is superior to other methods in respect to required time of testing. However, several aspects of the testing hardware and test procedures have been identified as a result of this program that need improvement, as discussed below. It is also concluded that the self-weight consolidation test is a simple yet valuable addition to any program of soft soil consolidation

testing. The material properties determined in this test would be unmeasurable in any other known manner because of the extremely low stresses.

161. A primary concern during development of test procedures for the LSCRS device has been that the test be conducive to accomplishment during a normal 8-hr work day. Due to the relatively wide spacing of pore pressure measurement ports and the fact that pore pressure distribution is largely determined as the moving boundary passes a port, relatively high strain rates are required to move the boundary past a sufficient number of ports during the test. These high strain rates lead to a concentration of excess pore pressure dissipation near the drained boundaries that makes it more difficult to properly analyze and interpret test data. The test can be significantly improved by the addition of more closely spaced pressure measurement ports and also decreasing the diameter of these ports to more nearly approach point measurements.

162. The addition of more closely spaced pressure ports will enable the use of slower strain rates and a much thinner sample while accomplishing the test during the desirable 8-hr time period. The use of slower strain rates will reduce the maximum excess pore pressure generated and promote more uniform conditions in the sample. The use of a thinner sample also promotes more uniform conditions, which is also a very desirable test trait.

163. As presently designed, the porous stones transmitting load to the load cells are inset from the main chamber wall and thus cover a reduced area. This condition makes it difficult to accurately calculate effective stresses at the sample's boundary due to the unknown pattern of stress redistribution at the inset. Tests performed during this study were apparently fast enough to produce 100 percent excess pore pressure generation within the material and this pressure was assumed equal to the effective stress at the boundary.

Measurements which were made at the boundary supported this assumption. However, when slower strain rates are used and generated excess pore pressures within the material are less than 100 percent of drained boundary effective stress, a more accurate measurement of this boundary effective stress is required. It is therefore recommended that the device be modified to eliminate the insets at the boundaries to allow load measurement over the entire cross-sectional area of the sample.

164. In general, it is recommended that validation testing in a modified LSCRS device be continued to fine-tune both the device and analysis procedures. The use of the self-weight consolidation test device and analysis procedures is recommended as a valuable supplement to other consolidation testing in order to define consolidation properties at the higher void ratios.

REFERENCES

Bromwell, L. G., and Carrier, W. D. 1979. "Consolidation of Fine-Grained Mining Wastes," Proceedings of the Sixth Panamerican Conference on Soil Mechanics and Foundation Engineering, Lima, Vol 1, pp 293-304.

Cargill, K. W. 1982. "Consolidation of Soft Layers by Finite Strain Analysis," Miscellaneous Paper GL-82-3, US Army Engineer Waterways Experiment Station, Vicksburg, Miss.

_____. 1983. "Procedures for Prediction of Consolidation in Soft, Fine-Grained Dredged Material," Technical Report D-83-1, US Army Engineer Waterways Experiment Station, Vicksburg, Miss.

Gibson, R. E., England, G. L., and Hussey, M. J. L. 1967. "The Theory of One-Dimensional Consolidation of Saturated Clays. I. Finite Non-Linear Consolidation of Thin Homogeneous Layers," Geotechnique, Vol 17, No. 3, pp 261-273.

Gibson, R. E., Schiffman, R. L., and Cargill, K. W. 1981. "The Theory of One-Dimensional Consolidation of Saturated Clays. II. Finite Non-Linear Consolidation of Thick Homogeneous Layers," Canadian Geotechnical Journal, Vol 18, No. 2, pp 280-293.

Imai, G. 1981. "Experimental Studies on Sedimentation Mechanisms and Sediment Formation of Clay Materials," Soils and Foundations, Japanese Society of Soil Mechanics and Foundation Engineering, Vol 21, No. 1.

Mikasa, M. 1965. "The Consolidation of Soft Clay, A New Consolidation Theory and Its Application," Reprint from Civil Engineering in Japan, Japan Society of Civil Engineers, Tokyo.

Monte, J. L., and Krizek, R. J. 1976. "One-Dimensional Mathematical Model for Large-Strain Consolidation," Geotechnique, Vol 26, No. 3, pp 495-510.

Olson, R. E., and Ladd, C. C. 1979. "One-Dimensional Consolidation Problems," Journal of the Geotechnical Engineering Division, American Society of Civil Engineers, Vol 105, GT1, pp 11-30.

Orthenblad, A. 1930. "Mathematical Theory of the Process of Consolidation of Mud Deposits," Journal of Mathematics and Physics, Vol 9, No. 2, pp 73-149.

Pane, V. 1981. One-Dimensional Finite Strain Consolidation, M.S. Thesis, Department of Civil Engineering, University of Colorado, Boulder, Colo.

Schiffman, R. L. 1980. "Finite and Infinitesimal Strain Consolidation," Journal of the Geotechnical Engineering Division, American Society of Civil Engineers, Vol 106, No. GT2, pp 115-119.

Smith, R. E., and Wahls, H. E. 1969. "Consolidation Under Constant Rates of Strain," Journal of the Soil Mechanics and Foundations Division, American Society of Civil Engineers, Vol 95, No. SM2, pp 519-539.

Terzaghi, K. 1924. "Die Theorie der Hydrodynamishen Spanungserscheinungen und ihr Erdbautechnisches Auswendungsgebeit," Proceedings, First International Congress of Applied Mechanics, Vol 1, Delft, The Netherlands, pp 288-294.

_____. 1925. "Principles of Soil Mechanics: IV - Phenomena of Cohesion of Clay," Engineering News Record, Vol 95, No. 22.

Umehara, Y., and Zen, K. 1980. "Constant Rate of Strain Consolidation for Very Soft Clayey Soils," Soils and Foundations, Vol 20, No. 2, pp 79-95.

_____. 1982. "Consolidation and Settling Characteristics of Very Soft Contaminated Sediments," Management of Bottom Sediments Containing Toxic Substances; Proceedings of the 6th US/Japan Experts Meeting, US Army Engineer Waterways Experiment Station, Vicksburg, Miss.

US Army Corps of Engineers. 1980. "Laboratory Soils Testing," EM 1110-2-1906, Office, Chief of Engineers, Washington, DC.

Wissa, A. E. Z., et al. 1971. "Consolidation at Constant Rate of Strain," Journal of the Soil Mechanics and Foundations Division, American Society of Civil Engineers, Vol 97, No. SM10, pp 1393-1413.

Znidarcic, D. 1982. Laboratory Determination of Consolidation Properties of Cohesive Soil, Ph.D Thesis, Department of Civil Engineering, University of Colorado, Boulder, Colo.

Znidarcic, D., and Schiffman, R. L. 1981. "Finite Strain Consolidation: Test Conditions," Journal of the Geotechnical Engineering Division, American Society of Civil Engineers, Vol 107, No. GT5, pp 684-688.

APPENDIX A: USER'S GUIDE FOR COMPUTER PROGRAM CRST

1. This appendix provides information useful to users of the Computer Program CRST (Controlled Rate of Strain Test), including a general description of the program processing sequence, definitions of principal variables, and format requirements for problem input. The program was originally written for use on the WES Time-Sharing System, but could be readily adapted to batch processing through a card reader and high-speed line printer. Some output format changes would be desirable if the program were used in batch processing to improve efficiency.

2. The program is written in FORTRAN IV computer language with seven-digit line numbers. However, characters 8 through 79 are formatted to conform to the standard FORTRAN statement when reproduced in spaces 1 through 72 of a computer card. Program input is through a quick access type file previously built by the user. Output is either to the time-sharing terminal or to a quick access file at the option of the user. Specific program options will be fully described in the remainder of this appendix.

3. A listing of the program is provided in Appendix B. Typical problem input and solution output are contained in this appendix.

Program Description and Components

4. CRST is composed of the main program ad six subroutines. It is broken down into subprograms to make modification and understanding easier. The program is also well documented throughout with comments, so a detailed description will not be given. However, an overview of the program structure is shown in Figure A1, and a brief statement about each part follows:

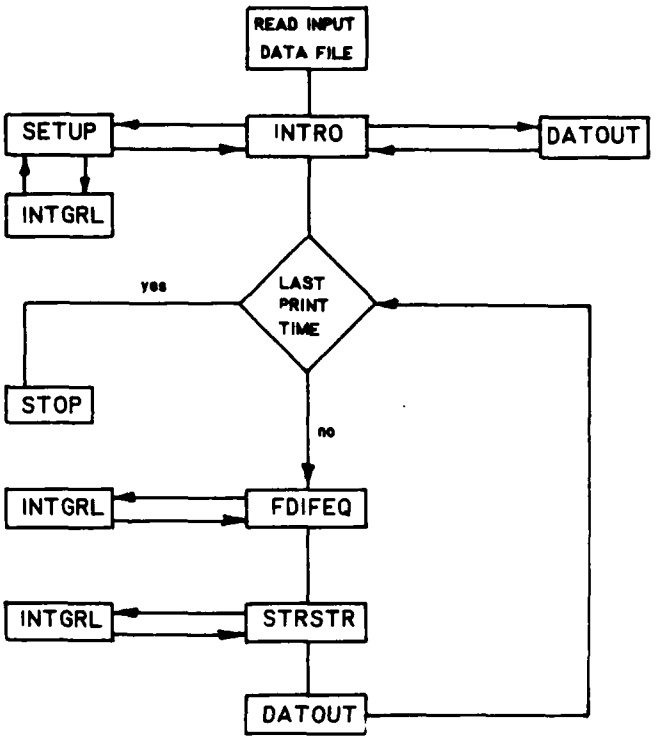

Figure A1. Flow diagram of computer program CRST

a. Main program. In this part, problem options and input data are read and the various subroutines are called to print initial data, calculate consolidation to specified times, calculate stresses, and print solution output.

b. Subroutine INTRO. This subprogram causes a heading to be printed, prints soil and calculation data, and prints initial conditions in the test specimen.

c. Subroutine SETUP. SETUP calculates the initial void ratios, coordinates, stresses, and pore pressures in the test specimen. It also calculates the various void ratio functions:

$$\frac{k}{1+e}, \frac{d\sigma'}{de}, \alpha(e), \text{ and } \beta(e)$$

from input relationships between void ratio, effective stress, and permeability (see Cargill (1982) for complete description of these void ratio functions).*

d. Subroutine FDIFEQ. This is where consolidation is actually calculated. A finite difference equation is solved for each total point in the test specimen at each time step between specified

---

* All references cited in this appendix are included in the References at the end of the main test.

output times. Void ratio functions and new conditions at top and bottom boundaries are also recalculated at each time step. The void ratio profile is also adjusted at each time step to require agreement between calculated and induced settlement. Just before each output time, consistency and stability criteria are checked.

e. Subroutine STRSTR. Here, the current convective coordinates, soil stresses, and pore pressures are calculated for each output time. Final void ratios for a constant ram load and current settlement are also calculated for use in determining percent consolidation.

f. Subroutine INTGRL. This subroutine evaluates the void ratio integral used in determining convective coordinates, settlements, and soils stresses. The procedure is by Simpson's rule for odd or even numbered meshes.

g. Subroutine DATOUT. DATOUT prints the results of consolidation calculations and initial conditions in tabular form.

Variables

5. The following is a list of the principal variables and variable arrays that are used in the Computer Program CRST. The meaning of each variable is also given along with other pertinent information about it. If the variable name is followed by a number in parentheses, it is an array, and the number denotes the current array dimensions. If these dimensions are not sufficient for the problem to be run, they must be increased throughout the program. A more detailed description of the variables concerning coordinates and void ratio functions can be found in Cargill (1982).

A(15) the Lagrangian coordinate of each space mesh point in the test specimen.

AF(15) the function $\alpha(e)$ corresponding to the current void ratios at each space mesh point in the test specimen

ALPHA(51) the function $\alpha(e)$ corresponding to the void ratios input when describing the void ratio-effective stress and permeability relationships for the test specimen.

BETA(51) the function $\beta(e)$ corresponding to the void ratios input when describing the void ratio-effective stress and permeability relationships for the test specimen.

BF(15) the function $\beta(e)$ corresponding to the current void ratios at each space mesh point in the test specimen.

BP the hydrostatic backpressure to which the test specimen is subjected during testing.

DA the difference between the Lagrangian coordinates of space mesh points in the test specimen.

DSDE(51) the calculated value of $\frac{d\sigma'}{de}$ corresponding to the void ratios input when describing the void ratio-effective stress relationship for the test specimen.

DZ the difference between the material or reduced coordinates of space mesh points in the test specimen.

E(15) the current void ratios at each space mesh point in the test specimen.

EØØ the initial void ratio assumed by the fine-grained material after initial sedimentation and before consolidation.

EFIN(15) the final (100 percent primary consolidation) void ratios at each space mesh point in the test specimen if the ram load were held constant at its current value.

EFS(15) the effective stress at each space mesh point in the test specimen.

ELL	the total height of the test specimen in material or reduced coordinates.
ES(51)	the void ratios input when describing the void ratio-effective stress and permeability relationships in the test specimen.
F(15)	the void ratios at each space mesh point of the previous time step in the test specimen.
FINT(15)	the void ratio integrals evaluated from the bottom to the subscripted space mesh point in the test specimen.
GMC	the buoyant unit weight of the fine-grained material solids.
GMS	the unit weight of the fine-grained material solids.
GMW	the unit weight of water.
GS	the specific gravity of the fine-grained material solids.
H	the initial height of the unconsolidated test specimen in Lagrangian coordinates.
HØ	the height of the test specimen at the start of testing in Lagrangian coordinates. May be unconsolidated height or height after self-weight consolidation.
HW	the height of the free-water surface above the bottom of the test specimen.
IN	an integer denoting the input mode or device for initial problem data which has the value "10" in the present program.
IOUT	an integer denoting the output mode or device for recording the results of program computations in a user's format which has the value "11" in the present program.

NBDIV — the number of parts into which the initial test specimen is divided for computation purposes.

ND — the total number of calculation points in the space mesh of the test specimen. Includes bottom image point.

NDOPT — an integer denoting the following options:

1 = test specimen is freely drained from the top only.

2 = test specimen is freely drained from the top and bottom.

NNN — an integer counter which is used in tracking the total number of time steps through which consolidation has proceeded.

NOPT — an integer denoting the following options:

1 = test specimen is initially unconsolidated.

2 = test specimen is initially consolidated under its own self weight.

NPROB — an integer used as a label for the current consolidation problem.

NPT — an integer denoting the following options:

1 = make a complete computer run, printing soil data, initial conditions, and current conditions for all specified print times.

2 = make a complete computer run but do not print soil data and initial conditions.

3 = terminate computer run after printing soil data and initial conditions.

NS — the number of data points used in describing the void ratio-effective stress and permeability relationships in the test specimen. The number should be sufficient to cover the full range of expected or possible void ratios.

NST — an integer line number used on each line of input data.

NTD — the total number of calculation points in the space mesh of the test specimen. Includes top and bottom image points.

NTIME — the number of data output times during the computer simulation of a controlled rate of strain test.

PK(51) — the function $\frac{k}{1 + e}$ corresponding to the void ratios input when describing the void ratio-permeability relationship in the fine-grained material.

PRINT(50) — the real times at which current conditions in the consolidation test will be output.

RK(51) — the permeabilities input when describing the void ratio-permeability relationship in the fine-grained material.

RN — a multiplier used to change the values of input permeabilities. Used to study the effects of a changed permeability without rewriting entire data input file.

RS(51) — the effective stresses input when describing the void ratio-effective stress relationship in the fine-grained material.

SETT — the current total settlement in the test specimen due to calculated consolidation. Calculated from void ratio integral.

SFIN	the final settlement in the test specimen if the ram load is held constant.
TAU	the value of the time step in the finite difference calculations.
TIMEØ	the time at which the current calculation loop began.
TIME	the real time value after each time step.
TPRNT	the real time value of the next output point.
TOS(15)	the current total stress at each space mesh point in the test specimen.
U(15)	the current excess pore pressure at each space mesh point in the test specimen.
UØ(15)	the current static pore pressure at each space mesh point in the test specimen.
UCON	the current degree of consolidation in the test specimen.
UW(15)	the current total pore pressure at each space mesh point in the test specimen.
V(50)	the various upper boundary velocities to which the specimen will be exposed during the controlled rate of strain test.
VEL	the current actual velocity of the top boundary of the test specimen.
VEL1	the effective velocity of the top boundary of the test specimen.
VEL2	the effective velocity of the bottom boundary of the test specimen.

VSETØ — the total settlement in the test specimen calculated from the velocity of the upper boundary and elapsed time at the time at which the current calculation loop began.

VSET — the current total settlement in the test specimen calculated from the velocity of the upper boundary and elapsed time.

VRI1 — the total void ratio integral in the test specimen when the test begins.

XI(15) — the current convective coordinate of each space mesh point in the test specimen.

Z(15) — the material or reduced coordinate of each space mesh point in the test specimen.

Problem Data Input

6. The method of inputting problem data in CRST is by a free field data file containing line numbers. The line number must be eight characters or less for ease in file editing and must be followed by a blank space. The remaining items of data on each line must be separated by a comma or blank space. Real data may be either written in exponential or fixed decimal formats, but integer data must be written without a decimal.

7. For a typical problem run, the data file should be sequenced in the following manner:

a. NST,NPROB,NPT,NOPT,NDOPT,RN

b. NST,H,EØØ,GS,GMW,HW,BP,NS

c. NST,ES(I),RS(I),RK(I)

d. NST,TAU,NBDIV,VEL,NTIME

e. NST,PRINT(I),V(I)

It should be pointed out here that NSI may be any positive integer but must increase throughout the file so that it will be read in the correct sequence in the time-sharing system. It should also be noted that there are NS of line type c and NTIME of line type e .

8. All input data having particular units must be consistent with all other data. For example, if specimen thickness is in inches and time is in minutes, then permeability must be in inches per minute. If stresses are in pounds per square inch, then unit weights must be in pounds per cubic inch. Any system of units is permissible so long as consistency is maintained.

9. An example of an input data file is shown in Figure A2. This is the file used for simulated test number 12 which was discussed in Part III of this report.

Program Execution

10. Once an input data file has been built as described in the previous section, the program is executed on the WES Time-Sharing System by the following FORTRAN command:

RUN RØGEØ4Ø/CRST,R#(filename)"1Ø";"11"

where: (filename) = the name of the previously built file in the user's catalog which contains the input data set as described in paragraph 7 above.

```
*LIST  DF10

101    12    1    2    2    1.0
102    6.    12.    2.7    0.0361111    12.    0.    24
200    12.0    0.0          8.64E-03
201    11.5    4.00E-03     5.40E-03
202    11.0    8.89E-03     3.38E-03
203    10.5    1.36E-02     2.14E-03
204    10.0    1.96E-02     1.32E-03
205     9.5    2.87E-02     8.34E-04
206     9.0    4.17E-02     5.22E-04
207     8.5    6.07E-02     3.28E-04
208     8.0    8.82E-02     2.05E-04
209     7.5   12.71E-02     1.30E-04
210     7.0   18.47E-02     8.16E-05
211     6.5   26.81E-02     5.10E-05
212     6.0   39.03E-02     3.23E-05
213     5.5   56.94E-02     2.02E-05
214     5.0   81.25E-02     1.20E-05
215     4.5   12.50E-01     7.14E-06
216     4.0   22.08E-01     3.98E-06
217     3.5   42.92E-01     2.05E-06
218     3.0   85.42E-01     9.24E-07
219     2.8   11.25E-00     6.24E-07
220     2.6   14.58E-00     4.06E-07
221     2.4   19.31E-00     2.45E-07
222     2.2   25.14E-00     1.46E-07
223     2.0   33.19E-00     8.46E-08
300  1.    10    3.0E-03    19
401     60    3.E-03
402    120    3.E-03
403    240    2.E-03
404    241    2.E-03
405    245    2.E-03
406    250    2.E-03
407    360    2.E-03
408    480    1.E-03
409    485    1.E-03
410    960    1.E-03
411   1440    7.5E-04
412   1445    7.5E-04
413   1920    7.5E-04
414   2400    5.E-04
415   2405    5.E-04
416   2880    5.E-04
417   3360    2.5E-04
418   3365    2.5E-04
419   3840    2.5E-04
```

Figure A2. Example of input data file for computer program CRST

Computer Output

11. Execution by the above command will cause output to be printed on the time-sharing device. If it is desired to save the output in a file for later printing, the filename should be inserted before the output mode code "11."

12. Program output is formatted for the eighty character line of a time-sharing terminal. Since printing at a time-sharing terminal is relatively slow, an option is provided which can be used to eliminate some data which may be repetitions of previous problem runs. All options are fully described in the previous sections of this appendix. Figure A3 contains a sample of output data also from simulated test number 12 of Part III.

**********CURRENT CONDITIONS IN SAMPLE**********

XI COORDINATE	E VOID RATIO	EFFECTIVE STRESS	*PORE PRESSURE* TOTAL	EXCESS
3.17784	5.01152	0.80690	0.31858	-0.00000
2.88840	5.50927	0.56608	0.57268	0.24365
2.57893	5.88107	0.43290	0.71987	0.37966
2.25505	6.13536	0.35722	0.81008	0.45818
1.92193	6.28221	0.32133	0.86084	0.49691
1.58447	6.32355	0.31122	0.88596	0.50984
1.24751	6.26089	0.32654	0.88565	0.49736
0.91585	6.09624	0.36678	0.86022	0.45996
0.59404	5.82949	0.45138	0.79007	0.37819
0.28713	5.45232	0.59258	0.66278	0.23982
0.	4.97402	0.83523	0.43333	0.00000

TIME	DELTA	VELOCITY SETTLEMENT	CALCULATED SETTLEMENT	DEGREE CONSOLIDATION
1440.000	0.04615	2.16000	2.16005	0.839524

VELOCITY = 0.10000E-02 (FOR PRIOR TIME)

Figure A3. Example of computer output for program CRST

APPENDIX B: CRST PROGRAM LISTING

1. The following is a complete listing of CRST (Controlled Rate of Strain Test) as written for the WES time-sharing system.

```
C     CONTROLLED RATE OF STRAIN TEST BY FINITE STRAIN THEORY
C
C
C            ************************************************
C            *                                              *
C            *                    CRST                      *
C            *                                              *
C            *                  AN ANALYSIS                 *
C            *                                              *
C            *                    OF                        *
C            *                                              *
C            *        THE CONTROLLED RATE OF STRAIN         *
C            *                                              *
C            *            CONSOLIDATION TEST BY             *
C            *                                              *
C            *             FINITE STRAIN THEORY             *
C            *                                              *
C            ************************************************
C
C
C     ****************************************************************
C     *                                                              *
C     * "CRST" COMPUTES THE VOID RATIOS, TOTAL AND EFFECTIVE STRESS, *
C     * PORE WATER PRESSURES, AND DEGREES OF CONSOLIDATION FOR HOMO- *
C     * GENEOUS SOFT CLAY WITH AN IMPERMEABLE OR FREE DRAINING LOWER *
C     * BOUNDARY AND A FREE DRAINING UPPER BOUNDARY MOVING AT A      *
C     * CONTROLLED VELOCITY.  THE VOID RATIO-EFFECTIVE STRESS AND    *
C     * VOID RATIO-PERMEABILITY RELATIONSHIPS ARE INPUT AS POINT     *
C     * VALUES AND THUS MAY ASSUME ANY FORM.                         *
C     *                                                              *
C     ****************************************************************
C
C
      COMMON  BP,DA,DZ,E00,ELL,GMC,GMS,GMW,GS,H,HW,IN,IOUT,NBDIV,
     &        ND,NDIV,NPROB,NPT,NS,NTD,NTIME,SETT,SFIN,TAU,TIMEO,
     &        TIME,TPRNT,UCON,VEL,VSET0,VSET,VRI1,HO,NOPT,NDOPT,V(50),
     &        VEL1,VEL2,
     &        A(15),AF(15),ALPHA(51),BETA(51),BF(15),DSDE(51),E(15),
     &        EFIN(15),EFS(15),ES(51),F(15),FINT(15),PK(51),PRINT(50),
     &        RK(51),RS(51),TOS(15),U(15),UO(15),UW(15),XI(15),Z(15)
C
C     ...SET INPUT AND OUTPUT MODES
      IN = 10
      IOUT = 11
C
C     ...READ PROBLEM INPUT FROM FREE FIELD DATA FILE
C     .....CONTAINING LINE NUMBERS
      READ(IN,100) NST,NPROB,NPT,NOPT,NDOPT,RN
      READ(IN,100) NST,H,E00,GS,GMW,HW,BP,NS
      DO 1  I=1,NS
      READ(IN,100) NST,ES(I),RS(I),RK(I)
      RK(I) = RK(I) * RN
```

```
    1 CONTINUE
      READ(IN,100) NST,TAU,NBDIV,VEL,NTIME
      DO 2  I=1,NTIME
      READ(IN,100) NST,PRINT(I),V(I)
    2 CONTINUE
  100 FORMAT(V)
C
C     ...PRINT INPUT DATA AND MAKE INITIAL CALCULATIONS
      CALL INTRO
      IF (NPT .EQ. 3) STOP
C
C     ...PERFORM CALCULATIONS TO EACH PRINT TIME AND OUTPUT RESULTS
      DO 3  K=1,NTIME
      TPRNT = PRINT(K)
      CALL FDIFEQ
      CALL STRSTR
      CALL DATOUT
      VEL = V(K)
    3 CONTINUE
C
C
      STOP
      END
C
C
      SUBROUTINE INTRO
C
C     ************************************************
C     * INTRO PRINTS INPUT DATA AND RESULTS OF INITIAL *
C     * CALCULATIONS IN TABULAR FORM.                  *
C     ************************************************
C
C
      COMMON  BP,DA,DZ,E00,ELL,GMC,GMS,GMW,GS,H,HW,IN,IOUT,NBDIV,
     &        ND,NDIV,NPROB,NPT,NS,NTD,NTIME,SETT,SFIN,TAU,TIME0,
     &        TIME,TPRNT,UCON,VEL,VSET0,VSET,VRI1,H0,NOPT,NDOPT,V(50),
     &        VEL1,VEL2,
     &        A(15),AF(15),ALPHA(51),BETA(51),BF(15),DSDE(51),E(15),
     &        EFIN(15),EFS(15),ES(51),F(15),FINT(15),PK(51),PRINT(50),
     &        RK(51),RS(51),TOS(15),U(15),U0(15),UW(15),XI(15),Z(15)
C     ...PRINT HEADING AND PROBLEM NUMBER
      WRITE(IOUT,100)
      WRITE(IOUT,101)
      WRITE(IOUT,102)
      WRITE(IOUT,103)
      WRITE(IOUT,104) NPROB
C
      CALL SETUP
C
C     ...PRINT SOIL DATA
      WRITE(IOUT,105)
      WRITE(IOUT,106)
```

```
      WRITE(IOUT,107)
      WRITE(IOUT,108) H,ELL,GS
      IF (NPT .EQ. 2) GOTO 2
      WRITE(IOUT,109)
      WRITE(IOUT,110)
      DO 1  I=1,NS
      WRITE(IOUT,111) I,ES(I),RS(I),RK(I),PK(I),BETA(I),
     &                DSDE(I),ALPHA(I)
    1 CONTINUE
C
C     ...PRINT CALCULATION DATA
    2 WRITE(IOUT,112)
      WRITE(IOUT,113)
      WRITE(IOUT,114)
      WRITE(IOUT,115) TAU,NBDIV,VEL,HW,BP
C
C     ...PRINT INITIAL CONDITIONS
      CALL DATOUT
C
C     ...FORMATS
  100 FORMAT(1H1/////9X,60(1H*))
  101 FORMAT(22X,34HCONSOLIDATION OF SOFT CLAYS DURING)
  102 FORMAT(22X,34HTHE CONTROLLED RATE OF STRAIN TEST)
  103 FORMAT(9X,60(1H*))
  104 FORMAT(9X,14HPROBLEM NUMBER,I4)
  105 FORMAT(/////21(1H*),28HCOMPRESSIBLE CLAY PROPERTIES,20(1H*))
  106 FORMAT(//12X,6HSAMPLE,10X,6HHEIGHT,10X,16HSPECIFIC GRAVITY)
  107 FORMAT(11X,9HTHICKNESS,7X,9HOF SOLIDS,11X,9HOF SOLIDS)
  108 FORMAT(12X,F6.3,8X,F10.7,13X,F5.3)
  109 FORMAT(//8X,4HVOID,2X,9HEFFECTIVE,3X,5HPERM-,5X,5HK/1+E)
  110 FORMAT(4X,8HI  RATIO,4X,6HSTRESS,3X,8HEABILITY,4X,2HPK,7X,
     &       4HBETA,6X,4HDSDE,5X,5HALPHA)
  111 FORMAT(2X,I3,1X,F6.3,6E10.3)
  112 FORMAT(/////28(1H*),16HCALCULATION DATA,27(1H*))
  113 FORMAT(///3X,3HTAU,10X,6HNUMBER,6X,12HTOP BOUNDARY,6X,
     &       6HHEIGHT,10X,4HBACK)
  114 FORMAT(14X,9HDIVISIONS,7X,8HVELOCITY,7X,8HOF WATER,7X,8HPRESSURE)
  115 FORMAT(1X,F6.3,10X,I3,10X,E10.4,6X,F6.3,6X,F10.3)
C
C
      RETURN
      END
C
C
      SUBROUTINE SETUP
C
C     ******************************************************
C     * SETUP MAKES INITIAL CALCULATIONS AND MANIPULATIONS *
C     * OF INPUT DATA FOR LATER USE.                       *
C     ******************************************************
```

```
C
      COMMON  BP,DA,DZ,E00,ELL,GMC,GMS,GMW,GS,H,HW,IN,IOUT,NBDIV,
     &        ND,NDIV,NPROB,NPT,NS,NTD,NTIME,SETT,SFIN,TAU,TIME0,
     &        TIME,TPRNT,UCON,VEL,VSET0,VSET,VRI1,H0,NOPT,NDOPT,V(50),
     &        VEL1,VEL2,
     &        A(15),AF(15),ALPHA(51),BETA(51),BF(15),DSDE(51),E(15),
     &        EFIN(15),EFS(15),ES(51),F(15),FINT(15),PK(51),PRINT(50),
     &        RK(51),RS(51),TOS(15),U(15),U0(15),UW(15),XI(15),Z(15)
C
C     ...INITIALIZE VARIABLES
      VEL1 = VEL
      VEL2 = 0.0
      TIME = 0.0
      TIME0 = 0.0
      UCON = 0.0
      SETT = 0.0
      SFIN = 0.0
      VSET = 0.0
      VSET0 = 0.0
C
C     ...SET CONSTANTS
      NDIV = NBDIV + 1
      ND = NDIV + 1
      NTD = ND + 1
      GMS = GS * GMW
      GMC = GMS - GMW
      ELL = H / (1.0+E00)
      DA = H / FLOAT(NBDIV)
      DZ = ELL / FLOAT(NBDIV)
      H0 = H
      VRI1 = E00 * ELL
C
C     ...CALCULATE INITIAL COORDINATES AND SET VOID RATIOS
      Z(2) = 0.0 ; A(2) = 0.0  ; XI(2) = 0.0
      F(2) = E00 ; E(2) = E00
      DO 1  I=3,ND
      II = I-1
      Z(I) = Z(II) + DZ
      A(I) = A(II) + DA
      XI(I) = A(I)
      E(I) = E00
      F(I) = E00
    1 CONTINUE
C
C     ...CALCULATE INITIAL STRESSES AND PORE PRESSURES
      DO 2  I=2,ND
      U0(I) = GMW*(HW-XI(I)) + BP
      U(I) = GMC * (ELL-Z(I))
      UW(I) = U0(I) + U(I)
      EFS(I) = 0.0
      TOS(I) = UW(I)
    2 CONTINUE
```

```
C
C     ...CALCULATE VOID RATIO FUNCTIONS
C     .....PERMEABILITY FUNCTION
      DO 3  I=1,NS
      PK(I) = RK(I) / (1.0+ES(I))
    3 CONTINUE
C     .....SLOPE OF PERMEABILITY FUNCTION --BETA
C     .....AND SLOPE OF VOID RATIO-EFF STRESS CURVE -- DSDE
      CD = ES(2) - ES(1)
      BETA(1) = (PK(2)-PK(1)) / CD
      DSDE(1) = (RS(2)-RS(1)) / CD
      L = NS-1
      DO 4  I=2,L
      II = I-1 ; IJ = I+1
      CD = ES(IJ) - ES(II)
      BETA(I) = (PK(IJ)-PK(II)) / CD
      DSDE(I) = (RS(IJ)-RS(II)) / CD
    4 CONTINUE
      CD = ES(NS) - ES(L)
      BETA(NS) = (PK(NS)-PK(L)) / CD
      DSDE(NS) = (RS(NS)-RS(L)) / CD
C     .....PERMEABILITY FUNCTION TIMES DSDE -- ALPHA
      DO 5  I=1,NS
      ALPHA(I) = PK(I) * DSDE(I)
    5 CONTINUE
C
C     ...INITIALIZE VOID RATIO FUNCTION FOR SAMPLE
      DO 6  I=2,ND
      AF(I) = ALPHA(1)
      BF(I) = BETA(1)
    6 CONTINUE
      IF (NOPT .EQ. 1) RETURN
C
C     ...RECALCULATE FOR FULLY CONSOLIDATED SAMPLE
      DO 10  I=2,ND
      DO 7  N=2,NS
      S1 = U(I) - RS(N)
      IF (S1 .LE. 0.0) GOTO 8
    7 CONTINUE
      E(I) = ES(NS) ; GOTO 9
    8 NN = N-1
      E(I) = ES(N) + S1*(ES(NN)-ES(N))/(RS(NN)-RS(N))
    9 EFS(I) = U(I)
      F(I) = E(I)
      U(I) = 0.0
   10 CONTINUE
C
C     ...CALCULATE VOID RATIO INTEGRAL
      CALL INTGRL(E,DZ,ND,FINT)
      VRI1 = FINT(ND)
      UCON = 1.0
C
```

```
C     ...CALCULATE XI COORDINATES AND REMAINING STRESSES
      DO 11  I=2,ND
      XI(I) = Z(I) + FINT(I)
      UO(I) = GMW*(HW-XI(I)) + BP
      UW(I) = UO(I)
      TOS(I) = UW(I) + EFS(I)
   11 CONTINUE
      HO = XI(ND)
C
C
      RETURN
      END
C
C
      SUBROUTINE FDIFEQ
C
C     ********************************************************************
C     * FDIFEQ CALCULATES NEW VOID RATIOS AS THE SOIL IS CONSTANTLY *
C     * STRAINED BY AN EXPLICIT FINITE DIFFERENCE SCHEME BASED ON   *
C     * PREVIOUS VOID RATIOS.  SOIL PARAMETER FUNCTIONS ARE         *
C     * CONTINUOUSLY UPDATED TO CORRESPOND WITH CURRENT VOID RATIOS.*
C     ********************************************************************
C
      COMMON  BP,DA,DZ,EOO,ELL,GMC,GMS,GMW,GS,H,HW,IN,IOUT,NBDIV,
     &        ND,NDIV,NPROB,NPT,NS,NTD,NTIME,SETT,SFIN,TAU,TIMEO,
     &        TIME,TPRNT,UCON,VEL,VSETO,VSET,VRI1,HO,NOPT,NDOPT,V(50),
     &        VEL1,VEL2,
     &        A(15),AF(15),ALPHA(51),BETA(51),BF(15),DSDE(51),E(15),
     &        EFIN(15),EFS(15),ES(51),F(15),FINT(15),PK(51),PRINT(50),
     &        RK(51),RS(51),TOS(15),U(15),UO(15),UW(15),XI(15),Z(15)
C
C     ...SET CONSTANTS
      NNN = 1
      EFST = GMC * ELL
      CF = TAU / (GMW*DZ)
      DZ2 = DZ * 2.0
C
C     ...LOOP THROUGH FINITE DIFFERENCE EQUATIONS UNTIL PRINT TIME
C
C     ...CALCULATE VOID RATIO OF BOTTOM IMAGE POINT
    1 DO 2  I=2,NS
      C1 = E(2) - ES(I)
      IF (C1 .GE. 0.0) GOTO 3
    2 CONTINUE
      DSED = DSDE(NS) ; GOTO 4
    3 II = I-1
      DSED = DSDE(I) + C1*(DSDE(I)-DSDE(II))/(ES(I)-ES(II))
    4 F(1) = F(3) + DZ2*((GMC/DSED)-(VEL2*GMW/AF(2)))
C
C     ...CALCULATE VOID RATIO OF TOP IMAGE POINT
      DO 5  I=2,NS
      C1 = E(ND) - ES(I)
```

```
      IF (C1 .GE. 0.0) GOTO 6
    5 CONTINUE
      DSED = DSDE(NS) ; GOTO 7
    6 II = I-1
      DSED = DSDE(I) + C1*(DSDE(I)-DSDE(II))/(ES(I)-ES(II))
    7 F(NTD) = F(NDIV) - DZ2*((GMC/DSED)-(VEL1*GMW/AF(ND)))
C
C     ...CALCULATE VOID RATIOS FOR REMAINDER OF MATERIAL
      DO 8  I=2,ND
      II = I-1 ; IJ = I+1
      DF = (F(IJ)-F(II)) / 2.0
      DF2DZ = (F(IJ)-F(I)*2.0+F(II)) / DZ
      AC = (AF(IJ)-AF(II)) / DZ2
      E(I) = F(I) - CF*(DF*(GMC*BF(I)+AC)+DF2DZ*AF(I))
    8 CONTINUE
      TIME1 = TAU * FLOAT(NNN)
      VSET1 = TIME1 * VEL
      VSET = VSET0 + VSET1
C
C     ...CHECK FOR AGREEMENT BETWEEN
C     .....INDUCED SETTLEMENT AND CALCULATED SETTLEMENT
      CALL INTGRL(E,DZ,ND,FINT)
      CEAV = FINT(ND) / ELL
      CVEL = ((H0-VSET)/ELL) - 1.0
      PC = (CEAV-CVEL) / CEAV
      IF (ABS(PC) .LE. 0.0001) GOTO 14
      DO 15  I=2,ND
      E(I) = (1.0-PC) * E(I)
   15 CONTINUE
C
C     ...SET ZERO EXCESS PRESS AT DRAINED BOTTOM BOUNDARY
   14 IF (NDOPT .EQ. 1) GOTO 16
      DO 20  N=2,NS
      C1 = E(ND) - ES(N)
      IF (C1 .GE. 0.0) GOTO 21
   20 CONTINUE
      EFS(ND) = RS(NS) ; GOTO 22
   21 NN = N-1
      EFS(ND) = RS(N) + C1*(RS(N)-RS(NN))/(ES(N)-ES(NN))
   22 EFS(2) = EFS(ND) + EFST
      DO 23  N=2,NS
      S1 = EFS(2) - RS(N)
      IF (S1 .LE. 0.0) GOTO 24
   23 CONTINUE
      E(2) = ES(NS) ; GOTO 16
   24 NN = N-1
      E(2) = ES(N) + S1*(ES(NN)-ES(N))/(RS(NN)-RS(N))
C
C     ...RESET BOUNDARY VELOCITIES
      C1 = F(2) - E(2)
      C2 = C1
      DO 25  I=3,ND
```

```
      II = I-1
      DELE = F(I) - E(I)
      C2 = C2 + DELE
      IF (DELE .LE. (F(II)-E(II))) C1 = C1+DELE
   25 CONTINUE
      VEL2 = -VEL * C1 / C2
      VEL1 = VEL2 + VEL
C
C     ...RESET FOR NEXT LOOP
   16 DO 11  I=2,ND
      F(I) = E(I)
      DO 9  N=2,NS
      C1 = E(I) -ES(N)
      IF (C1 .GE. 0.0) GOTO 10
    9 CONTINUE
      AF(I) = ALPHA(NS)
      BF(I) = BETA(NS) ; GOTO 11
   10 NN = N-1
      C = C1 / (ES(N)-ES(NN))
      AF(I) = ALPHA(N) + C*(ALPHA(N)-ALPHA(NN))
      BF(I) = BETA(N) + C*(BETA(N)-BETA(NN))
   11 CONTINUE
C
C     ...CHECK FOR PRINT TIME
      TIME = TIME0 + TIME1
      NNN = NNN + 1
      IF (TIME .LT. TPRNT) GOTO 1
      VSET0 = VSET
      TIME0 = TIME
C
C     ...CHECK STABILITY AND CONSISTENCY
      STAB = ABS((DZ**2*GMW)/(2.0*AF(ND)))
      IF (STAB .LT. TAU) WRITE(IOUT,100) NPROB
      CONS = ABS((2.0*AF(2))/(GMC*BF(2)))
      IF (CONS .LE. DZ) WRITE(IOUT,101) NPROB
C
C     ...FORMATS
  100 FORMAT(/////10(1H*),25HSTABILITY ERROR---PROBLEM,I3)
  101 FORMAT(/////10(1H*),27HCONSISTENCY ERROR---PROBLEM,I3)
C
C
      RETURN
      END
C
C
      SUBROUTINE STRSTR
C
C     ************************************************************
C     * STRSTR CALCULATES EFFECTIVE STRESSES, TOTAL STRESSES,    *
C     * PORE WATER PRESSURES, NEW COORDINATES, AND SETTLEMENTS,  *
C     * BASED ON CURRENT VOID RATIO AND VOID RATIO INTEGRAL.     *
C     ************************************************************
```

```
C
      COMMON  BP,DA,DZ,EOO,ELL,GMC,GMS,GMW,GS,H,HW,IN,IOUT,NBDIV,
     &        ND,NDIV,NPROB,NPT,NS,NTD,NTIME,SETT,SFIN,TAU,TIMEO,
     &        TIME,TPRNT,UCON,VEL,VSETO,VSET,VRI1,HO,NOPT,NDOPT,V(50),
     &        VEL1,VEL2,
     &        A(15),AF(15),ALPHA(51),BETA(51),BF(15),DSDE(51),E(15),
     &        EFIN(15),EFS(15),ES(51),F(15),FINT(15),PK(51),PRINT(50),
     &        RK(51),RS(51),TOS(15),U(15),UO(15),UW(15),XI(15),Z(15)
C
C     ...CALCULATE VOID RATIO INTEGRAL
      CALL INTGRL(E,DZ,ND,FINT)
C
C     ...CALCULATE XI COORDINATES
      DO 3  I=2,ND
      XI(I) = Z(I) + FINT(I)
C
C     ...CALCULATE STRESSES
      DO 1  N=2,NS
      C1 = E(I) - ES(N)
      IF (C1 .GE. 0.0) GOTO 2
    1 CONTINUE
      EFS(I) = RS(NS) ; GOTO 3
    2 NN = N-1
      EFS(I) = RS(N) + C1*(RS(N)-RS(NN))/(ES(N)-ES(NN))
    3 CONTINUE
      WL = HW - XI(ND) + FINT(ND)
      DO 4  I=2,ND
      UO(I) = GMW*(HW-XI(I)) + BP
      TOS(I) = EFS(ND) + (GMW*(WL-FINT(I))) + (GMS*(ELL-Z(I))) + BP
      UW(I) = TOS(I) - EFS(I)
      U(I) = UW(I) - UO(I)
    4 CONTINUE
C
C     ...CALCULATE FINAL VOID RATIOS FOR CONSTANT RAM LOAD
      DO 7  I=2,ND
      S1 = EFS(ND) + GMC*(ELL-Z(I))
      DO 5  N=2,NS
      S2 = S1 - RS(N)
      IF (S2 .LE. 0.0) GOTO 6
    5 CONTINUE
      EFIN(I) = ES(NS) ; GOTO 7
    6 NN = N-1
      EFIN(I) = ES(N) + S2*(ES(NN)-ES(N))/(RS(NN)-RS(N))
    7 CONTINUE
C
C     ...CALCULATE SETTLEMENT AND PERCENT CONSOLIDATION
      CALL INTGRL(EFIN,DZ,ND,FINT)
      SFIN = VRI1 - FINT(ND)
      SETT = HO - XI(ND)
      UCON = SETT / SFIN
C
C
```

```
      RETURN
      END
C
C
      SUBROUTINE INTGRL(E,DZ,N,F)
C
C     ************************************************
C     * INTGRL EVALUATES THE VOID RATIO INTEGRAL TO  *
C     * EACH MESH POINT IN THE MATERIAL.             *
C     ************************************************
C
      DIMENSION E(15),F(15)
C
C     ...BY SIMPSONS RULE FOR ALL ODD NUMBERED MESH POINTS
      F(2) = 0.0
      DO 1  I=4,N,2
      F(I) = F(I-2) + DZ*(E(I-2)+4.0*E(I-1)+E(I))/3.0
    1 CONTINUE
C
C     ...BY SIMPSONS 3/8 RULE FOR EVEN NUMBERED MESH POINTS
      DO 2  I=5,N,2
      F(I) = F(I-3) + DZ*(E(I-3)+3.0*(E(I-2)+E(I-1))+E(I))*(3.0/8.0)
    2 CONTINUE
C
C     ...BY DIFFERENCES FOR FIRST INTERVAL
      F2 = DZ*(E(3)+4.0*E(4)+E(5))/3.0
      F(3) = F(5) - F2
C
C
      RETURN
      END
C
C
      SUBROUTINE DATOUT
C
C     ************************************************************
C     * DATOUT PRINTS RESULTS OF CONSOLIDATION CALCULATIONS      *
C     * AND BASE DATA IN TABULAR FORM.                           *
C     ************************************************************
C
      COMMON  BP,DA,DZ,E00,ELL,GMC,GMS,GMW,GS,H,HW,IN,IOUT,NBDIV,
     &        ND,NDIV,NPROB,NPT,NS,NTD,NTIME,SETT,SFIN,TAU,TIMEO,
     &        TIME,TPRNT,UCON,VEL,VSET0,VSET,VRI1,HO,NOPT,NDOPT,V(50),
     &        VEL1,VEL2,
     &        A(15),AF(15),ALPHA(51),BETA(51),BF(15),DSDE(51),E(15),
     &        EFIN(15),EFS(15),ES(51),F(15),FINT(15),PK(51),PRINT(50),
     &        RK(51),RS(51),TOS(15),U(15),U0(15),UW(15),XI(15),Z(15)
C
C     ...PRINT CURRENT CONDITIONS
      WRITE(IOUT,100)
      WRITE(IOUT,101)
      WRITE(IOUT,102)
```

```
      WRITE(IOUT,103)
      DO 1  J=2,ND
      I = ND+2-J
      WRITE(IOUT,104) XI(I),E(I),EFS(I),UW(I),U(I)
    1 CONTINUE
C
C     ...PRINT OTHER DATA
      WRITE(IOUT,105)
      WRITE(IOUT,106)
      WRITE(IOUT,103)
      WRITE(IOUT,107) TIME,DZ,VSET,SETT,UCON
      WRITE(IOUT,108) VEL
C
C     ...FORMATS
  100 FORMAT(1H1/////22(1H*),28HCURRENT CONDITIONS IN SAMPLE,20(1H*))
  101 FORMAT(//5X,2HXI,14X,1HE,10X,9HEFFECTIVE,10X,15H*PORE PRESSURE*)
  102 FORMAT(1X,10HCOORDINATE,5X,10HVOID RATIO,7X,6HSTRESS,10X,
     &       5HTOTAL,9X,6HEXCESS)
  103 FORMAT(/)
  104 FORMAT(2X,F8.5,7X,F8.5,6X,F10.5,2(5X,F10.5))
  105 FORMAT(///29X,8HVELOCITY,6X,10HCALCULATED,8X,6HDEGREE)
  106 FORMAT(5X,4HTIME,6X,5HDELTA,8X,10HSETTLEMENT,5X,10HSETTLEMENT,
     &       5X,13HCONSOLIDATION)
  107 FORMAT(1X,F10.3,2X,F8.5,2(5X,F10.5),5X,F10.6)
  108 FORMAT(/5X,11HVELOCITY = ,E11.5,3X,16H(FOR PRIOR TIME))
C
C
      RETURN
      END
```

APPENDIX C: USER'S GUIDE FOR COMPUTER PROGRAM LSCRS

1. This appendix provides information useful to users of the Computer Program LSCRS (Large Strain, Controlled Rate of Strain) including a general description of the program processing sequence, definitions of principal variables, and format requirements for problem input. The program was originally written for use on the WES Time-Sharing System but could be readily adapted to batch processing through a card reader and high-speed line printer. Some output format changes would be desirable if the program were used in batch processing to improve efficiency.

2. The program is written in FORTRAN IV computer language with eight-digit line numbers. However, characters 9 through 80 are formatted to conform to the standard FORTRAN statement when reproduced in spaces 1 through 72 of a computer card. Program input is through a quick access type file previously built by the user. Output is either to the time-sharing terminal or to a quick access file at the option of the user. Specific program options will be fully described in the remainder of this appendix.

3. A listing of the program is provided in Appendix D. Typical problem input and solution output are contained in this appendix.

Program Description and Components

4. LSCRS is composed of the main program and three subroutines. It is broken down into subprograms to make modification and understanding easier. The program is also well documented throughout with comments, so a detailed description will not be given. However, an overview of the program structure is shown in Figure C1, and a brief statement about each part follows:

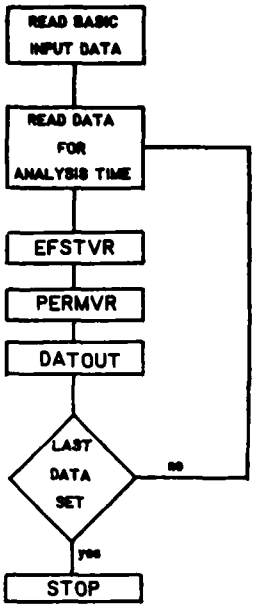

Figure C1. Flow diagram of computer program LSCRS

a. Main program. In this part, problem options, data describing the material tested, and data collected during the test are read from a free field data file. Basic parameters including initial material coordinates and self-weight at vertical space mesh points are utilized and the various subroutines to analyze the data and output results are called.

b. Subroutine EFSTVR. This subprogram calculates the void ratio-effective stress relationship at each analysis time based on input data and the results of previous calculations.

c. Subroutine PERMVR. Here, the relationship between void ratio and permeability is calculated at each analysis time from input pore pressure distribution, boundary velocity, and calculated void ratio distribution.

d. Subroutine DATOUT. DATOUT prints the results of program calculation in tabular form for each analysis time and a summary of the derived void ratio-effective stress relationship.

Variables

5. The following is a list of the principal variables and variable arrays that are used in the Computer Program LSCRS. The meaning of each variable is also given along with other pertinent information about it. If the variable name is followed by a number in parentheses, it is an array, and the number denotes the current array dimensions. If these dimensions are not

sufficient for the problem to be run, they must be increased throughout the program.

CC(100)	the fine-grain material's compression index associated with a particular void ratio. The compression index represents the slope of the e-log σ' curve from the associated void ratio to the next higher void ratio selected to represent the curve.
CPC	the percent difference between the known volume of solids in the tested specimen and the volume of solids deduced from the calculated void ratio distribution which is used to adjust the calculated solids in the center portion of the sample where there is zero effective stress.
DH(50)	the difference between space mesh points in the current data set.
DH1(50)	the difference between space mesh points in the previous data set.
DUDXI(15)	the slope of the excess pore pressure distribution curve in units of pressure per actual length at each vertical space mesh point in the tested material.
DZ	the uniform spacing of mesh points in material coordinates used for making an initial estimate of material self-weight between each mesh point.

DZ1(50)	the actual spacing of mesh points in material coordinates for the current data set.
E(15)	the current void ratio at each vertical space mesh point in the tested material.
EI(15)	the initial void ratio at each vertical space mesh point in the fine-grained material before testing began.
EFS(15)	the current effective stress at each vertical space mesh point in the tested material.
ELL	the total depth of solids in the test specimen in material or reduced coordinates.
ES(100)	the void ratio associated with a particular effective stress which is used to define the fine-grained material's void ratio-effective stress relationship.
EV1(50)	the average void ratio between space mesh points in the previous data set.
EV(50)	the average void ratio between space mesh points in the current data set.
GMC	the buoyant unit weight of the fine-grained material solids.
GMS	the unit weight of the fine-grained material solids.
GMW	the unit weight of water.
GS	the specific gravity of the fine-grained material solids.

H	the current height of the test specimen in convective coordinates.
HØ	the initial height of the test specimen in convective coordinates.
IN	an integer denoting the input mode or device for initial problem data which has the value "10" in the present program.
IOUT	an integer denoting the output mode or device for recording the results of program computations in a user's format which has the value "11" in the present program.
L	an integer denoting the space mesh point number at which a constant excess pore pressure approximately equal to the boundary effective stress begins in the tested specimen.
M	an integer denoting the space mesh point number at which a constant excess pore pressure approximately equal to the boundary effective stress ends in the tested specimen.
NC	an integer denoting the following options: 1 = test specimen is totally unconsolidated or exists at a uniform void ratio throughout its depth. 2 = test specimen consolidated under its own weight and exists initially at the input void ratio distribution.

ND	the total number of vertical space mesh points in the test specimen or number of data points to be used in describing the material's initial conditions and later pore pressure distribution curves.
NDM1	an integer denoting one less than ND.
NDOPT	an integer denoting the following options: 1 = test specimen is freely drained from the top only. 2 = test specimen is freely drained from the top and bottom.
NP	the current total number of points used to define the fine-grained material's void ratio-effective stress relationship.
NST	an integer line number used on each line of input data.
NSTOP	an integer denoting the following: 1 = last set of data to be entered for this test. 2 = file contains additional sets of data for this test. 3 = first set of data to be entered for this test and more sets follow.
NTEST	an integer used to denote a test number for labeling purposes.
PD	the total percent difference between the known volume of solids in the tested specimen and the

	calculated volume of solids at each analysis time.
PERM(15)	the current value of the fine-grained material's permeability calculated for each vertical space mesh point in the test specimen.
RS(100)	the effective stress associated with a particular void ratio which is used in defining the fine-grained material's void ratio-effective stress relationship.
SW	the total buoyant self-weight per unit area of the test specimen.
SWI(15)	the approximate incremental buoyant self-weight per unit area at each vertical space mesh point in the test specimen.
TIME	the time at which an intermediate analysis is conducted to determine consolidation properties in the test specimen. Measured from the start of the test.
TIMEØ	the time at which the last intermediate analysis was performed or the time at which testing starts.
U(15)	the current excess pore pressure at each vertical space mesh point in the tested material.
UZ	the total volume of solids per unit area between the space mesh points denoted by L and M.

UE	the void ratio in the zone between the space mesh points denoted by L and M.
VEL	the actual velocity of the top boundary of the test specimen.
VELB	the apparent velocity of the bottom boundary of the test specimen.
VELT	the apparent velocity of the top boundary of the test specimen
XI(15)	the current convective coordinate of each vertical space mesh point in the test specimen.
Z(15)	the material or reduced coordinate of each vertical space mesh point in the test specimen.

Problem Data Input

6. The method of inputting problem data in LSCRS is by a free field data file containing line numbers. The line number must be eight characters or less for each in file editing and must be followed by a blank space. The remaining items of data on each line must be separated by a comma or blank space. Real data may be either written in exponential or fixed decimal formats, but integer data must be written without a decimal.

7. For a typical problem run, the data file should be sequenced in the following manner:

a. NST,NTEST,NDOPT,ND,NP,NC

b. NST,TIMEØ,HØ,ELL,GMW,GS

c. NST,XI(I),EI(I)

d. NST,ES(I),RS(I),CC(I)

e. NST,TIME,VEL,EFS(ND),L,M,NSTOP

f. NST,XI(I),U(I)

It should be pointed out here that NST may be any positive integer but must increase throughout the file so that it will be read in the correct sequence in the time-sharing system. It should also be noted that there are ND of line types c except that line type c is omitted when NC = 1 , that there are NP of line types d , and that line types e and f are repeated for each analysis time. In general, there are ND of line type f also except that the points between L and M will be generated by the program and need not be entered.

8. All input data having particular units must be consistent with all other data. For example, if specimen thickness is in inches and time is in minutes, then permeability must be in inches per minute. If stresses are in pounds per square inch, then unit weights must be in pounds per cubic inch. Any system of units is permissible so long as consistency is maintained.

9. An example of an input data file is shown in Figure C2. This is a portion of the file used for the Drum Island example discussed in Part VI.

Program Execution

10. Once an input data file has been built as described in the previous section, the program is executed on the WES Time-Sharing System by the following FORTRAN command:

```
RUN RØGEØ4Ø/LSCRS,R#(filename)"10";"11"
```

```
#LIST DFDI

100    2    2    24    3    1
110    0.    5.12    .4263    .03611    2.6
151    11.0    2.80E-03    0.30
152    10.0    6.90E-03    2.553
153     9.0    1.45E-02    3.101
300    55.    7.33E-03    2.68    6    19    3
301    0.00    0.00
302    0.025    2.00
303    0.05    2.30
304    0.10    2.57
305    0.15    2.65
306    0.40    2.68
319    4.15    2.68
320    4.40    2.65
321    4.45    2.57
322    4.50    2.30
323    4.525    2.00
324    4.55    0.00
400    125.    5.6E-03    5.30    8    17    0
401    0.00    0.00
402    0.025    3.15
403    0.05    3.80
404    0.10    4.54
405    0.15    4.90
406    0.20    5.14
407    0.25    5.25
408    0.70    5.30
417    3.40    5.30
418    3.90    5.25
419    3.95    5.14
420    4.00    4.90
421    4.05    4.54
422    4.10    3.80
423    4.125    3.15
424    4.15    0.00
500    210.    4.7E-03    8.70    10    15    0
501    0.00    0.00
502    0.025    4.7
503    0.05    5.8
504    0.10    7.1
505    0.15    7.7
506    0.20    8.1
507    0.25    8.35
508    0.30    8.53
509    0.35    8.62
510    0.80    8.70
515    2.90    8.70
516    3.35    8.62
517    3.40    8.53
```

Figure C2. Example of input data file for computer program LSCRS (Continued)

```
518    3.45    8.35
519    3.50    8.1
520    3.55    7.7
521    3.60    7.1
522    3.65    5.8
523    3.675   4.7
524    3.70    0.00
600    320.    3.8E-03    12.08    10    15    0
601    0.00    0.00
602    0.025   5.9
603    0.05    7.6
604    0.10    9.6
605    0.15   10.2
606    0.20   11.0
607    0.25   11.4
608    0.30   11.7
609    0.35   11.9
610    0.80   12.08
615    2.40   12.08
616    2.85   11.9
617    2.90   11.7
618    2.95   11.4
619    3.00   11.0
620    3.05   10.2
621    3.10    9.6
622    3.15    7.6
623    3.175   5.9
624    3.20   0.00
700    450.    3.3E-03    14.20    12    13    1
701    0.00    0.00
702    0.025   5.0
703    0.05    7.0
704    0.10    9.4
705    0.15   10.9
706    0.20   11.9
707    0.25   12.9
708    0.30   13.3
709    0.35   13.7
710    0.40   13.9
711    0.55   14.1
712    0.90   14.20
713    1.85   14.20
714    2.20   14.1
715    2.35   14.0
716    2.40   13.7
717    2.45   13.3
718    2.50   12.9
719    2.55   11.9
720    2.60   10.9
721    2.65    9.4
722    2.70    7.0
723    2.725   5.0
724    2.75    0.00
```

Figure C2. (Concluded)

where: (filename) = the name of the previously built file in the user's catalog which contains the input data as described in paragraph 7 above.

Computer Output

11. In the above command, "11" indicates normal program output is to be printed at the time-sharing terminal. The program is easily modified to utilize other modes of input and output by simply changing the mode identifiers in the main program to whatever is desired.

12. Program output is formatted for the eighty character line of a time-sharing terminal. Figure C3 contains a sample of output data also from the example previously addressed.

TEST NUMBER 2

**********CURRENT CONDITIONS IN SAMPLE**********

XI COORDINATES	Z	E VOID RATIO	EFFECTIVE STRESS	K PERMEABILITY
2.7500	0.4251	1.5297	0.1420E 02	0.2908E-06
2.7250	0.4157	1.8396	0.9201E 01	0.4101E-06
2.7000	0.4072	2.0146	0.7202E 01	0.9483E-06
2.6500	0.3914	2.3205	0.4803E 01	0.1385E-05
2.6000	0.3770	2.6007	0.3304E 01	0.2086E-05
2.5500	0.3635	2.8122	0.2305E 01	0.2500E-05
2.5000	0.3511	3.2796	0.1306E 01	0.3382E-05
2.4500	0.3398	3.5911	0.9075E 00	0.5501E-05
2.4000	0.3297	4.2994	0.5086E 00	0.
2.3500	0.3212	5.4704	0.2096E 00	0.
2.2000	0.2995	6.3140	0.1107E 00	0.
1.8500	0.2596	9.2551	0.1200E-01	0.
0.9000	0.1670	9.2551	0.1200E-01	0.
0.5500	0.1271	6.2762	0.1139E 00	0.
0.4000	0.1044	4.9324	0.3150E 00	0.
0.3500	0.0954	4.2800	0.5161E 00	0.7714E-05
0.3000	0.0853	3.5821	0.9171E 00	0.6195E-05
0.2500	0.0740	3.2719	0.1318E 01	0.3725E-05
0.2000	0.0616	2.8087	0.2319E 01	0.2713E-05
0.1500	0.0481	2.5978	0.3320E 01	0.2244E-05
0.1000	0.0337	2.3173	0.4821E 01	0.1480E-05
0.0500	0.0179	2.0126	0.7222E 01	0.1014E-05
0.0250	0.0093	1.8379	0.9224E 01	0.4303E-06
0.	0.	1.5284	0.1422E 02	0.3031E-06

TIME	PERCENT DIFFERENCE	TOTAL VELOCITY	TOP VELOCITY	BOTTOM VELOCITY
450.00	0.29280E 00	0.33000E-02	-0.16212E-02	0.16788E-02

MEASURED SOLIDS VOLUME = 0.42630

RECAP OF VOID RATIO - EFFECTIVE STRESS RELATIONSHIP

VOID RATIO	EFFECTIVE STRESS	COMPRESSION INDEX
11.00000	0.28000E-02	0.30000E 00
10.00000	0.69000E-02	0.25530E 01
9.00000	0.14500E-01	0.31010E 01
3.69566	0.80310E 00	0.30425E 01
2.85262	0.21523E 01	0.19691E 01
2.52550	0.37550E 01	0.13534E 01
2.20471	0.55194E 01	0.19177E 01
1.92490	0.81659E 01	0.16449E 01

Figure C3. Example of computer output for program LSCRS

APPENDIX D: LSCRS PROGRAM LISTING

1. The following is a complete listing of LSCRS (Large Strain, Controlled Rate of Strain) as written for the WES time-sharing system.

```
C     LSCRS - LARGE STRAIN CONTROLLED RATE OF STRAIN
C
C
C     ****************************************************************
C     *                                                              *
C     * LSCRS ANALYSES THE LARGE STRAIN CONTROLLED RATE OF STRAIN    *
C     * TEST FOR THE DETERMINATION OF THE VOID RATIO - EFFECTIVE     *
C     * STRESS AND VOID RATIO - PERMEABILITY RELATIONSHIPS BASED     *
C     * ON AN INPUT STARTER E-LOGP CURVE, LSCRS TEST DATA, AND       *
C     * THE EQUATIONS OF CONTINUITY.                                 *
C     *                                                              *
C     ****************************************************************
C
C
      COMMON  CPC,DZ,ELL,GMC,GMW,GS,HO,H,IN,IOUT,L,M,ND,NDM1,
     &        NDOPT,NP,NSTOP,PD,SW,TIMEO,TIME,VEL,VELB,VELT,
     &        UZ,UE,
     &        CC(100),DH(50),DH1(50),DUDXI(50),DZ1(50),E1(50),
     &        E(50),EFS(50),ES(100),EV1(50),EV(50),PERM(50),
     &        RS(100),SWI(50),U(50),XI(50),Z(50)
C
C     ...SET INPUT AND OUTPUT MODES
      IN = 10
      IOUT = 11
C
C     ...READ PROBLEM INPUT DATA FROM FREE FIELD DATA FILE
      READ(IN,100) NST,NTEST,NDOPT,ND,NP,NC
      READ(IN,100) NST,TIMEO,HO,ELL,GMW,GS
      IF (NC .EQ. 1) GOTO 2
C
C     ...READ INITIAL VOID RATIOS FOR CONSOLIDATED SAMPLE
      READ(IN,100) NST,XI(1),E1(1)
      DO 1  I=2,ND
      READ(IN,100) NST,XI(I),E1(I)
      EV1(I) = (E1(I)+E1(I-1)) / 2.0
      DH1(I) = XI(I) - XI(I-1)
    1 CONTINUE
C
C     ...READ INITIAL E-LOG P CURVE
    2 DO 3  I=1,NP
      READ(IN,100) NST,ES(I),RS(I),CC(I)
    3 CONTINUE
C
C     ...INITIALIZE VARIABLES
      EO = (HO/ELL) - 1.0
      UE = EO
      GMS = GS * GMW
      GMC = GMS - GMW
      NDM1 = ND - 1
```

```
      SW = ELL * GMC
      Z(ND) = ELL
      DZ = ELL / FLOAT(NDM1)
      XI(1) = 0.0 ; DH(1) = 0.0 ; DH1(1) = 0.0
      Z(1) = 0.0
      SWI(1) = SW
      SWI(ND) = 0.0
      DO 4  I=2,NDM1
      Z(I) = Z(I-1) + DZ
      SWI(I) = SW - Z(I)*GMC
    4 CONTINUE
      IF (NC .EQ. 2) GOTO 11
C
C     ...SET INITIAL VOID RATIOS FOR UNCONSOLIDATED SAMPLE
      E1(1) = E0  ;  E(1) = E0
      DO 10  I=2,ND
      E1(I) = E0  ;  E(I) = E0
      EV1(I) = E0
   10 CONTINUE
C
C     ...READ PROBLEM DATA AT EACH ANALYSIS TIME
   11 READ(IN,100) NST,TIME,VEL,EFS(ND),L,M,NSTOP
      DO 12  I=1,ND
      IF (I .GT. L .AND. I .LT. M) GOTO 12
      READ(IN,100) NST,XI(I),U(I)
   12 CONTINUE
C
C     ...SET ADDITIONAL DATA POINTS
      H = XI(ND)
      XILM = XI(M) - XI(L)
      UZ = XILM / (1.0+UE)
      J = M-L
      IF (J .LE. 1) GOTO 14
      DXI = XILM / FLOAT(J)
      DO 13  I=L,(M-1)
      XI(I+1) = XI(I) + DXI
      U(I+1) = U(L)
   13 CONTINUE
C
C     ...SET DISTRIBUTION FACTOR
      CPC = (H-XILM) / H
      FAC = UZ / ELL
      IF (CPC .GE. FAC) CPC = FAC
C     ...PRINT TEST NUMBER
   14 WRITE(IOUT,101) NTEST
C
C     ...PERFORM ANALYSIS AND PRINT RESULTS
      CALL EFSTVR
      CALL PERMVR
      CALL DATOUT
C
C     ...RESET FOR NEXT SET OF DATA
```

```
      TIMEO = TIME
      DO 15  I=1,ND
      PERM(I) = 0.0
   15 CONTINUE
      IF (NSTOP .NE. 1) GOTO 11
C
C     ...FORMATS
  100 FORMAT(V)
  101 FORMAT(1H1//5X,12HTEST NUMBER ,I3)
  102 FORMAT(1H1//5X,25HCHECK INITIAL VOID RATIOS)
C
C
      STOP
      END
C
C
      SUBROUTINE EFSTVR
C
C     ************************************************************
C     * EFSTVR CALCULATES THE EFFECTIVE STRESS - VOID RATIO      *
C     * RELATIONSHIP AT EACH ANALYSIS TIME BASED ON INPUT DATA   *
C     * AND PREVIOUS CALCULATIONS.                               *
C     ************************************************************
C
C
      COMMON  CPC,DZ,ELL,GMC,GMW,GS,HO,H,IN,IOUT,L,M,ND,NDM1,
     &        NDOPT,NP,NSTOP,PD,SW,TIMEO,TIME,VEL,VELB,VELT,
     &        UZ,UE,
     &        CC(100),DH(50),DH1(50),DUDXI(50),DZ1(50),E1(50),
     &        E(50),EFS(50),ES(100),EV1(50),EV(50),PERM(50),
     &        RS(100),SWI(50),U(50),XI(50),Z(50)
C
C     ...CALCULATE DISTANCE BETWEEN DATA POINTS
      DO 1  I=2,ND
      DH(I) = XI(I) - XI(I-1)
      IF (NSTOP .EQ. 3) DH1(I) = DH(I)
    1 CONTINUE
C
C     ...ESTIMATE VOID RATIOS AT TEST DATA POINTS
      DO 5  I=1,ND
      IF (U(I) .GE. EFS(ND)) GOTO 5
      EFS(I) = EFS(ND) + SWI(I) - U(I)
      DO 3  N=1,NP
      S1 = RS(N) - EFS(I)
      IF (S1 .GE. 0.0) GOTO 4
    3 CONTINUE
      E(I) = ES(NP) - CC(NP)*ALOG10(EFS(I)/RS(NP))
      IF (E(I) .GT. UE) E(I) = UE
      GOTO 5
    4 E(I) = ES(N) - CC(N)*ALOG10(EFS(I)/RS(N))
      IF (E(I) .GT. UE) E(I) = UE
    5 CONTINUE
```

```
C
C     ...CHECK ESTIMATED SOLIDS AGAINST KNOWN VOLUME
      DO 6  I=2,ND
      IF (U(I) .GE. EFS(ND)) E(I) = UE
      II = I-1
      EAV = (E(I)+E(II)) / 2.0
      Z(I) = Z(II) + (DH(I)/(1.0+EAV))
      DZ1(I) = Z(I) - Z(II)
    6 CONTINUE
C
C     ...ADJUST SOLIDS VOLUME AS NECESSARY
      DIF = (ELL - Z(ND)) * CPC
      IF (DIF .LE. 0.0) DIF = 0.0
      UZ = UZ + DIF
      UE = ((XI(M)-XI(L))/UZ) - 1.0
      Z(ND) = Z(ND) + DIF
      PC = (ELL-Z(ND)) / ELL
      DL = Z(ND) - UZ
      DDL = ELL - UZ
      FAC = DDL / DL
      PD = PC * 100.
      DO 7  I=2,L
      DZ1(I) = DZ1(I) * FAC
      Z(I) = Z(I-1) + DZ1(I)
    7 CONTINUE
      Z(M) = Z(L) + UZ
      DO 8  I=(M+1),ND
      DZ1(I) = DZ1(I) * FAC
      Z(I) = Z(I-1) + DZ1(I)
    8 CONTINUE
C
C     ...CALCULATE AVERAGE VOID RATIO AND EFFECTIVE STRESS
C     .....NEXT TO DRAINED BOUNDARY
      AVX = 0.0 ; AVZ = 0.0 ; AVS = 0.0
      AV = XI(ND) * 0.98
      IF (AV .LT. XI(M)) AV = XI(M)
      DO 9  I=(M+1),ND
      IF (XI(I) .LT. AV) GOTO 9
      AVZ = AVZ + DZ1(I)
      AVX = AVX + DH(I)
      AES = (EFS(I) + EFS(I-1)) / 2.0
      AVS = AVS + (AES*DZ1(I))
    9 CONTINUE
      EAV = (AVX/AVZ) - 1.0
      ESV = AVS / AVZ
C
C     ...EXTEND VOID RATIO - EFF STRESS RELATIONSHIP
      IF (EAV .GT. ES(NP)) GOTO 19
      NP = NP + 1
      ES(NP) = EAV
      RS(NP) = ESV
      CC(NP) = (ES(NP)-ES(NP-1)) / ALOG10(RS(NP-1)/RS(NP))
```

```
C
C     ...CALCULATE FINAL VOID RATIO DISTRIBUTION
   19 DO 22  I=1,ND
      E(I) = UE
      IF (U(I) .GE. EFS(ND)) GOTO 22
      EFS(I) = EFS(ND) + SWI(I) - U(I)
      DO 20  N=2,NP
      S1 = RS(N) - EFS(I)
      IF (S1 .GE. 0.0) GOTO 21
   20 CONTINUE
      E(I) = ES(NP) - CC(NP)*ALOG10(EFS(I)/RS(NP))
      IF (E(I) .GT. UE) E(I) = UE
      GOTO 22
   21 E(I) = ES(N) - CC(N)*ALOG10(EFS(I)/RS(N))
      IF (E(I) .GT. UE) E(I) = UE
   22 CONTINUE
      DO 23  I=2,ND
      II = I-1
      EV(I) = (E(I)+E(II)) / 2.0
      Z(I) = Z(II) + (DH(I)/(1.0+EV(I)))
      DZ1(I) = Z(I) - Z(II)
   23 CONTINUE
      PC = (ELL-Z(ND)) / ELL
      PD = PC * 100.
      DIF = ELL - Z(ND)
      IF (DIF .LE. 0.0) DIF = 0.0
      UZ = UZ + DIF
      UE = ((XI(M)-XI(L))/UZ) - 1.0
C
C     ...CALCULATE EFFECTIVE STRESS AT INTERIOR NODES
      DO 32  I=2,NDM1
      IF (E(I) .GE. ES(1))  EFS(I) = 0.0
      IF (E(I) .GE. ES(1)) GOTO 32
      DO 30  N=2,NP
      IF (E(I) .GE. ES(N)) GOTO 31
   30 CONTINUE
      EFS(I) = EXP10(ALOG10(RS(NP))-((E(I)-ES(NP))/CC(NP)))
      GOTO 32
   31 EFS(I) = EXP10(ALOG10(RS(N))-((E(I)-ES(N))/CC(N)))
   32 CONTINUE
C
C
      RETURN
      END
C
C
      SUBROUTINE PERMVR
C
C     ************************************************************
C     * PERMVR CALCULATES THE PERMEABILITY - VOID RATIO          *
C     * RELATIONSHIP AT EACH ANALYSIS TIME BASED ON INPUT        *
C     * DATA AND CALLCULATED VOID RATIO DISTRIBUTION.            *
C     ************************************************************
```

```
C
C
      COMMON  CPC,DZ,ELL,GMC,GMW,GS,HO,H,IN,IOUT,L,M,ND,NDM1,
     &        NDOPT,NP,NSTOP,PD,SW,TIMEO,TIME,VEL,VELB,VELT,
     &        UZ,UE,
     &        CC(100),DH(50),DH1(50),DUDXI(50),DZ1(50),E1(50),
     &        E(50),EFS(50),ES(100),EV1(50),EV(50),PERM(50),
     &        RS(100),SWI(50),U(50),XI(50),Z(50)
C
C     ...CALCULATE APPARENT VELOCITIES AT TOP AND BOTTOM
      C1 = E1(1) - E(1)
      C2 = E1(M) - E(M)
      DO 2  I=2,ND
      II = I-1
      DELE = E1(I) - E(I)
      IF (U(I) .GT. U(II)) C1 = C1 + DELE
      IF (U(I) .LT. U(II)) C2 = C2 + DELE
    2 CONTINUE
      C3 = C1 + C2
      DT = TIME - TIMEO
      VELB = VEL * (C1/C3)
      VELT = VELB - VEL
      IF (NDOPT .EQ. 2) GOTO 3
      VELB = 0.0
      VELT = -VEL
C
C     ...CALCULATE DUDXI AT EACH POINT IN SAMPLE
    3 DO 4  I=2,NDM1
      DUDXI(I) = (U(I+1)-U(I-1)) / (DH(I)+DH(I+1))
    4 CONTINUE
      DUDXI(1) = (U(2)-U(1)) / DH(2)
      DUDXI(ND) = (U(ND)-U(NDM1)) / DH(ND)
      IF (NDOPT .EQ. 1) DUDXI(1) = 0.0
      IF (NDOPT .EQ. 1) GOTO 6
C
C     ...CALCULATE PERMEABILITY AT EACH POINT IN SAMPLE
      PERM(1) = VELB*GMW / DUDXI(1)
      V = VELB
      DO 5  I=2,(L-1)
      C = DH(I) - DH1(I)
      IF (ABS(C) .GT. 0.0001) GOTO 6
      DEDT = (EV(I)-EV1(I)) / DT
      DEDT1 = DEDT / (1.0+EV(I))
      V = V + DEDT1*DH(I)
      PERM(I) = V*GMW / DUDXI(I)
      IF (PERM(I) .LE. 0.0) PERM(I) = 0.0
    5 CONTINUE
    6 PERM(ND) = VELT*GMW / DUDXI(ND)
      V = VELT
      DO 7  I=M,NDM1
      J = ND+M-I
```

```
      C = DH(J) - DH1(J)
      IF (ABS(C) .GT. 0.0001) GOTO 9
      DEDT = (EV(J)-EV1(J)) / DT
      DEDT1 = DEDT / (1.0+EV(J))
      V = V - DEDT1*DH(J)
      PERM(J) = V*GMW / DUDXI(J)
      IF (PERM(J) .LE. 0.0) PERM(J) = 0.0
    7 CONTINUE
C
C     ...RESET FOR NEXT TIME
      E1(1) = E(1)  ;  EV1(1) = EV(1)  ;  DH1(1) = DH(1)
    9 DO 8  I=2,ND
      E1(I) = E(I)
      EV1(I) = EV(I)
      DH1(I) = DH(I)
    8 CONTINUE
C
C
      RETURN
      END
C
C
      SUBROUTINE DATOUT
C
C     ************************************************************
C     * DATOUT PRINTS RESULTS OF PROGRAM CALCULATIONS AT EACH    *
C     * ANALYSIS TIME PLUS A RECAP OF VOID RATIO - EFFECTIVE     *
C     * STRESS RELATIONSHIP.                                     *
C     ************************************************************
C
C
      COMMON  CPC,DZ,ELL,GMC,GMW,GS,HO;H,IN,IOUT,L,M,ND,NDM1,
     &        NDOPT,NP,NSTOP,PD,SW,TIMEO,TIME,VEL,VELB,VELT,
     &        UZ,UE,
     &        CC(100),DH(50),DH1(50),DUDXI(50),DZ1(50),E1(50),
     &        E(50),EFS(50),ES(100),EV1(50),EV(50),PERM(50),
     &        RS(100),SWI(50),U(50),XI(50),Z(50)
C
C     ...PRINT CURRENT CONDITIONS
      WRITE(IOUT,100)
      WRITE(IOUT,101)
      WRITE(IOUT,102)
      WRITE(IOUT,103)
      DO 1  I=1,ND
      J = ND+1-I
      WRITE(IOUT,104) XI(J),Z(J),E(J),EFS(J),PERM(J)
    1 CONTINUE
      WRITE(IOUT,105)
      WRITE(IOUT,106)
      WRITE(IOUT,103)
      WRITE(IOUT,107) TIME,PD,VEL,VELT,VELB
      WRITE(IOUT,112) ELL
```

```
C
C     ...RECAP VOID RATIO - EFF STRESS RELATIONSHIP
      IF (NSTOP .NE. 1) RETURN
      WRITE(IOUT,108)
      WRITE(IOUT,109)
      WRITE(IOUT,110)
      WRITE(IOUT,103)
      DO 2  I=1,NP
      WRITE(IOUT,111) ES(I),RS(I),CC(I)
    2 CONTINUE
C
C     ...FORMATS
  100 FORMAT(//6X,18(1H*),28HCURRENT CONDITIONS IN SAMPLE,18(1H*))
  101 FORMAT(///11X,2HXI,10X,1HZ,12X,1HE,9X,9HEFFECTIVE,10X,1HK)
  102 FORMAT(12X,11HCOORDINATES,8X,10HVOID RATIO,6X,6HSTRESS,6X,
     &       12HPERMEABILITY)
  103 FORMAT(/)
  104 FORMAT(8X,F7.4,5X,F7.4,5X,F8.4,5X,E10.4,5X,E10.4)
  105 FORMAT(///17X,7HPERCENT,8X,5HTOTAL,10X,3HTOP,10X,6HBOTTOM)
  106 FORMAT(5X,4HTIME,7X,10HDIFFERENCE,5X,3(8HVELOCITY,6X))
  107 FORMAT(2X,F8.2,5X,E12.5,3(2X,E12.5))
  108 FORMAT(///10X,39HRECAP OF VOID RATIO - EFFECTIVE STRESS ,
     &       12HRELATIONSHIP)
  109 FORMAT(//19X,4HVOID,7X,9HEFFECTIVE,4X,11HCOMPRESSION)
  110 FORMAT(18X,5HRATIO,9X,6HSTRESS,8X,5HINDEX)
  111 FORMAT(16X,F10.5,3X,E12.5,2X,E12.5)
  112 FORMAT(//17X,25HMEASURED SOLIDS VOLUME = ,F10.5)
C
C
      RETURN
      END
```

APPENDIX E: RESULTS OF SELF-WEIGHT CONSOLIDATION TESTING

1. This appendix contains figures depicting the final void ratio distribution, history of sample deformation, and the chosen exponential relationship between void ratio and effective stress which resulted from the self-weight consolidation testing of some typical soft dredged materials.

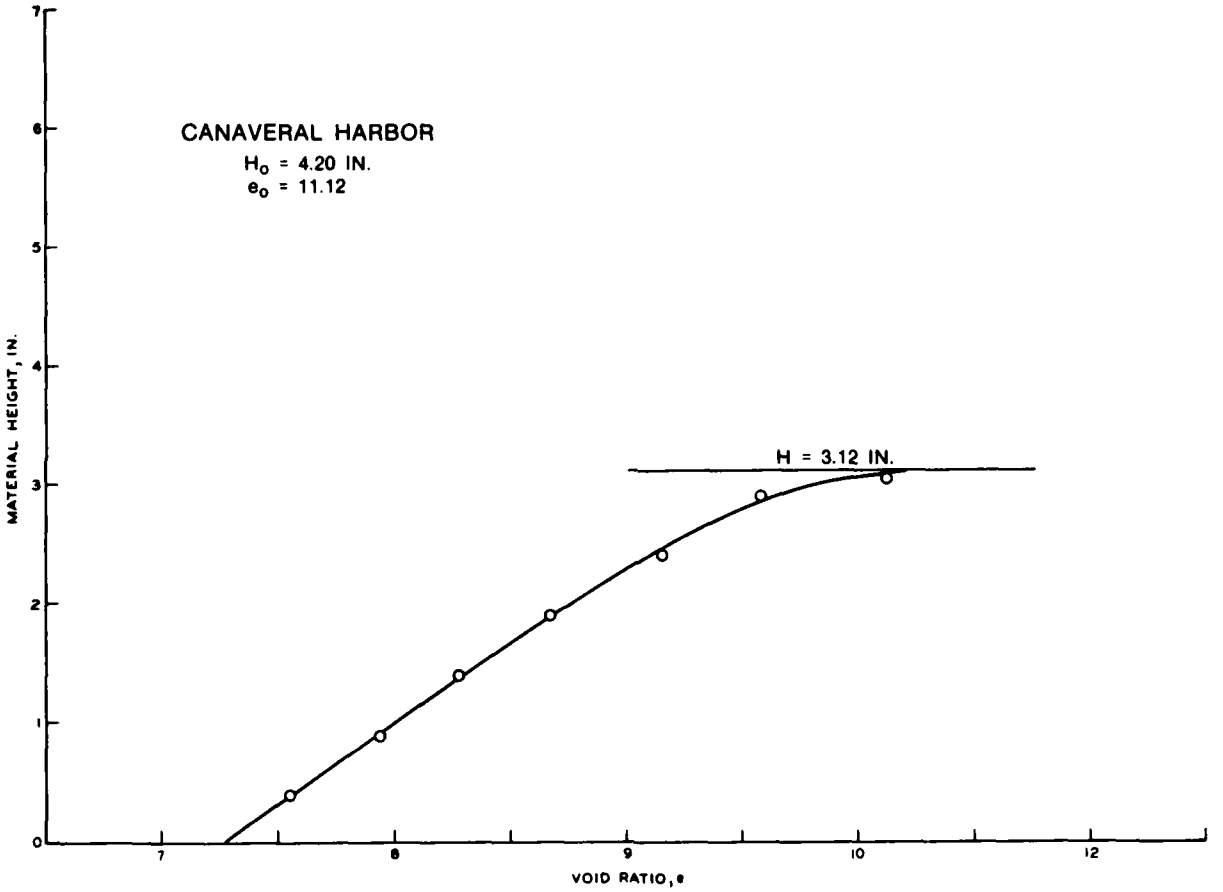

Figure E1. Final void ratio distribution after self-weight consolidation test of Canaveral Harbor material, e_o = 11.12

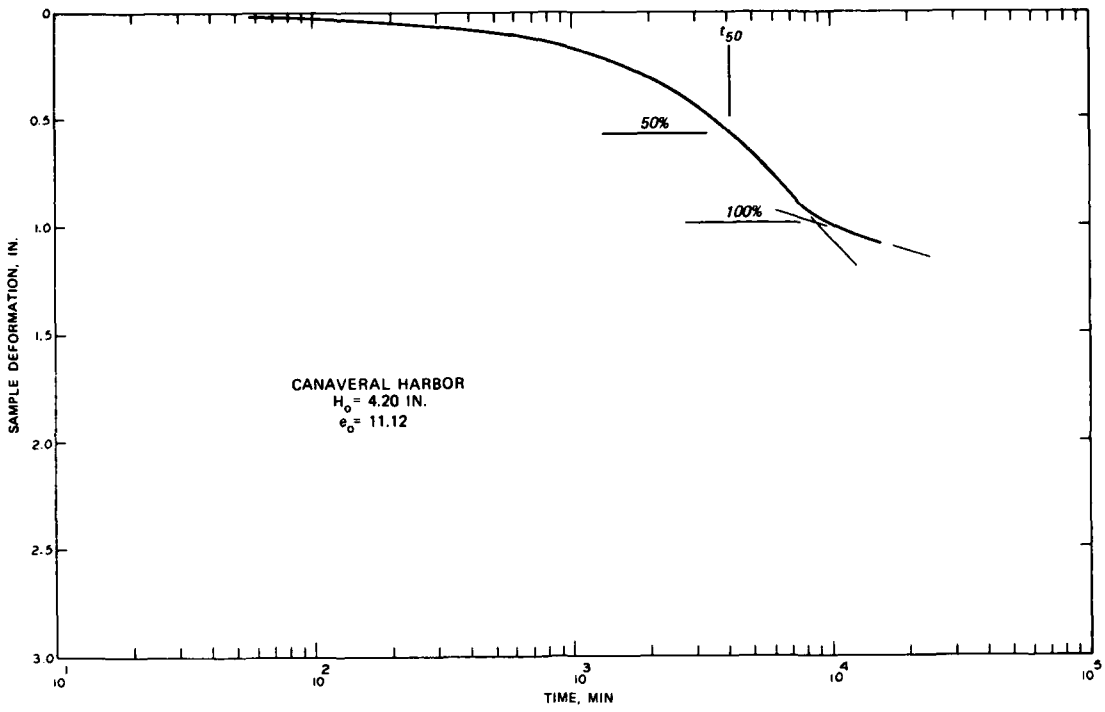

Figure E2. Sample deformation during self-weight consolidation test of Canaveral Harbor material, e_o = 11.12

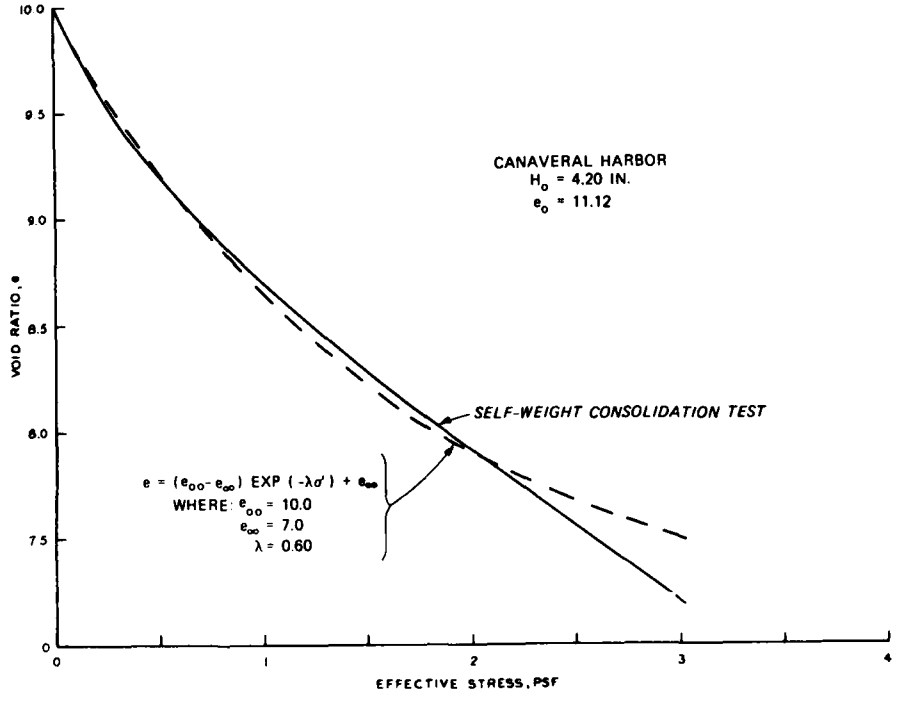

Figure E3. Exponential relationship between void ratio and effective stress chosen to represent results of self-weight consolidation test on Canaveral Harbor material, e_o = 11.12

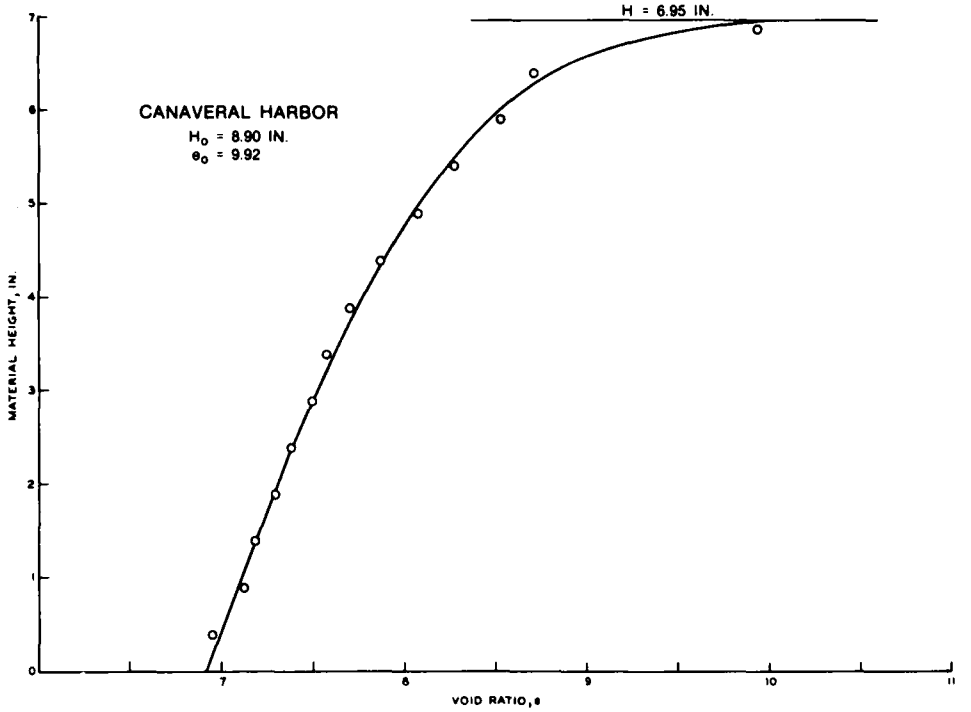

Figure E4. Final void ratio distribution after self-weight consolidation test of Canaveral Harbor material, $e_o = 9.92$

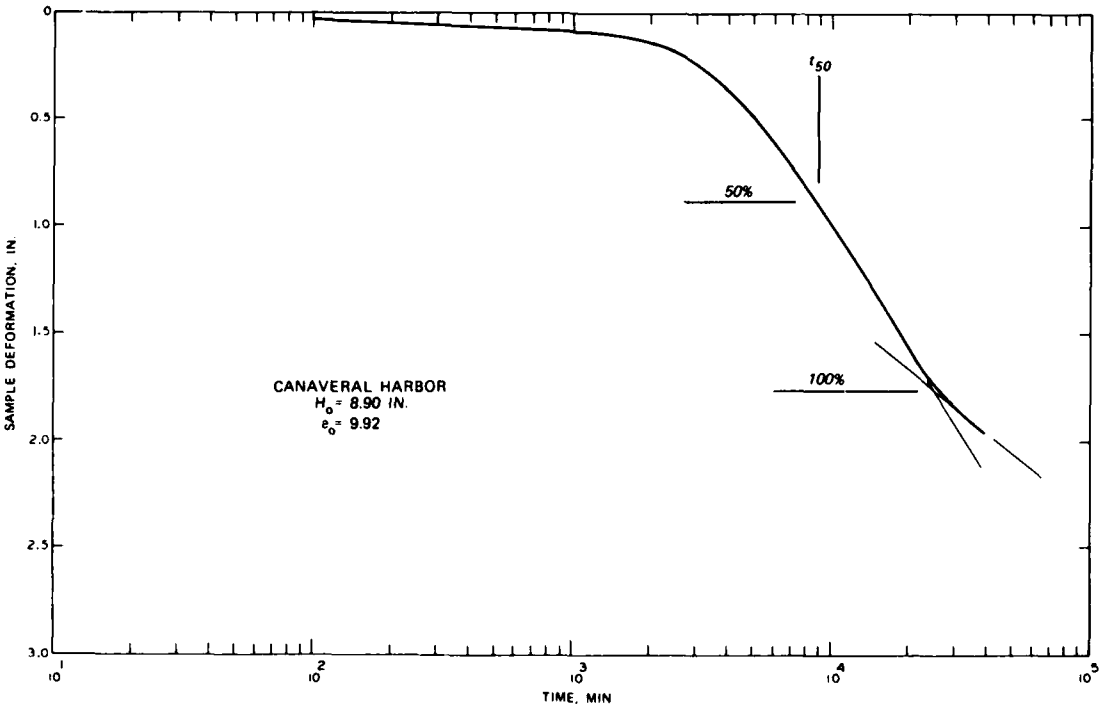

Figure E5. Sample deformation during self-weight consolidation test of Canaveral Harbor material, $e_o = 9.92$

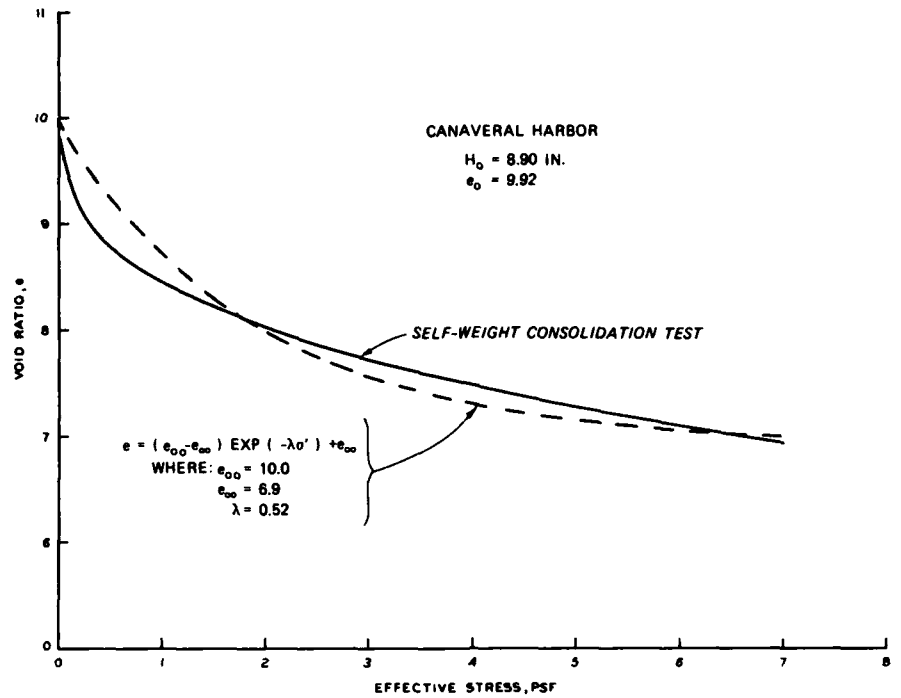

Figure E6. Exponential relationship between void ratio and effective stress chosen to represent results of self-weight consolidation test on Canaveral Harbor material, e_o = 9.92

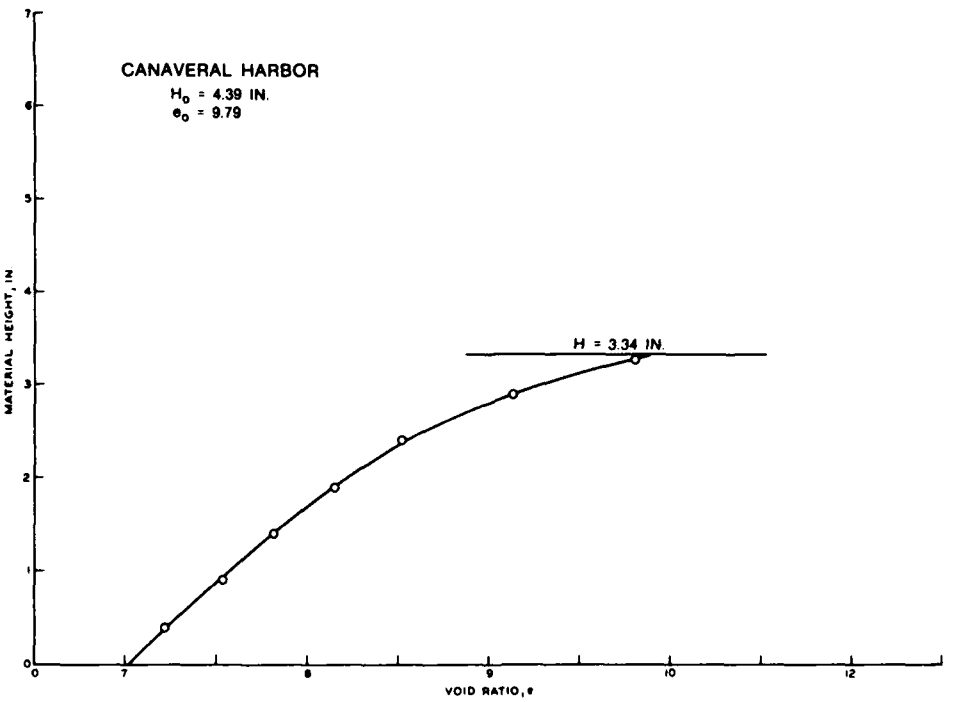

Figure E7. Final void ratio distribution after self-weight consolidation test of Canaveral Harbor material, e_o = 9.79

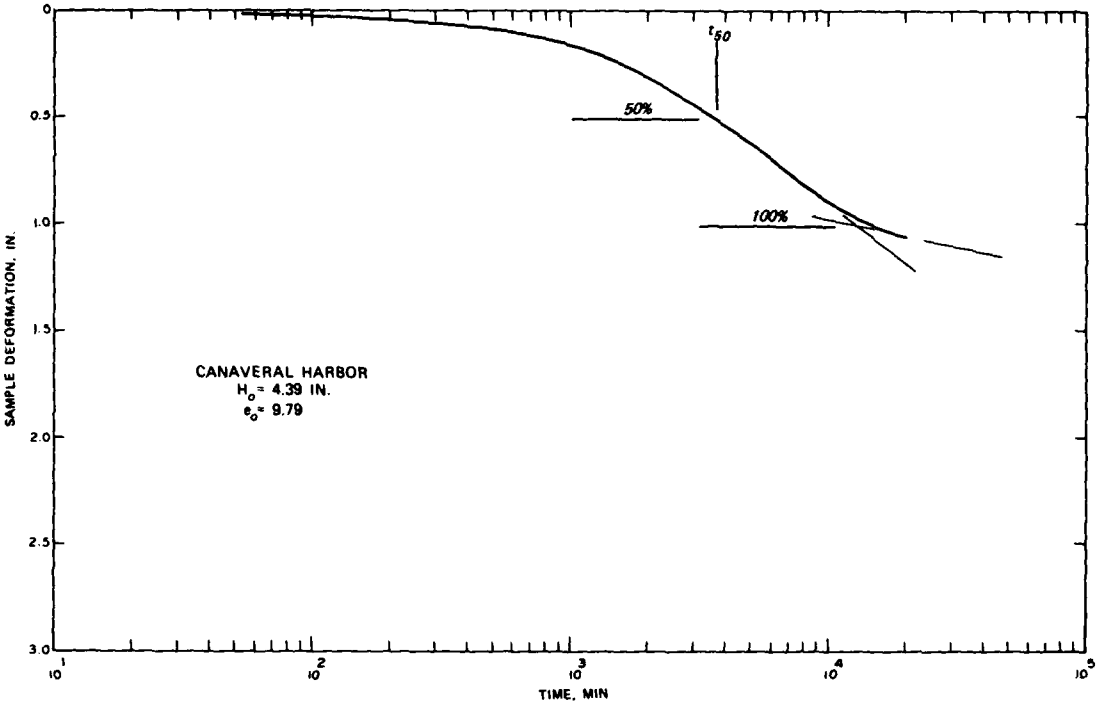

Figure E8. Sample deformation during self-weight consolidation test of Canaveral Harbor material, e_o = 9.79

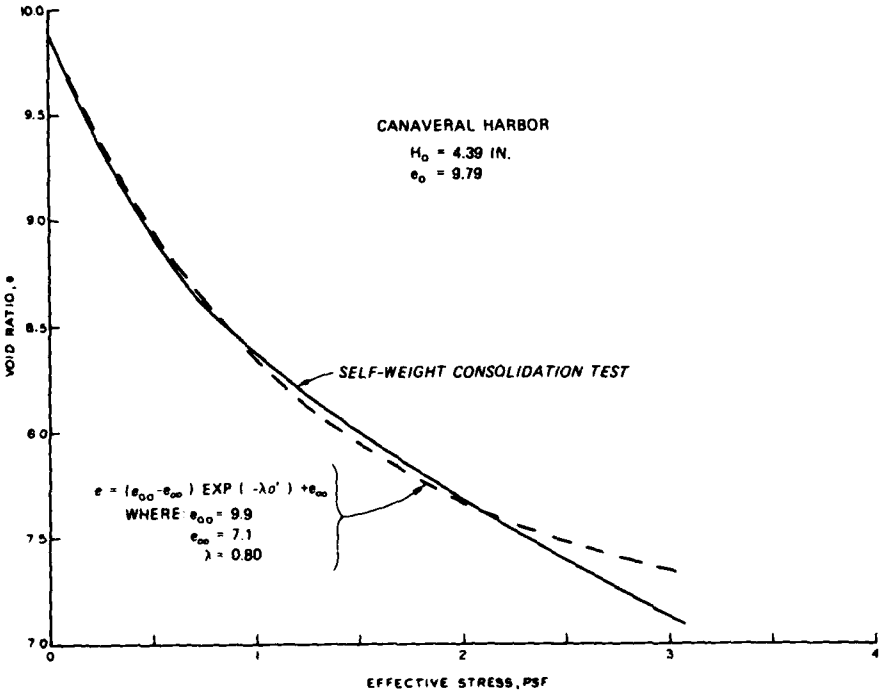

Figure E9. Exponential relationship between void ratio and effective stress chosen to represent results of self-weight consolidation test on Canaveral Harbor material, e_o = 9.79

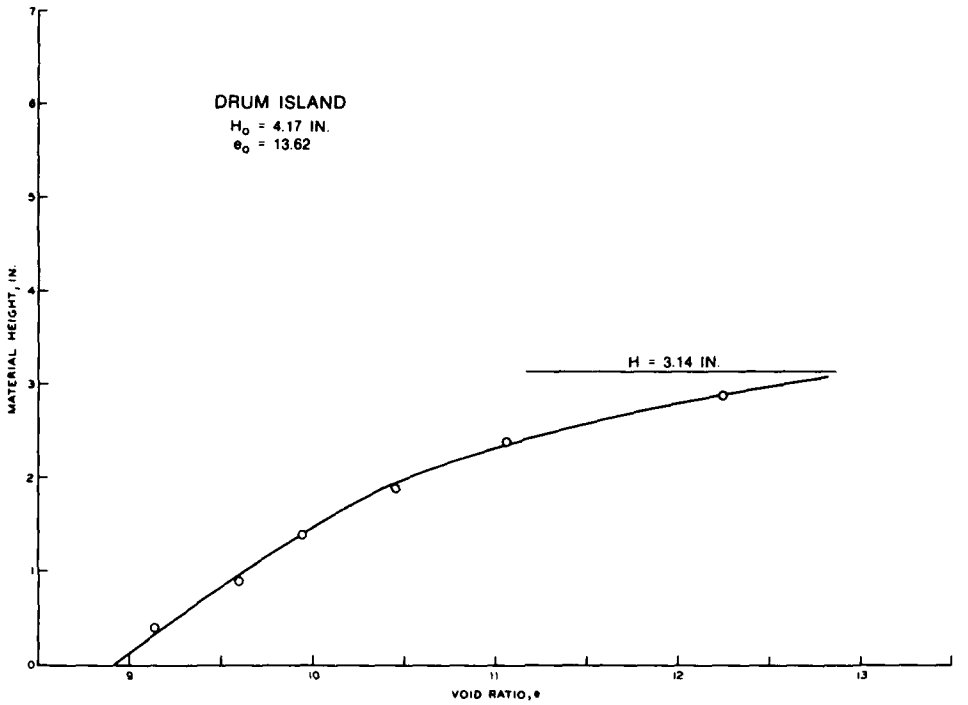

Figure E10. Final void ratio distribution after self-weight consolidation test of Drum Island material, e_o = 13.62

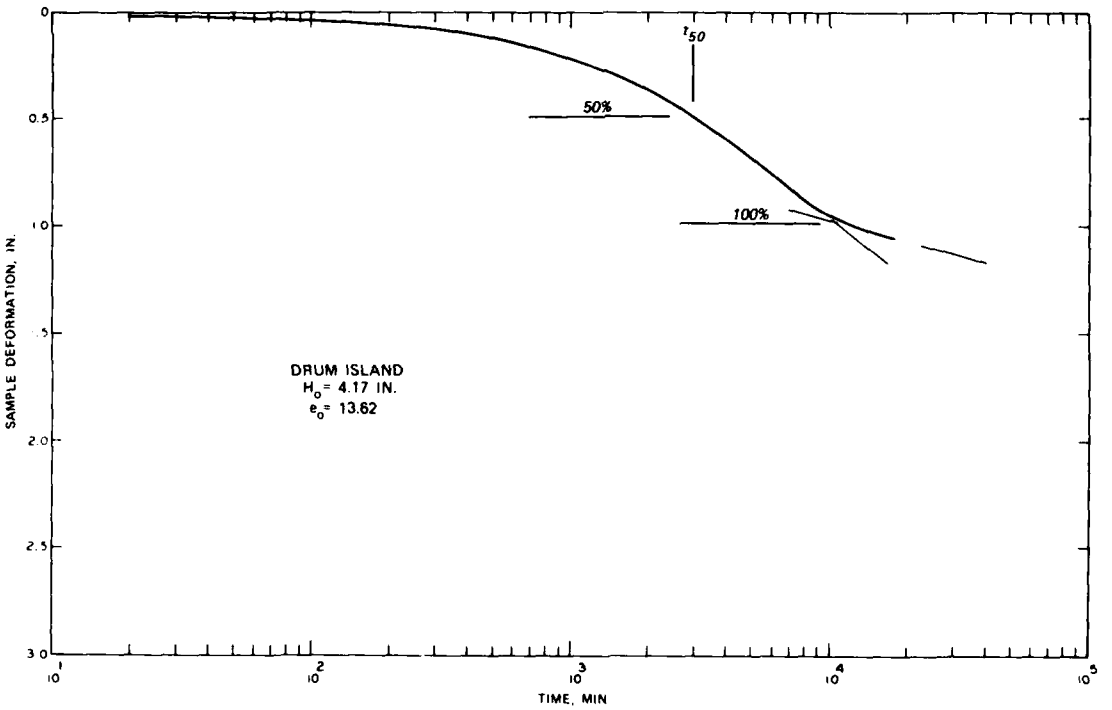

Figure E11. Sample deformation during self-weight consolidation test of Drum Island material, e_o = 13.62

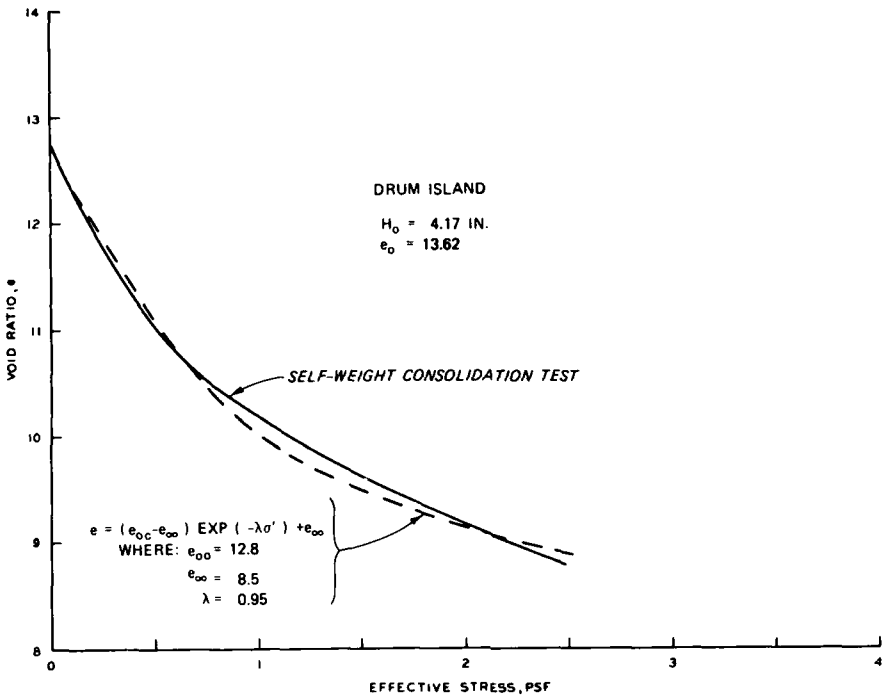

Figure E12. Exponential relationship between void ratio and effective stress chosen to represent results of self-weight consolidation test on Drum Island material, e_o = 13.62

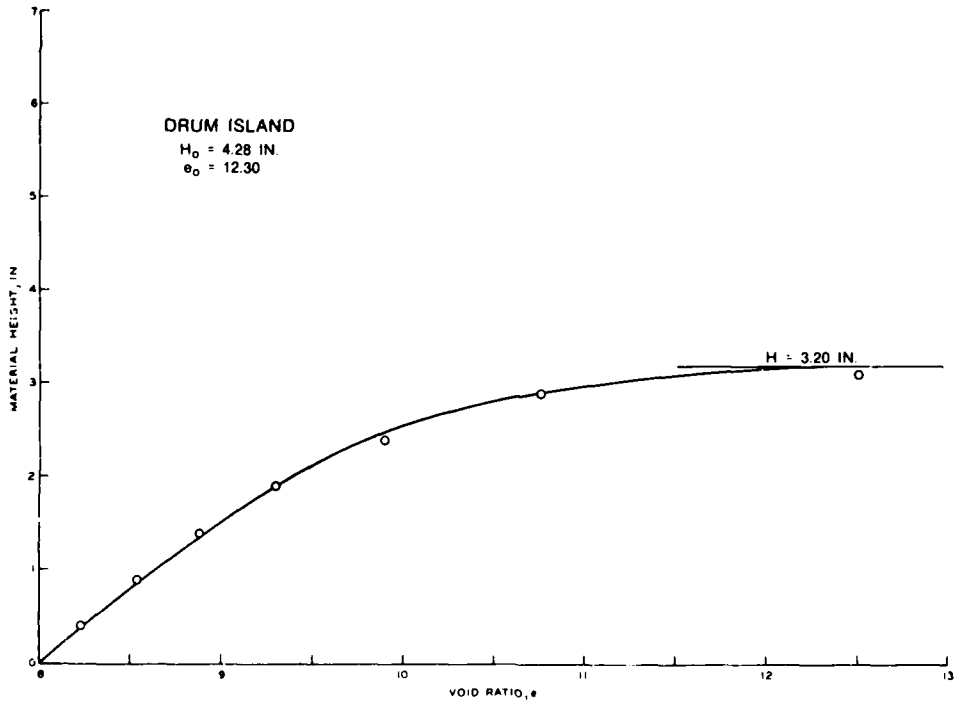

Figure E13. Final void ratio distribution after self-weight consolidation test of Drum Island material, e_o = 12.30

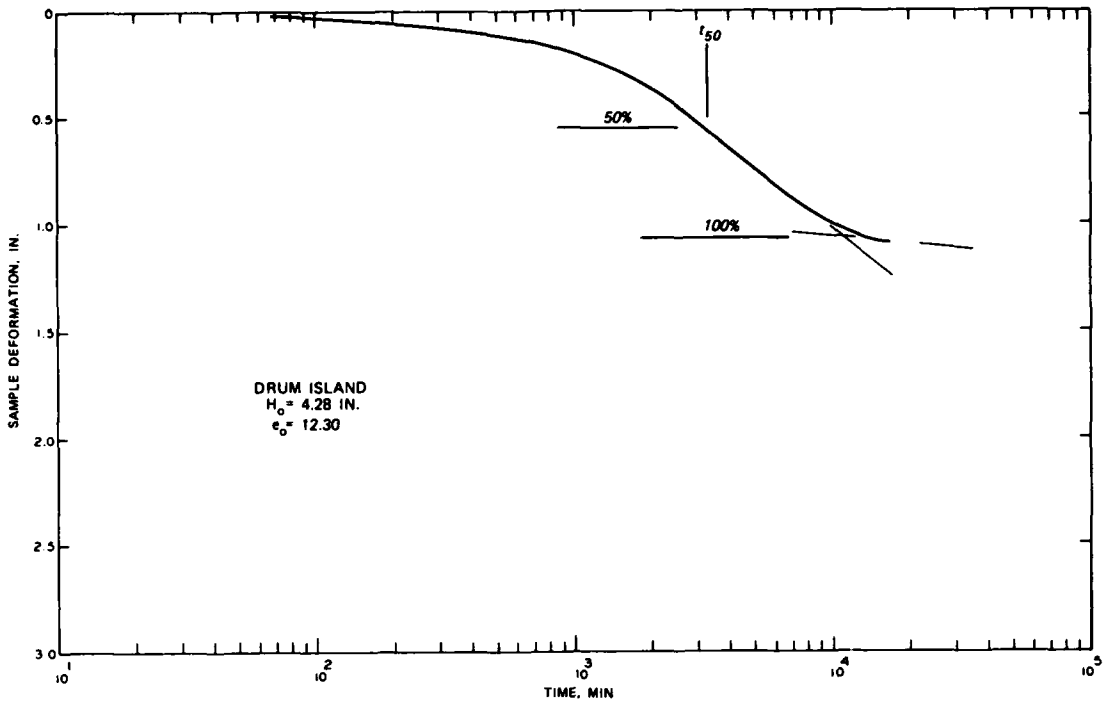

Figure E14. Sample deformation during self-weight consolidation test of Drum Island material, e_o = 12.30

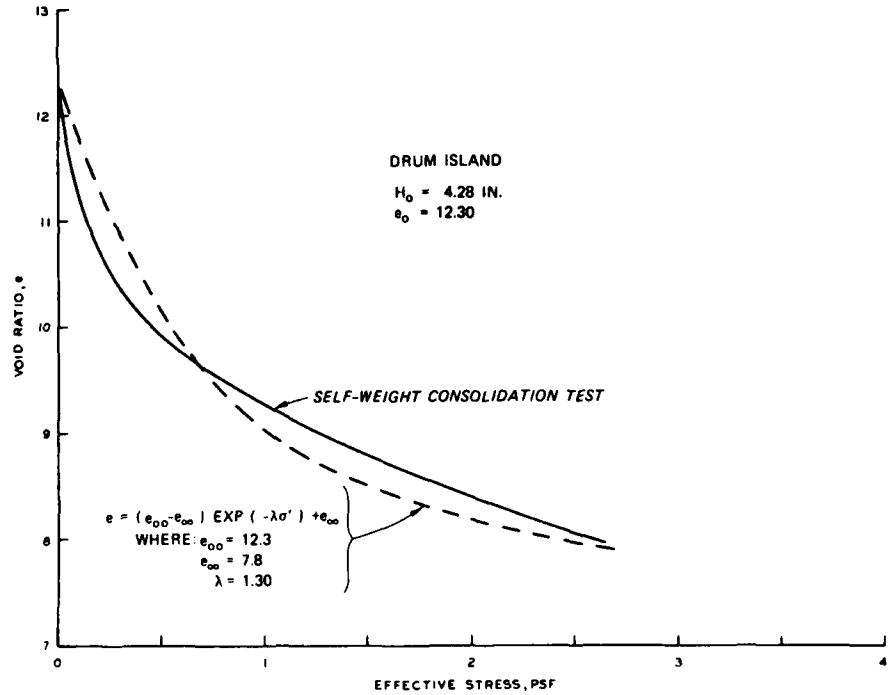

Figure E15. Exponential relationship between void ratio and effective stress chosen to represent results of self-weight consolidation test on Drum Island material, e_o = 12.30

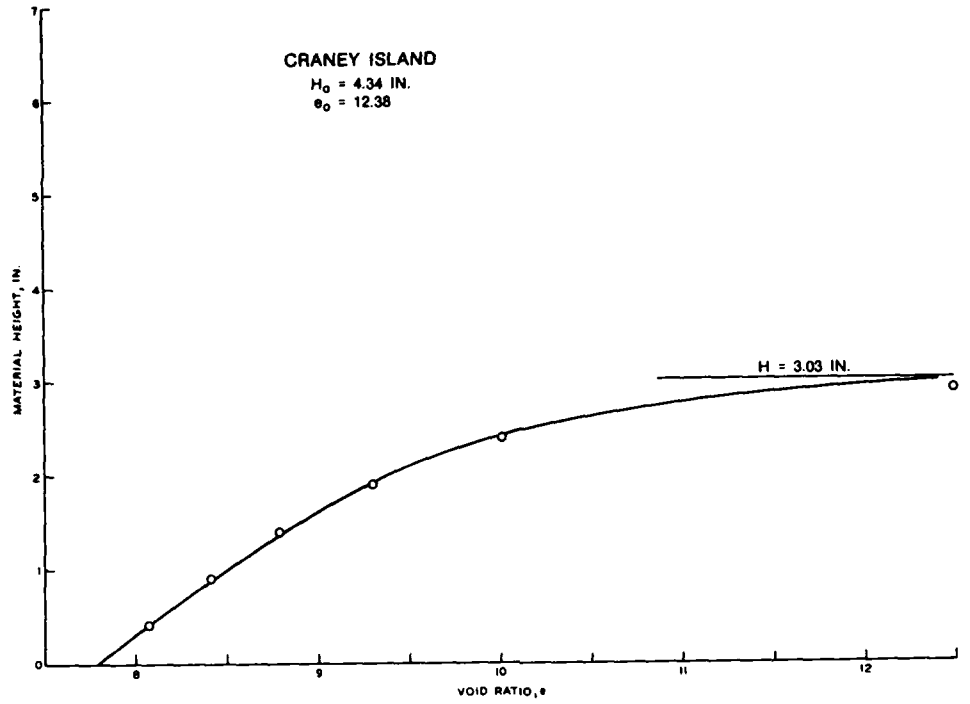

Figure E16. Final void ratio distribution after self-weight consolidation test of Craney Island material, e_o = 12.38

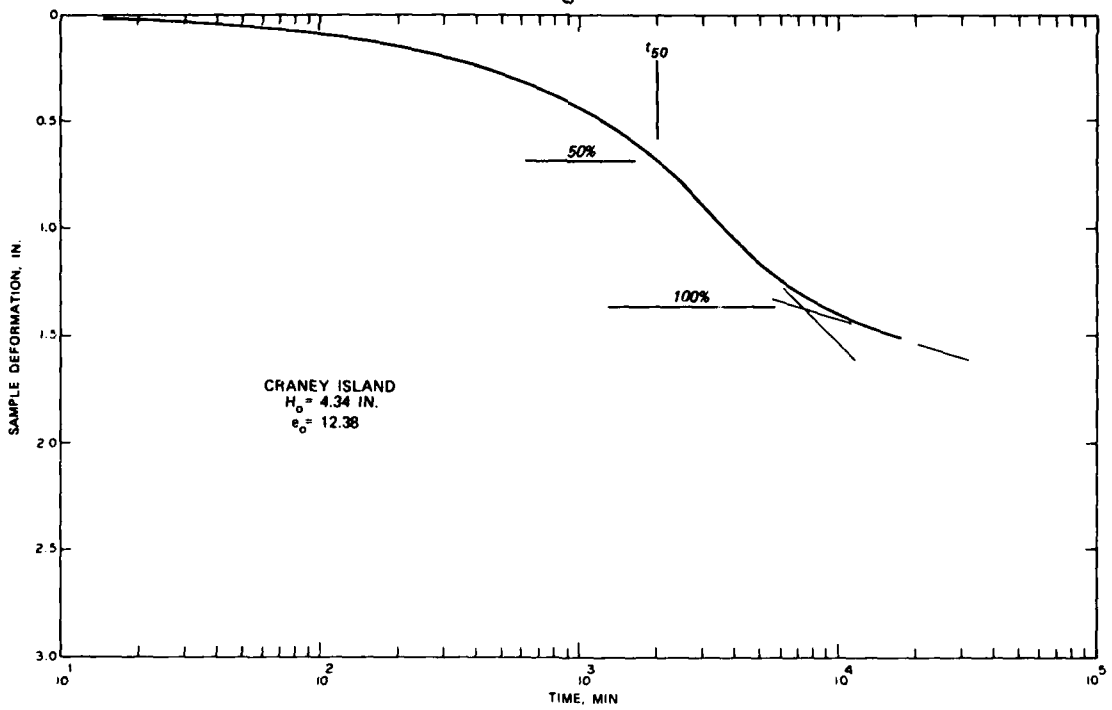

Figure E17. Sample deformation during self-weight consolidation test of Craney Island material, e_o = 12.38

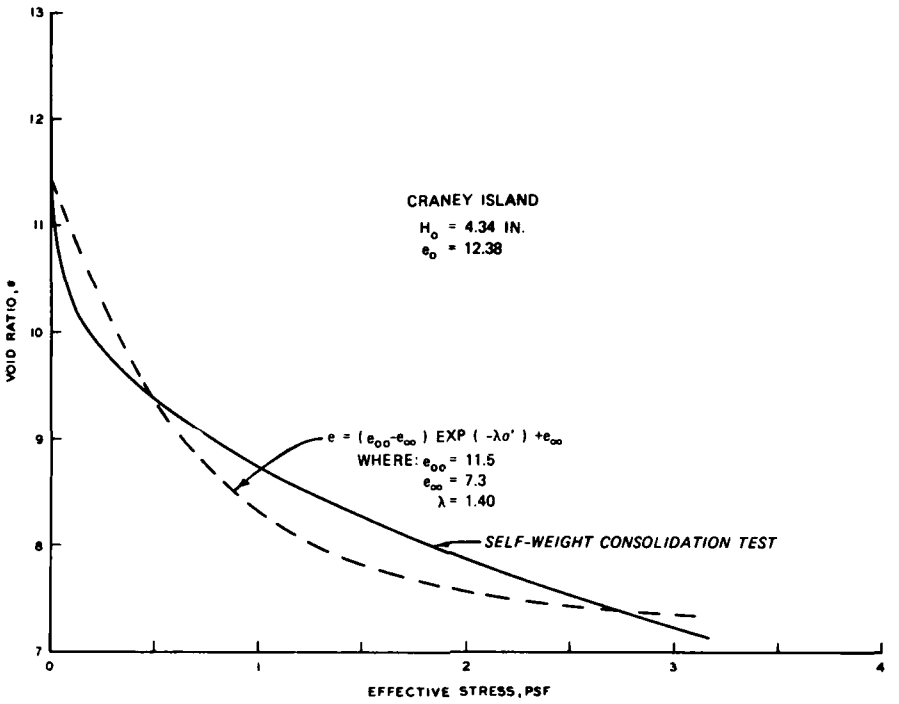

Figure E18. Exponential relationship between void ratio and effective stress chosen to represent results of self-weight consolidation test on Craney Island material, e_o = 12.38

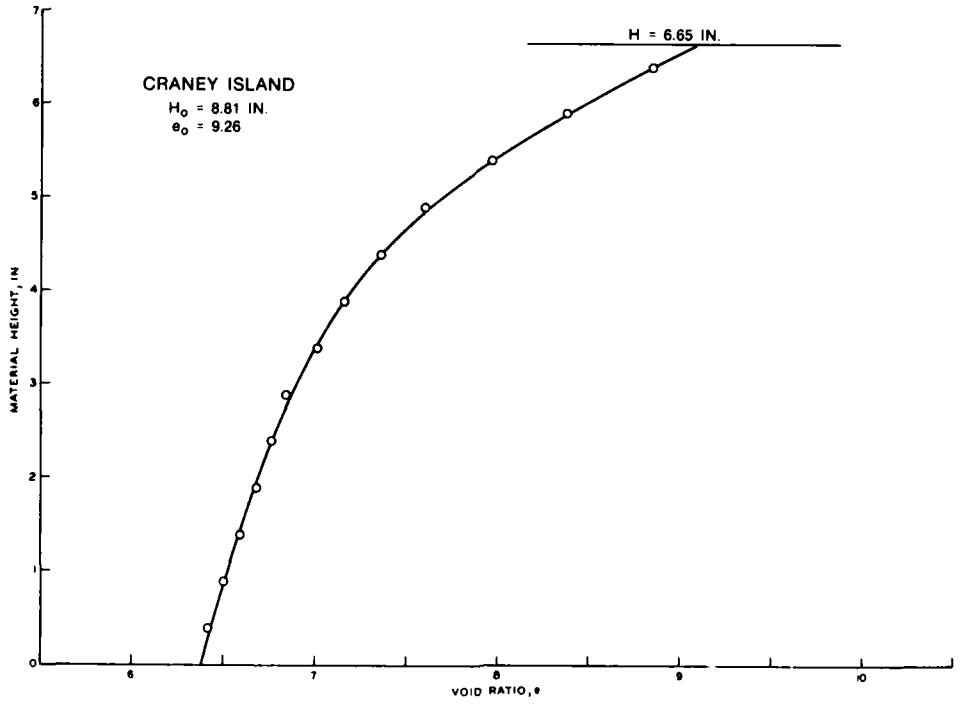

Figure E19. Final void ratio distribution after self-weight consolidation test of Craney Island material, e_o = 9.26

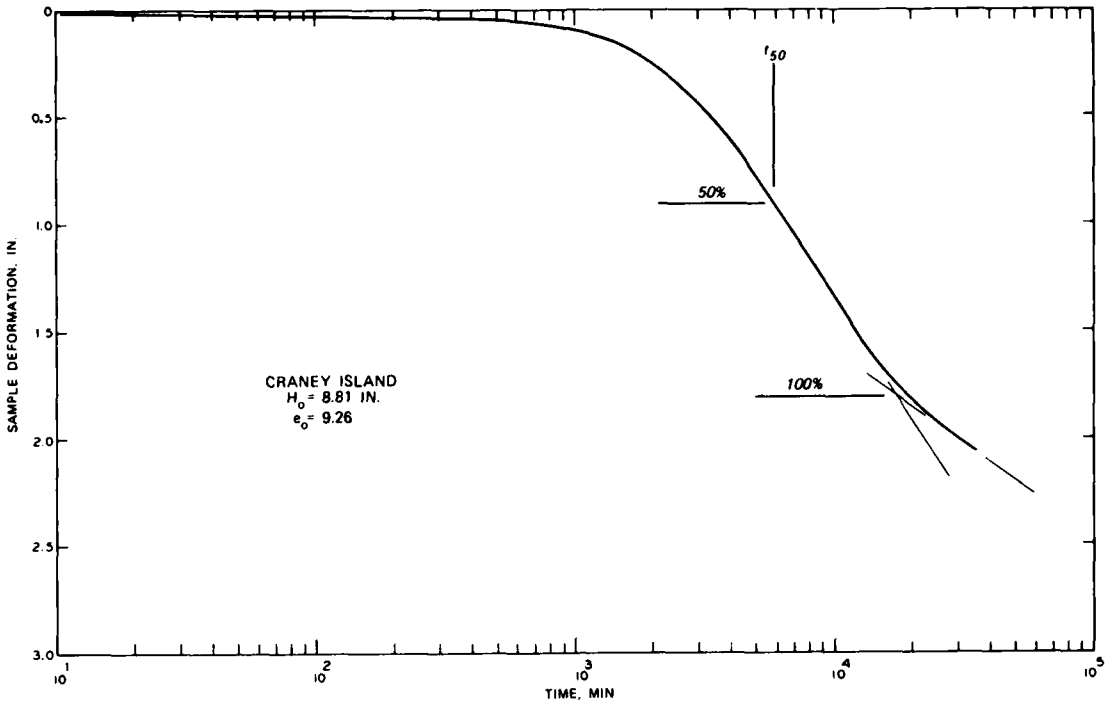

Figure E20. Sample deformation during self-weight consolidation test of Craney Island material, $e_o = 9.26$

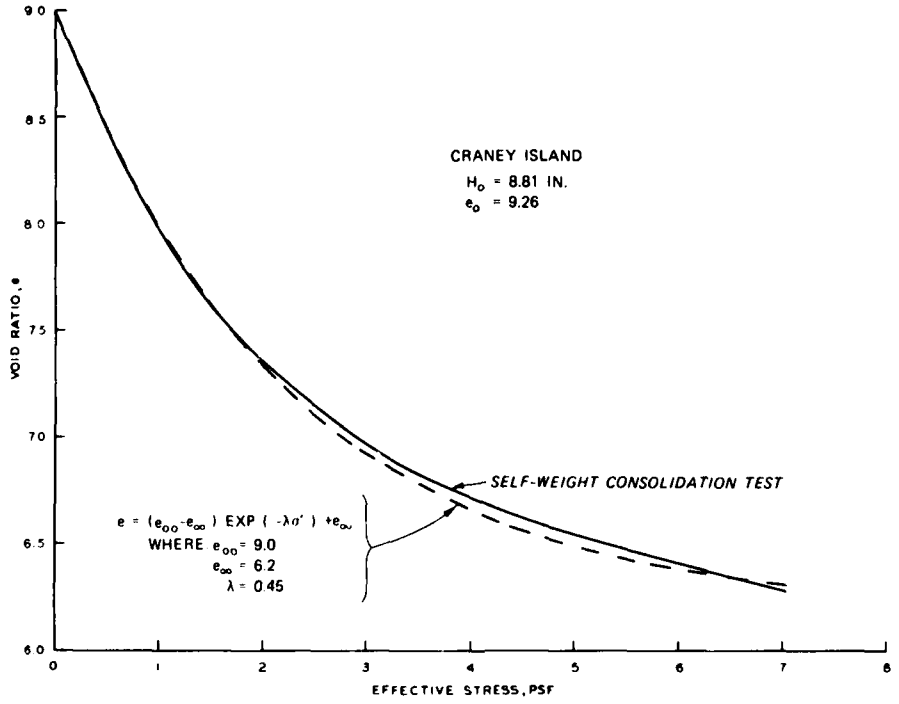

Figure E21. Exponential relationship between void ratio and effective stress chosen to represent results of self-weight consolidation test on Craney Island material, $e_o = 9.26$

APPENDIX F: EXCESS PORE PRESSURE DISTRIBUTIONS FROM LSCRS TESTING

1. This appendix contains figures depicting the excess pore pressure distribution at various times during LSCRS (Large Strain, Controlled Rate of Strain) testing of some typical soft dredged materials. In the figures, the open circles represent actual measurements made at each particular time. The solid circles represent points calculated from the curves in Figures 36. 42, 43, and 44 and the measured maximum excess pore pressure at each particular time.

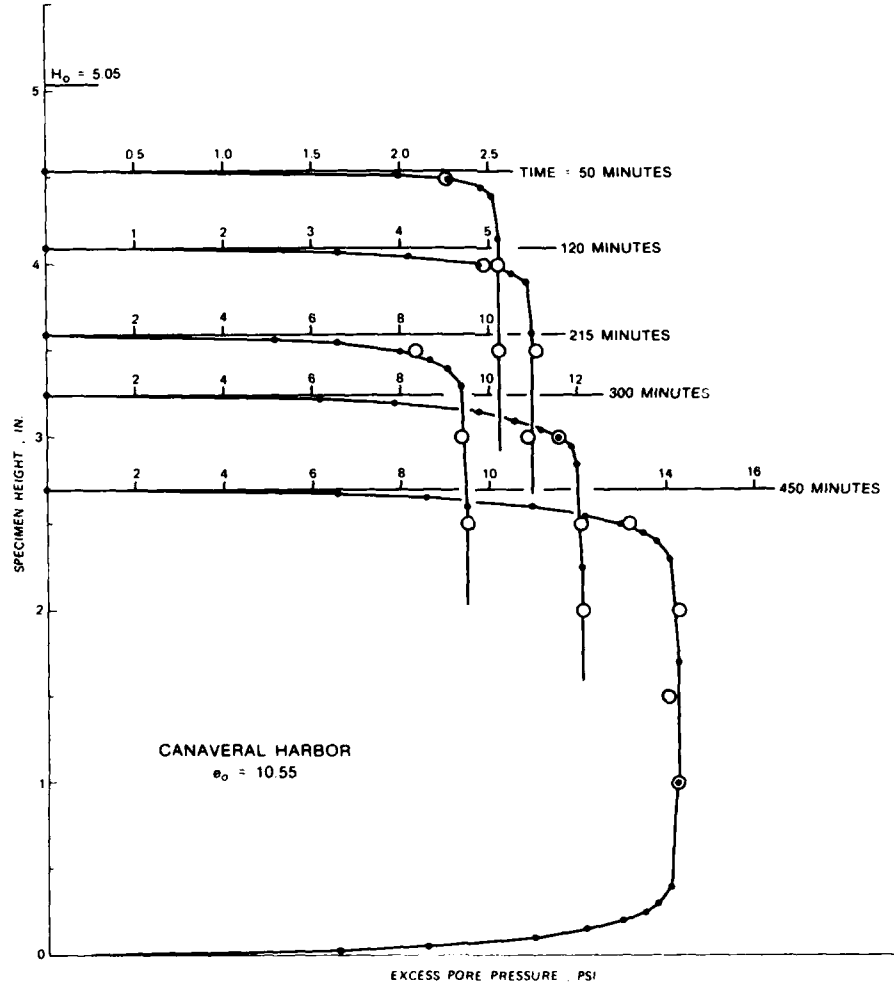

Figure F1. Excess pore pressure distributions during LSCRS test on Canaveral Harbor material, e_o = 10.55

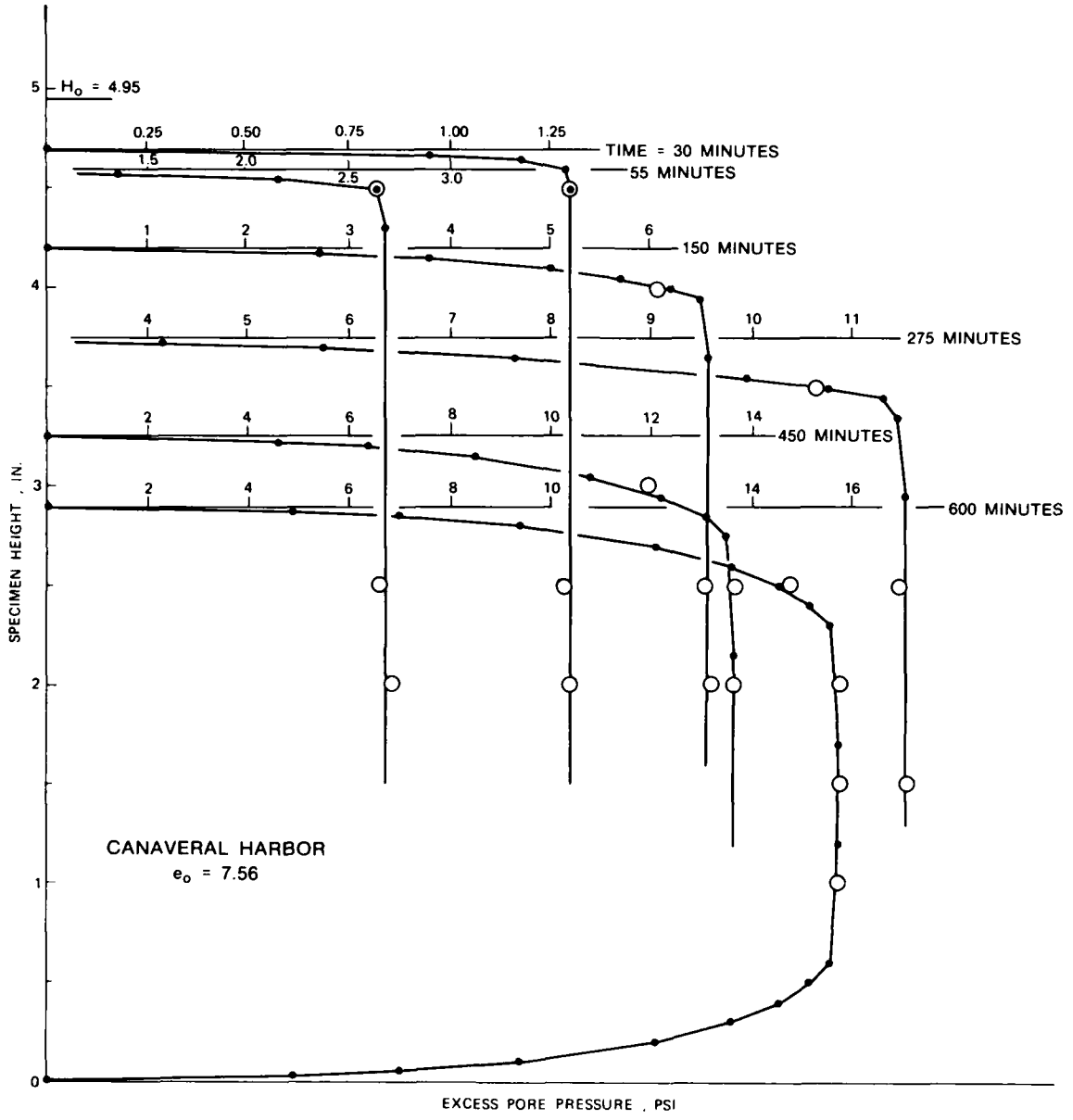

Figure F2. Excess pore pressure distributions during LSCRS test on Canaveral Harbor material, e_o = 7.56

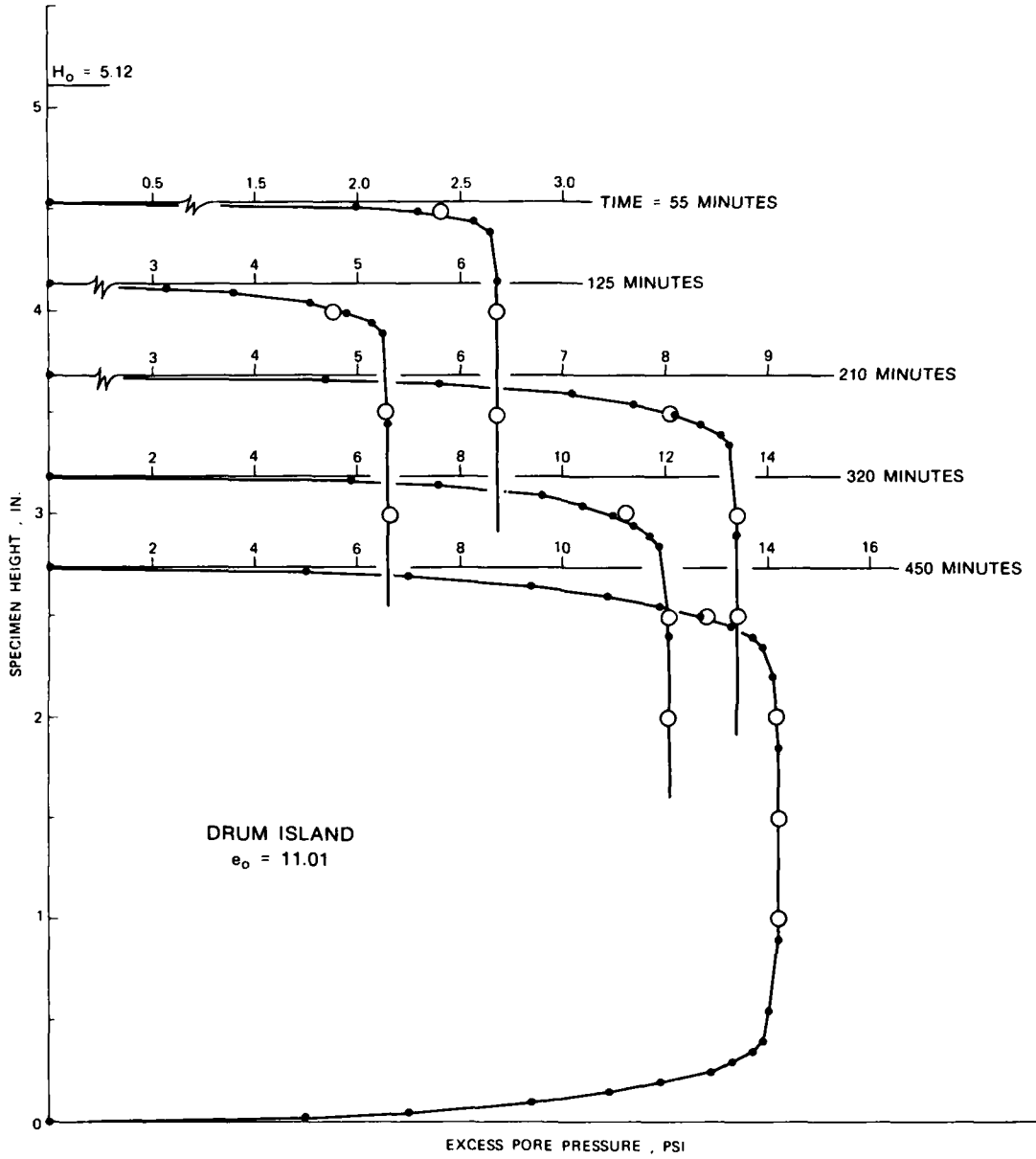

Figure F3. Excess pore pressure distributions during LSCRS test on Drum Island material, e_o = 11.01

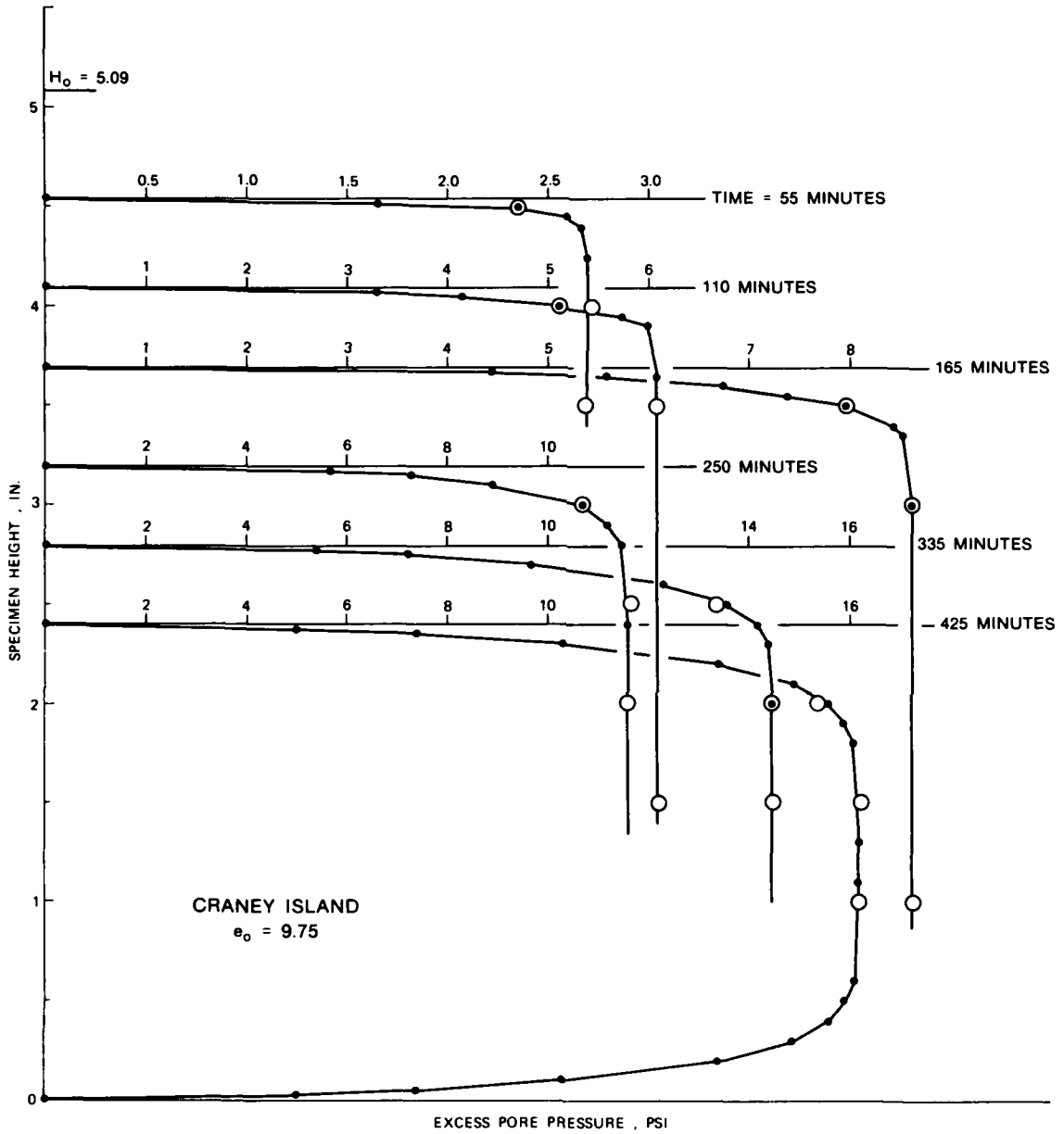

Figure F4. Excess pore pressure distributions during LSCRS test on Craney Island material, e_o = 9.75

END

10-86

DTIC